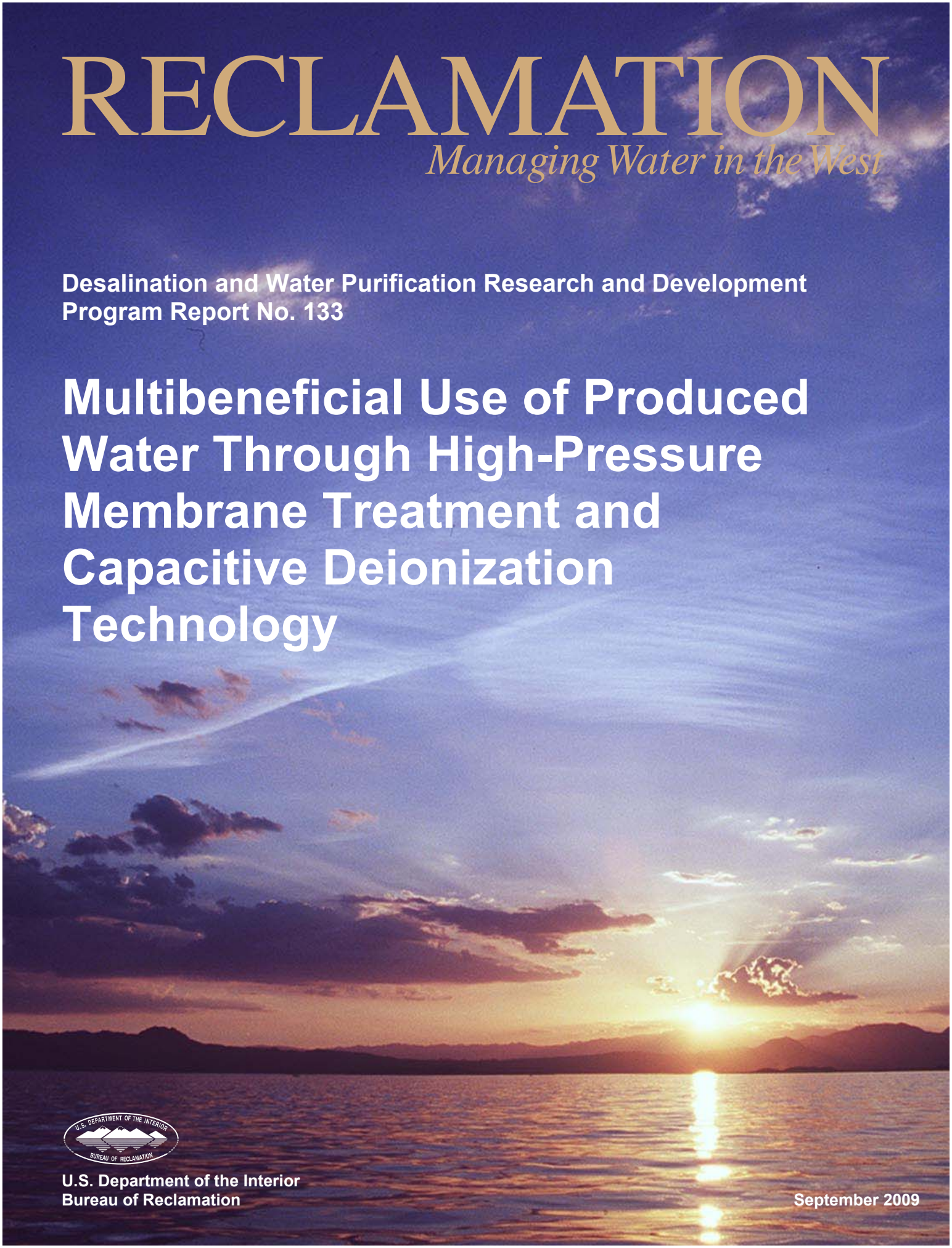

RECLAMATION

Managing Water in the West

Desalination and Water Purification Research and Development Program Report No. 133

Multibeneficial Use of Produced Water Through High-Pressure Membrane Treatment and Capacitive Deionization Technology

U.S. Department of the Interior
Bureau of Reclamation

September 2009

REPORT DOCUMENTATION PAGE

Form Approved
OMB No. 0704-0188

PLEASE DO NOT RETURN YOUR FORM TO THE ABOVE ADDRESS.

1. REPORT DATE *(DD-MM-YYYY)*	2. REPORT TYPE	3. DATES COVERED *(From - To)*
30-12-2005	Final Report	October 2004 to September 2005

4. TITLE AND SUBTITLE

Multibeneficial use of produced water through high-pressure membrane treatment and capacitive deionization technology

5a. CONTRACT NUMBER
Agreement No. 04-FC-81-1053

5b. GRANT NUMBER

5c. PROGRAM ELEMENT NUMBER

6. AUTHOR(S)
Jörg E. Drewes, Pei Xu, Dean Heil, and Gary Wang

5d. PROJECT NUMBER

5e. TASK NUMBER
Task C

5f. WORK UNIT NUMBER

7. PERFORMING ORGANIZATION NAME(S) AND ADDRESS(ES)

Colorado School of Mines
Golden, Colorado 80401-1887

8. PERFORMING ORGANIZATION REPORT NUMBER

9. SPONSORING/MONITORING AGENCY NAME(S) AND ADDRESS(ES)

Bureau of Reclamation
Denver Federal Center
PO Box 25007
Denver CO 80225-0007

10. SPONSOR/MONITOR'S ACRONYM(S)
Reclamation

11. SPONSOR/MONITOR'S REPORT NUMBER(S) DWPR No. 133

12. DISTRIBUTION/AVAILABILITY STATEMENT

Available from the National Technical Information Service
Operations Division, 5285 Port Royal Road, Springfield VA 22161

13. SUPPLEMENTARY NOTES

Report can be downloaded from Reclamation Web site: www.usbr.gov/pmts/water/publications/reports.html

14. ABSTRACT

Large volumes of produced water are generated during natural gas production. Beneficial use of produced water has become an attractive solution to produced water management by providing additional and reliable water supplies and reducing the cost for disposal. This project investigated the viability of using low-pressure reverse osmosis/nanofiltration membranes and capacitive deionization as potential techniques to treat produced water that meets nonpotable and potable water quality standards and providing conditions which allow an economical recovery of iodide. The study included laboratory- and field-scale tests with makeup waters representing various produced water chemistries, which were directed to identify key operational parameters and performance. The two technologies proposed were assessed in terms of technical and economic criteria.

15. SUBJECT TERMS

Produced water, desalination, water reuse, membrane treatment, capacitive deionization, reverse osmosis, nanofiltration, membrane fouling and cleaning, iodide recovery.

16. SECURITY CLASSIFICATION OF:			17. LIMITATION OF ABSTRACT	18. NUMBER OF PAGES	19a. NAME OF RESPONSIBLE PERSON
a. REPORT	b. ABSTRACT	a. THIS PAGE			Frank Leitz
U	U	U	SAR	142	19b. TELEPHONE NUMBER *(Include area code)* 303-445-2255

Desalination and Water Purification Research and Development Program Report No. 133

Multibeneficial Use of Produced Water Through High-Pressure Membrane Treatment and Capacitive Deionization Technology

Prepared for Reclamation Under Agreement No. 04-FC-81-1053

by

Jörg E. Drewes, Pei Xu, Dean Heil, and Gary Wang
Advanced Water Technology Center (AQWATEC)
Environmental Science and Engineering Division
Colorado School of Mines
Golden, Colorado

U.S. Department of the Interior
Bureau of Reclamation
Technical Service Center
Water and Environmental Services Division
Water Treatment Engineering Research Team
Denver, Colorado

February 2009

MISSION STATEMENTS

The mission of the Department of the Interior is to protect and provide access to our Nation's natural and cultural heritage and honor our trust responsibilities to Indian tribes and our commitments to island communities.

The mission of the Bureau of Reclamation is to manage, develop, and protect water and related resources in an environmentally and economically sound manner in the interest of the American public.

Disclaimer

The views, analysis, recommendations, and conclusions in this report are those of the authors and do not represent official or unofficial policies or opinions of the United States Government, and the United States takes no position with regard to any findings, conclusions, or recommendations made. As such, mention of trade names or commercial products does not constitute their endorsement by the United States Government.

Acknowledgement

The authors acknowledge the Desalination and Water Purification Research and Development Program, Bureau of Reclamation, for its financial, technical, and administrative assistance in funding and managing the project. The authors gratefully acknowledge CDT Systems, Inc., for providing capacitive deionization testing units and technical support. The authors thank Paul Mendell with Mendell Energy, Inc. for assisting in field testing and data analysis.

Table of Contents

List of Figures

List of Figures (continued)

List of Figures (continued)

List of Tables

Table *Page*

List of Tables (continued)

Acronyms

°C	degrees Celsius
°F	degrees Fahrenheit
Å	angstrom
AFM	atomic force microscopy
Ag/AgCl	silver/silver chloride
ATR	attenuated total reflection
BET	Brunauer-Emmet-Teller
BJH	Barrett, Joyner, and Halenda
BTEX	benzene, toluene, ethylbenzene and xylene
cm^2	square centimeter
Ca	calcium
$CaCO_3$	calcium carbonate
CCL	Contaminant Candidate List
CDI	capacitive deionization
CDT	capacitive deionization technology
cm	centimeter
cm^3/g	cubic centimeters per gram
CO_2	carbon dioxide
CSM	Colorado School of Mines
DBP	disinfection byproduct
DI	deionized
DOC	dissolved organic carbon
ED	electrodialysis
EDR	electrodialysis reversal
EDS	electron dispersive spectroscopy
EDTA	sodium ethylenediaminetetraacetate
ESEM	environmental scanning electron microscopy
ft^2	square foot
FT	flow-through
FTIR	Fourier transform infrared
g/cm^3	grams per cubic centimeter
gal	gallon
gfd	gallons per square foot per day
gpd	gallons per day

gpm	gallons per minute
HCl	hydrochloric acid
I	iodine
IC	ion chromatograph
ICP	Inductive Coupled Plasma
in	inch
IR	internal-recycle
kilogram	kg
kPa	kilopascal
kWh/g	kilowatthour per gram
L	liter
L/m^2 day·kPa	liter per day per square meter per kilopascal
L/mg·m	liters per milligram per meter
L/min	liters per minut
lb	pound
LLNL	Lawrence Livermore National Laboratory
m	meter
m^2	square meter
m^2/g	square meters per gram
m^3	cubic meter
$m^{3/}d$	cubic meters per day
MCT	mercury cadmium telluride
mg	magnesium
mg/g	milligrams per gram
mg/L	milligrams per liter
$MgCl_2$	magnesium chloride
MGD	million gallons per day
mL	milliliter
mm	millimeter
mmol/g	millimoles per gram
mol/g	moles per gram
MWCO	Molecular weight cutoff
N_2	nitrogen
Na	sodium
NaOh	sodium hydroxide
NF	nanofiltration

nm	nanometer
O&M	operation and maintenance
pCi/L	picocuries per liter
psi	pounds per square inch
Ra	mean roughness
RO	reverse osmosis
SAR	sodium adsorption ratio
SDI	silt density index
SDS	sodium dodecyl sulfate
SEC	size exclusion chromatography
TDS	total dissolved solids
TOC	total organic carbon
UF	ultrafiltration
ULPRO	ultra low pressure reverse osmosis
UV	ultraviolet
V	volt
WHO	World Health Organization
ZnSe	zinc selenide
µL	microliter
µm	micrometer
µS/cm	microsiemens per centimeter

1. Executive Summary

A substantial amount of produced water is generated during gas and oil production, and its disposal represents a significant component in the cost of producing oil and gas. Many areas in the United States where oil and gas operations are underway are also characterized by a lack of water for drinking water supply and agricultural needs. Produced water quality varies considerably depending upon the geographic location of the field, geological formation, and the type of hydrocarbon products being produced. Produced water usually has high total dissolved solids (TDS) concentrations and a high sodium adsorption ratio (SAR), which make it unsuitable for beneficial use without proper treatment. Coal-bed methane production from aquifers is a new approach in utilizing unconventional natural gas resources, and produced water generated from these operations is characterized by the absence of hydrocarbons and, in some cases, elevated concentrations of iodide.

High-pressure membranes such as reverse osmosis (RO) have been used to desalinate seawater and brackish water for more than 30 years and could offer a possible solution for a beneficial treatment of natural gas produced water. The advent of ultra-low pressure RO (ULPRO) membranes and tight nanofiltration (NF) membranes offers a viable option for produced water treatment because they can be as effective as RO in removing certain solutes from water while requiring lower feed pressure.

Capacitive deionization technology (CDT) with carbon-aerogel electrodes represents a novel process in desalination of brackish source water as compared to technologies like RO or electrodialysis. The ions are removed by charge separation, and the system is regenerated during the elimination of the electrical field by reversing electrodes polarity. Thus, common scaling problems associated with membrane and thermal processes can be avoided. The CDT process operates at ambient conditions and low voltages. It uses electrostatic regeneration rather than the harsh chemicals used for regeneration in related adsorptive treatment system.

This study investigated the viability of ULPRO/NF membranes and CDT as potential techniques to treat produced water by meeting nonpotable and potable water quality standards, and providing conditions which would allow an economical recovery of iodide. Laboratory-scale experiments and field tests were conducted to identify key operational parameters and treatment performance. Pretreatment, fouling, and cleaning issues of membranes and carbon aerogel electrodes were examined. Based on findings from laboratory and field tests as well as model simulations, the proposed technologies then were assessed in terms of technical and economic criteria, including water quality, iodide recovery,

production efficiency, operation considerations, energy and chemical consumption, and water production costs.

Membrane fouling and scaling is the biggest challenge to employing membrane technology in produced water treatment. The fouling propensity depended on membrane properties such as hydrophobicity and roughness. Chemical cleaning using caustic and anionic surfactant solutions was proved efficient to restore declined permeate flux. Compared to membrane technology, which often needs rigorous and complex pretreatment, CDT required minimum pretreatment (such as cartridge filters), and no chemicals for scaling control and chemical cleaning. Because of slow mass transport rate of ions adsorbing onto and desorbing from carbon aerogels, water recovery of CDT was low compared to RO process. A large amount of concentrate waste was produced during electrode regeneration and rinsing process. Membrane technology was more cost-effective than CDT and provided a better overall performance in terms of product water quality, iodide recovery, and energy consumption. Both the product water from CDT and membrane technologies required post-treatment for stabilization, removal of boron, and adjustment of SAR for agricultural irrigation. While CDT exhibited a potential alternative to brackish water desalination, the efficiency and system design need to be improved before the technology becomes economically feasible for commercialization.

2. Background and Introduction to the Project

2.1 Background

2.1.1 Produced Water Treatment

Operations of conventional and unconventional natural gas fields are growing rapidly to meet increased energy demands in the world. Large volumes of produced water are generated in gas production by dewatering aquifers in order to recover trapped gas. It is estimated that 10 times more water than gas is generated during gas production (DWPT Roadmap, 2003). Produced water management is critical to a sustainable natural gas operation because of environmental concerns, high disposal costs, and limited disposal options (IOGCC/ALL, 2006; ALL, 2003; Veil et al., 2004). Treating produced water for beneficial use is being investigated as an attractive alternative to traditional disposal methods, such as surface discharge or deep well injection (IOGCC/ALL, 2006; Veil et al., 2004), and offers an opportunity to augment water supplies in areas that lack fresh water supplies.

Produced waters vary widely in composition because they originate from differing geological formations with variable gas hydrocarbon compositions, and they differ by well development and maintenance. These factors affect the technical and economic feasibility of employing treatment technologies for utilizing produced water for beneficial use and meeting regulatory criteria for the targeted end use. The common constituents usually found in produced water include organic compounds such as oil; grease; benzene and phenols; and inorganic compounds such as sodium (Na), potassium (K), iron (Fe), calcium (Ca), magnesium (Mg), chloride (Cl), sulfate, carbonate, bicarbonate, silicate, and borate. Based on the quality and composition of produced water, desalination is often imperative to meet potable and nonpotable water reuse standards.

A number of techniques have been installed, piloted, or are in an experimental stage of development to meet discharge standards or for beneficial use of produced water. High-pressure membranes such as reverse osmosis (RO) have been used to desalinate seawater and brackish water for more than 30 years and offer a product water quality suitable for many beneficial reuse applications of produced water. The Texas Water Resources Institute developed small-scale, modular, transportable units capable of treating relatively small amounts of brine from oil and gas operations inexpensively. These small-scale units utilized nanofiltration (NF) and RO to remove contaminants from oilfield brines (Morales and Barrufet, 2002). Lee et al. (2002) combined a standard RO system with a bentonite clay membrane as a low-cost, low-efficiency membrane filtration system to remove salts in solid form from saline waters. These researchers

expected that this system could treat produced water more economically than conventional RO, with no need for chemical pretreatment. While preliminary results showed some promise, the work was performed at laboratory scale. The complexity of produced water qualities and prospect of a potential market have also drawn the attention of membrane manufacturers. Osmonics, Inc., tested unique membranes and membrane elements especially designed to treat produced water from oil and gas fields (Nicolaisen, 2002 and 2003). The proposed and field tested treatment train consisted of sequentially employed ultrafiltration (M-series, Osmonics), NF (Desal-5, Osmonics), and RO (Desal-3 or Desal-11, Osmonics) membranes. The extremely hydrophilic surface of the M-series membrane minimized membrane fouling that results from oil, grease, and fat. The surfaces of the Desal-3 RO membrane and Desal-5 NF membrane were designed to be very smooth, resulting in increased fouling resistance. While the Desal-5 NF membrane could be very effective in rejecting anions (such as sulfate, phosphate, etc.) and sodium chloride (NaCl) (rejected by up to 30 percent), remaining oil, grease, and fat after ultrafiltration (UF) treatment also were rejected. The final treatment using RO Desal-3 or Desal-11 resulted in water that met drinking water standards. This Osmonics system was specially designed to eliminate the severe fouling problem due to hydrocarbons present in many produced waters.

A pilot study was conducted to evaluate the technical and economic feasibility of treating oilfield-produced water for beneficial reuse at the Placerita Canyon Oil Field, Los Angeles County, California (Funston et al., 2002). Beneficial reuse options evaluated included industrial, irrigation, and potable water use. The major water quality challenges included: total dissolved solids ([TDS] ~ 5,800 milligrams per liter [mg/L]), temperature (170 degrees Fahrenheit [°F]), ammonia (10 mg/L), boron (16 mg/L), and organics. The produced water contained high levels of silica (255 mg/L), hardness (1,000 mg/L as calcium carbonate [$CaCO_3$]), and oil and grease that can potentially foul TDS removal processes such as RO. The pilot units consisted of warm softening, coconut shell filtration, cooling (fin-fan), trickling filter, ion exchange, and reverse osmosis. The warm softening process removed (~95 percent) hardness from the produced water. Silica levels in the softening effluent were 80 and 20 mg/L at a pH of 8.5 and 9.5, respectively. Silica level decreased to 3 mg/L when 400 mg/L of magnesium chloride ($MgCl_2$) were added. More than 95 percent of TDS was removed by RO. Effective removal of boron (~ 90 percent) was achieved at a pH of 10.5 or above. Ammonia was removed effectively (80 percent) at a pH of 8.7 or below.

Electrodialysis (ED) and electrodialysis reversal (EDR) systems also have been considered an alternative to produced water treatment (Spiegler and El-Sayed, 2001; IOGCC/ALL, 2006; Hayes and Arthur, 2004; Spitz, 2003). Frac Water Inc.

developed mobile ED treatment units for treating coal-bed methane (CBM)-produced water and reusing it in fracturing treatment. Several case studies suggested that the mobile treatment units treated the produced water with TDS ranging from 11,400 to 27,000 mg/L and sulfates from 4,000 to 14,000 mg/L (Spitz, 2003). The pretreatment included cartridge filtration to remove particulate matter, carbon filters to remove organic matter, and weak acid cation exchange to remove hardness and iron. ED treatment primarily recovers 80–90 percent of brackish water. The water quality was to meet the requirement for the basic gel fracturing fluids. Hayes and Arthur (2004) reported that ED could provide economical demineralization of produced water with TDS of about 8,300 to 10,000 mg/L, oil and grease with TDS of about 65 mg/L, and biological oxidation demand with TDS of more than 330 mg/L. Although ED/EDR is more resistant to membrane fouling and scaling than RO, the ED process is challenged by complex operation, high cost, and poor removal of organics and microbiological organisms.

Currently, ion exchange technologies have been commercially installed to treat CBM-produced water (IOGCC/ALL, 2006). Produced waters with a predominant sodium bicarbonate ($NaHCO_3$) makeup are frequently treated by the Higgins Loop continuous ion-exchange process. This process can achieve 97–99 percent water recovery, and 1–3 percent of the volume ends up as concentrated brine that is deep-injected or transported offsite by truck for disposal by class II deep injection wells (Beagle, 2006; Matthews, 2007). The treated water can be discharged or transferred for beneficial use when it meets regulatory discharge requirements. Significant cost disadvantages of ion-exchange processes are (1) the use of hydrochloric acid or sulfuric acid for resin regeneration that needs to be delivered to remote sites, (2) the generation of sodium-heavy brine that must be hauled over difficult terrain/dirt roads, and (3) the need for wastewater injection disposal into class III disposal wells. The Higgins Loop continuous ion-exchange process is usually limited to treatment of sodium-bicarbonate-type water and is not cost effective in treating other types of water, such as sodium chloride.

Previous pilot tests have shown that RO could provide good quality water by removing a large fraction of organic and inorganic constituents from produced water (Funston et al., 2002; Bellona and Drewes, 2002). Membrane fouling, however, deteriorates the membrane performance very quickly and results in increased operation costs due to high operating pressure and frequent clean-in-place cycles (Hayes and Arthur, 2004; Visvanathan et al., 2000). Depending on the produced water composition, free and dissolved oil can adhere to the membrane surface, resulting in a loss of permeability. The soluble hydrocarbons, including methane, volatile acids, and BTEX (benzene, toluene, ethylbenzene, and xylene) can cause biofilm growth on membrane surfaces. Particles and

soluble salts can precipitate onto the membrane surface, causing membrane scaling. Rigorous and complex pretreatment often is required for successful RO membrane application.

The advent of ultra-low pressure RO (ULPRO) membranes and nanofiltration membranes with high desalting degrees offers a viable option for produced water treatment because they can be as effective as RO in removing certain solutes from water while requiring considerably less feed pressure. Field experiments at Metropolitan Water District, California, designed to reduce salinity in Colorado River water showed that significant energy savings could be achieved by using ULPRO membranes as compared to previous generations of low-pressure RO membranes (Larson, 1999). Bellona and Drewes (2002) conducted a preliminary assessment using ULPRO (XLE, Dow/Filmtec) and NF membranes (TFC-S, Koch) for produced water from a production well of sandstone aquifer in Montana. The water sample represented brackish groundwater with the major constituents of sodium and chloride, and a conductivity of 11,000 microsiemens per centimeter (μS/cm). Both membranes achieved TDS rejections of more than 90 percent, meeting secondary TDS drinking water standards in the permeate. Samples from this production well consistently showed iodide (I) concentrations of more than 45 mg/L. During treatment with ULPRO membranes using a two-stage laboratory-scale unit, iodide was rejected at more than 97 percent using a feed pressure of 230 pounds per square inch (psi) in single pass at recoveries of 32 to 40 percent. It would make commercial iodine recovery economically attractive. Recovery of iodine from produced water could bring additional economic benefits to produced water treatment by off-setting membrane treatment costs, reducing the volume of the concentrate brine, and by creating an opportunity for augmenting nonpotable and potable water supplies in areas of severe water shortage.

2.1.2 Capacitive Deionization Technology

Capacitive deionization technology (CDT) with carbon-aerogel electrodes represents a novel process in desalination of brackish source water compared to technologies such as RO membranes or ED. Carbon aerogel is a special class of aerogels (air-filled foams) exhibiting ideal electrode material due to its high electrical conductivity, high specific surface area, and controllable pore size distribution (Farmer et al., 1996; Ying et al., 2002). In this process, water is passed between electrodes kept at a potential difference of about one volt; nonreducible and nonoxidizable ions are removed from the water by the imposed electrostatic field and held at the electrode surfaces. Adsorbed ions are desorbed from the surface of the electrodes by eliminating the electric field, resulting in the regeneration of the electrodes.

The major mechanisms related to the removal of charged constituents during electronic water treatment are physisorption, chemisorption, electrodeposition, and/or electrophoresis. The efficiency of CDT strongly depends upon the surface property of electrodes such as the surface area and adsorption properties (Pekala et al., 1998; Gabelich et al., 2002). The Lawrence Livermore National Laboratory (LLNL) began its research into CDT in the late 1980s. LLNL developed and optimized carbon aerogel materials, which multiplied the effective surface area of the deionization electrodes by a factor of 60,000, and dramatically improved their capacity to attract and hold charged water constituents.

In comparison to other desalination technologies, the CDT process exhibits several advantages: a simple, modular, plate-and-frame construction; operating at ambient conditions; no high-pressure pumps or heaters; and low voltages. The CDT systems remove ions by charge separation and the polarity of the electrodes is reversed between operation cycles. The scaling problems commonly associated with membrane and distillation processes therefore may be avoided. It uses electrostatic regeneration rather than the harsh chemicals used for regeneration in other adsorptive treatment systems. The CDT process might offer an attractive, energy-efficient alternative to thermal and membrane desalination processes. The CDT process, however, is only effective at removing ions and frequently requires additional techniques to meet product water quality of organics and microorganisms for discharge or beneficial use.

A disadvantage of the system appears to be the slow kinetics of transport of ions into and out of the highly porous electrodes. Several efforts have been made to improve the performance of the capacitor. Andelman and Walker (2004) used charge blocking layers (essentially ion exchange membranes) on the surface of the electrodes to limit migration of ions into and out of the electrodes and decrease the transition times between purifying and purging cycles. Shiue et al. (2005) improved significantly the efficiency of capacitive deionization (CDI) by using spiral-wound electrodes (activated carbon coated on titanium foil) cartridge in combination with online electrolytic ozonation. Ozone was produced by low-voltage electrolysis of water, and the electrolytic ozone could be placed either before or after the CDI. The electricity retrieved at the discharge of CDI operation could be reused for production of ozone. Water recovery of flow-through capacitor increased to more than 90 percent and energy recovery rate exceeded 30 percent. Noncharged species including organics and pathogens were reduced through online ozonation.

Laboratory-scale experiments have been conducted using brackish water (Welgemoed and Schutte, 2005; CDT Systems, Inc. Technical Report, 2003; Larson, 1999; Gabelich et al., 2002), seawater (Andelman, 1998; Shiue et al., 2005), and industrial waters (Farmer et al., 1996; Pekala et al., 1998; Tran et al.,

2002). However, the knowledge regarding treatment efficiencies of larger scale installations, economic analysis, and short- and long-term fouling/scaling issues of CDT systems has not been established.

2.2 Methodology Applied in the Project

The produced water examined in this study was generated in natural gas operations from sandstone aquifers. The tested water was characterized as brackish groundwater of sodium chloride type with TDS concentration of 5,300 mg/L, and no detectable hydrocarbons but elevated concentration of iodide. Iodine (I) is an essential and rare element with increasing demand in many industrial applications. The major end-uses of iodine include animal feed supplements, catalysts, inks and colorants, pharmaceuticals, photographic chemicals and films, sanitary and industrial disinfectants, and stabilizers (Roskill Report, 2002).

The objectives of this research project were to (1) investigate the viability of ULPRO/NF membranes and CDT as potential techniques to treat produced water while meeting nonpotable and potable water quality standards and (2) provide conditions that would allow an economical iodide recovery. Key elements of this investigation were costs associated with installation and operation. The study also studied fouling and cleaning issues of membranes and carbon aerogel electrodes during produced water treatment. The study included laboratory and field tests with makeup water representative of various produced water chemistries and water produced from a gas field to identify key operational parameters and performance issues.

3. Conclusions and Recommendations

3.1 Conclusions

- Flat-sheet experiments using high-pressure membranes and membrane surface characterization revealed that the degree of flux decline was dependent upon the physico-chemical properties of the membranes during produced water treatment. Hydrophobic and rough membranes exhibited a higher flux decline and lower chemical cleaning efficiency than smooth and/or hydrophilic membranes.

- Pretreatment including microfiltration, pH adjustment, and addition of antiscalants could alleviate membrane fouling significantly.

- Chemical cleaning using caustic and anionic surfactant solutions restored membrane permeability more efficiently than chemical cleaning using acids and metal chelating agents.

- The nanofiltration membrane (NF-90) required a low pressure for producing a high permeate flux. The salt rejection and iodide recovery by the NF-90, however, were much lower in comparison to the RO and ULPRO membranes tested. The permeate quality of the NF-90 met USEPA National Primary Drinking Water Standards, but exceeded the Secondary Standards regarding chloride and total dissolved salts.

- The two ULPRO membranes tested (TMG-10 and TFC-ULP) exhibited a high permeate flux while displaying a competitive rejection in comparison to the conventional RO membrane, notably the TMG-10 which showed a very stable rejection at low and high recoveries.

- Cost analysis showed that the ULPRO membrane system provided marginally lower overall operation and maintenance (O&M) costs than RO for meeting drinking water standards while treating produced water. The ULPRO membrane operation also resulted in lower treatment cost than RO and NF for meeting irrigation water standards, especially at high energy cost.

- The performance of the CDT system was consistent throughout the bench-scale experiments and the field test. Deterioration or fouling of the carbon aerogel electrodes was not observed during produced water treatment. Electrode fouling, however, might occur due to adsorption of organics during regeneration when the electrodes are uncharged.

- The sorption capacity of carbon aerogel (in moles per gram [mol/g] aerogel) in treating the produced water followed the order Na>>Ca>Mg>K for cations, and chlorine (Cl)>>bromine (Br)>I for anions.

- The maximum percentage of removal, however, followed a different trend in the order of organic acids (in terms of ultraviolet absorbance (UVA) at 254 nanometers [nm]) > I > Br > Ca > alkalinity > Mg > Na > Cl.

- Energy consumption increased exponentially with the applied current on the CDT electrodes. Lower power for electrode charging and discharging could lead to higher energy efficiency for salt removal.

- The treatment efficiency of CDT maintained a constant level over multiple stages.

- Due to the microporous nature of the aerogel structure (average pore size of 4.28 nm), the actual available surface area for ion sorption was about 33 percent of the measured Brunauer-Emmet-Teller (BET) area. Therefore, modifying pore size distribution is critical to improving sorption performance of the carbon aerogel electrodes.

- CDI could be an alternative for brackish water desalination, but the sorption capacity of the electrodes and operational performance merit further improvement.

- High-pressure membrane technologies provided a better overall performance in terms of product water quality and iodide recovery.

- Water cost of CDT process was much higher than that of all tested membranes due to its high downtime and low product water recovery.

- Cost analysis revealed that the ULPRO membrane system had marginally lower overall O&M costs than RO for meeting drinking water standards. The ULPRO membrane operation resulted in even lower treatment cost than RO and NF for meeting irrigation water standards, especially at higher energy rate.

3.2 Recommendations

1. Capacitive deionization is an alternative desalination process to treat produced water. The efficiency and production capacity of the system, however, needs to be improved before CDT becomes economically feasible to treat water at this level of salinity (TDS > 5,000 mg/L). The

results of the laboratory and field test allowed for the identification of the critical equipment and operational parameters which merit further improvements in design and optimization. These include:

- High capacitance and low cost of electrode materials
- Faster charging and discharging of electrodes
- Successful recovery of residual electricity
- Shorter regeneration time (downtime)
- Reduced waste of rinsing and regeneration water (avoid using product water) and higher recovery
- Reduced carryover volume (residual water volume) after regeneration

2. Findings of this study revealed that ULPRO membranes represent a viable technology for multibeneficial use of produced water.

4. Work Performed

The treatment objective of this study was to compare NF/ULPRO membranes with CDT in treating produced water to provide a water quality that met (1) irrigation water quality standards (TDS of 500–1,000 mg/L), (2) potable water quality standards (primary and secondary maximum contaminant levels [MCLs]), and (3) allowed an economical way to recover iodide. The study was designed for a period of 12 months with four main tasks.

4.1 Pre-Assessment Studies

4.1.1 Water Quality Analysis

A comprehensive water analysis was conducted to identify water quality constituents in produced water critical for membrane and CDT treatment. Analytical methods and sampling strategies followed protocols described in *Standard Methods* (APHA, 2005). The team established and followed standard operating procedures in collecting samples and conducting water quality analyses. Samples from the Jorgensen well, 40 miles from Havre, Montana, were collected at grab samples. The samples were put on ice and shipped to the Colorado School of Mines laboratory for analysis. Besides the initial water quality analysis, 19 samples were collected throughout the course of this study confirming the quality of this groundwater.

4.1.2 Bench-Scale Membrane Selection Tests

Bench-scale testing was conducted to preselect appropriate ULPRO and NF membranes with the focus on pretreatment, membrane fouling and cleaning, salt rejection, and iodide recovery using produced water generated from the Jorgenson production well in Montana. Two cross-flow flat sheet units (Osmonics Sepa II) were employed to test salt rejection and evaluate flux decline using appropriate ULPRO and NF membrane specimens. The candidate membranes included one RO membrane: TFC-HR (Koch Membrane Systems), three ULPRO membranes: XLE (Dow/Filmtec), TFC-ULP (Koch) and TMG-10 (Toray America), and three NF membranes: NF-90 (Dow/Filmtec), TFC-S (Koch) and ESNA (Hydranautics).

Membrane fouling was characterized using microscopic techniques, contact angle measurement, and electron dispersion spectrum (EDS), and Fourier transform infrared (FT-IR) spectroscopy.

4.1.3 Bench-Scale CDT Tests

Bench-scale CDT aquacells were tested with focus on fouling behavior of electrodes, regeneration effectiveness, and desalting efficiency. Experiments

were initiated with the assessment of the ion removal properties of the cell with synthetic solutions, progressed to the treatment of a synthetic surrogate of the produced water, and culminated in the treatment of produced water from the natural gas production site.

4.2 Laboratory-Scale Membrane Tests

The viability of ULPRO and NF membranes selected from bench-scale tests in treating produced water was further examined using 4040 spiral-wound elements in a two-stage laboratory-scale testing unit in a 1:1 array operated at a flux of approximately 0.20-0.77 $m^3/(m^2 \bullet d)$ (5–19 gfd, i.e., gallons of permeate produced per day divided by the area of membrane (ft^2)) depending on the membranes employed. The experiments were focused on recoveries and rejection using the water produced from the Jorgenson well. The laboratory-scale tests allowed transfer of research results to pilot- and full-scale applications.

4.3 CDT System Field Tests

In order to verify findings derived from laboratory bench-scale experiments, a field evaluation with a pilot-scale CDT unit was performed at the Jorgensen well in Montana over a period of 3 weeks. The field test examined the performance of CDT at a larger scale under "real" operational conditions. The consistency of bench- and pilot-scale testing regarding design, manufacture, and operation would allow scaling of the CDT process to industrial size treatment plants, which would be used to compare CDT process against membrane treatment based on technical and economic criteria.

Two commercial CDT aquacells (provided by CDT Systems, Inc., Dallas, TEXAS) were tested in the field under different operational conditions such as flow rate, charge/discharge current, and regeneration frequencies. During the experiments at this field site, the parameters for each test run, including flow rate, current, voltage, pH, conductivity, and temperature were collected automatically by Labview (National Instruments) as well as checked manually by handheld analytical instruments. Iodide concentration was measured at site by an ion-analyzer. Well water samples and CDT processed water samples were also shipped to the Colorado School of Mines for further comprehensive analysis.

4.4 Technical-Economic Assessment of Membrane and CDT Technologies

The two proposed desalination technologies for produced water treatment were compared in terms of water quality criteria and iodide recovery, specific production efficiency (water recovery and system down time), operation and design considerations, pre- and post-treatment, energy and chemical consumption, life cycle of system, and overall costs. The assessment was based on the results from laboratory and field tests as well as simulation using commercially available membrane design programs.

5. System Description

5.1 Methods of Water Quality Analysis

Water analysis for different target constituents was conducted employing Standard Methods (APHA, 2005). Iodide was analyzed using an EA 940 Expanded Ionanalyzer (Orion Research Inc, Boston, Massachusetts) with ThermoOrion Iodide and silver/silver chloride (Ag/AgCl) electrodes. Inorganic cations were measured with the Optima 3000 Inductive Coupled Plasma (ICP) Spectrometer (Perkin Elmer, Norwalk, Connecticut). Samples were prepared by 0.45-micrometer (μm) filtration and then acidified to pH 2.0 using nitric acid concentrate before instrumental analysis. Inorganic anions were measured with a Dionex DS600 Ion Chromatograph (IC) (Dionex, Sunnyvale, California) using an AS14A column and a sodium hydroxide eluent. Samples were prepared by 0.45-μm filtration before instrumental analysis.

Membrane fouling potential was assessed by the silt density index (SDI) calculated from the rate of plugging of a 0.45-μm membrane filter (47 millimeters [mm] in diameter, Nuclepore polyester, Whatman, Clifton, New Jersey). The schematic of the laboratory apparatus used to measure SDI is shown in figure 1. The SDI was measured at 209.5 kilo Pascal (kPa) or 30 psi using the standard Test Method D4189-95 (2002) according to equation (1). Deionized water (type II water obtained from a laboratory water purification system (U.S. Filters, Warrendale, Pennsylvania)) was used as non-plugging reference water. Since the time to collect 500 milliliters (mL) of the tested water represented more than 110 percent of the non-plugging time, a sample size of 100 mL was used for the SDI measurement.

$$SDI = (\%P_{30}/T) = [1-(ti/tf)]*100/T \quad (1)$$

Where $\%P_{30}$ = percent at 30 psi feed pressure

T = total elapsed flow time, (minute [min])

t_i = time to collect initial 100 mL of sample, (s)

t_f = after test time T, time to collect final 100 mL of sample, (s)

For the SDI measurement, total elapsed flow time T is often set for 15 minutes. However, due to the high fouling potential of the tested water, the $\%P_{30}$ exceeded 75 percent in this study, which is the recommended value of the method. Thus, 5 minutes was used as the total elapsed time T. Water temperature before and after the test was 19.4 degrees Celsius (°C) or 67.1 degrees °F.

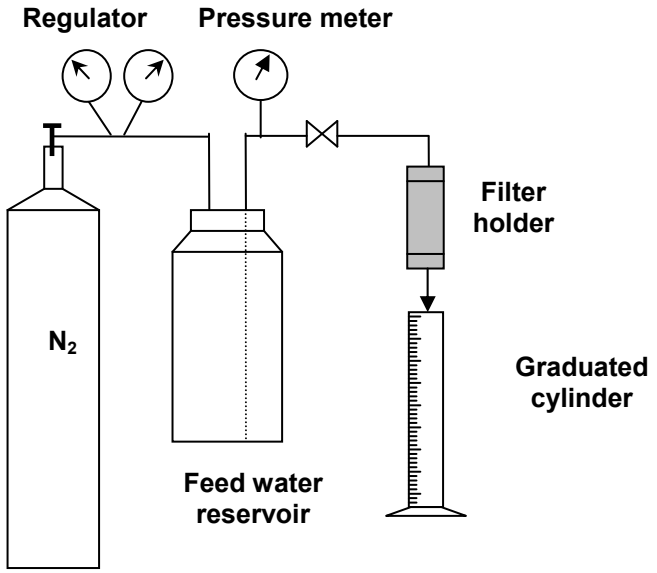

Figure 1. Schematic of SDI test apparatus.

5.2 Bench-Scale Membrane Testing

Two standard laboratory cross-flow membrane filtration units (Sepa CF II, GE Osmonics, Minnetonka, Minnesota) were employed in rejection tests and membrane fouling experiments (figures 2 and 3). The dimensions of the cells are 14.6 centimeters (cm) by 9.5 cm by 0.86 millimeters (mm) or 5.75 inches (in) by 3.74 in by 34 mil for channel length, width, and height, respectively. These channel dimensions provide an effective membrane area of 139 square centimeters (cm^2) per unit and a cross-sectional flow area of 0.82 cm^2. Given the channel height of 34 mil and controlled flow rate, the test cell can simulate hydrodynamic conditions of a spiral-wound element that often has a spacer thickness of 31 mil. The test cells of the units were rated for operating pressures up to 689.5 kPa or 100 psi.

The experiments were carried out at a pressure of 80 psi (558.8 kPa) and a feed flow rate of 500 milliliters per minute (mL/min), resulting in a feed cross-flow velocity of 10 centimeters per second (cm/s). The feed water temperature was kept at 11±1 °C (51.8±1.8 °F) by a stainless steel water cooling system, simulating the onsite well water temperature. Feedwater to the units was the microfiltered produced water processed through a 5 μm cartridge and a 0.45-μm filter bag (Cole-Parmer, Vernon Hills, Illinois). To avoid inorganic scaling, the pH of the microfiltered produced water was adjusted to 6.0 using a hydrochloric acid (HCl) solution. Approximately 50 liters (13.2 gallons) of the microfiltered water was stored in a drum and pumped into the parallel membrane test cell setup

by splitting feedwater into two parallel streams. The fouling tests were operated in a recycling mode in which all concentrates and permeates were recirculated into the feed drum. The membrane specimens were preserved for membrane characterization and future reference.

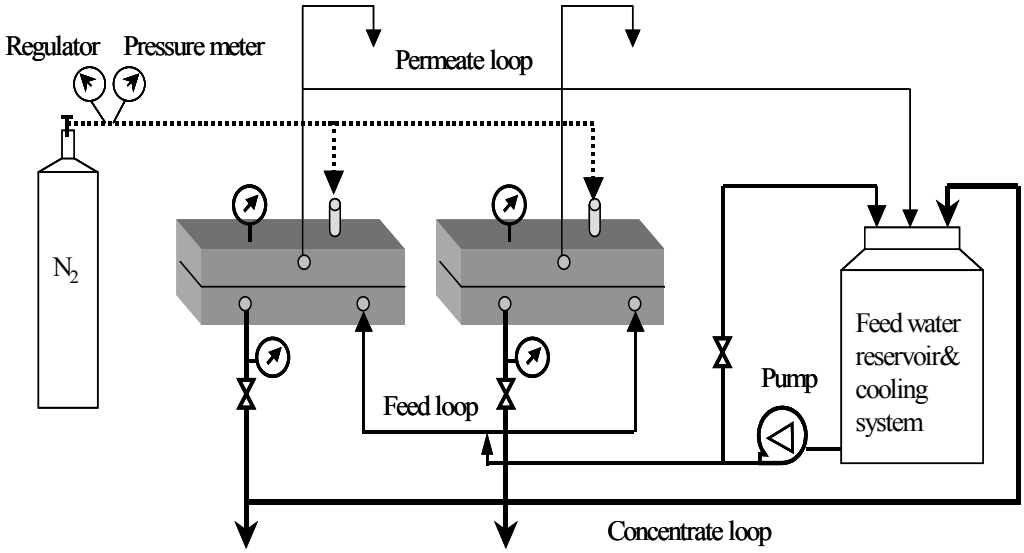

Figure 2. Schematic of the flat-sheet membrane units (Osmonics Sepa II) for rejection and fouling tests.

Figure 3. Flat-sheet membrane units in the laboratory for rejection and fouling tests.

Prior to fouling and rejection experiments, virgin (new) membrane specimens were placed in the units and rinsed with deionized (DI) water at 558.8 kPa (80 psi) for 2 hours to compact the membrane and eliminate impurities attached to the membrane surface. Pure water permeability was recorded for each membrane

specimen to ensure that the membranes used for the experiments were comparable.

The effect of adding antiscalants on flux decline was assessed using the antiscalant Hypersperse MDC700 from GE Betz (Trevose, Pennsylvania) at a concentration of 3 mg/L. In addition to hydraulic cleaning, the efficiency of chemical cleaning was examined with hydrochloric acid, citric acid, and sodium hydroxide (NaOH) as an alkaline solution; sodium ethylenediaminetetraacetate (EDTA) as a metal chelating agent; and sodium dodecyl sulfate (SDS) as an anionic surfactant. These chemical agents are common ingredients in commercial chemical cleaning solutions for organic and inorganic fouled membranes. Hydraulic and chemical cleaning was conducted for 10 minutes at ambient temperature. After chemical cleaning, the membrane was flushed with type II (deionized) water for 10 minutes to remove any residual agents and to measure pure water permeability.

All chemicals used were of reagent grade from Mallinckrodt (St. Louis, Missouri) and Fisher Scientific Inc. (Fairlawn, New Jersey).

5.3 Membrane Characteriziation

Membranes selected for this study are characterized as thin-film composite polyamide membranes and all are commercially available in the United States. The candidate membranes included one RO membrane: TFC-HR (Koch Membrane Systems); three ULPRO membranes: XLE (Dow/Filmtec), TFC-ULP (Koch) and TMG-10 (Toray America); and three NF membranes: NF-90 (Dow/Filmtec), TFC-S (Koch), and ESNA (Hydranautics). The RO and ULPRO membranes TFC-HR, TMG-10, TFC-ULP and XLE had MWCO below 100 Dalton and high salt rejection above 99 percent reported by the manufacturers. The NF membranes NF-90, TFC-S, and ESNA had a molecular weight cutoff (MWCO) of 200 Dalton with varying desalting degree from 90, 85, and 70 percent, respectively. The physical-chemical properties of the virgin (unused) membranes are summarized in table 1.

Table 1. Characterization of membrane properties

Membrane type	TFC-HR	XLE	TMG-10	TFC-ULP	TFC-S	NF-90	ESNA
Type	RO Koch	ULPRO Dow/ Filmtec	ULPRO Toray	ULPRO Koch	NF Koch	NF Dow/ Filmtec	NF Hydra-nautics
Salt rejection (manufacturer)	99.4%	99%	99.4%	99%	85%	90%	70%
pH range (long term)	4–11	4-11	2–11	4–11	4–11	4–11	3–10
Pure water permeability (liters per square meter per day) kilopascal [L/(m^2·day·kPa)] (25 °C)	0.84	2.16	2.20	1.95	2.64	2.49	1.05
Contact angle (degree)	35.0	66.3	54.5	38.0	57.4	63.2	57
Mean roughness (nm)	64	73	44	42	73	64	29

5.3.1 Pure Water Permeability Measurement

The pure water permeability of membranes was measured with type II water using a bench-scale cross flow flat sheet membrane unit (Sepa CF II, GE Osmonics, Minnetonka, Minnesota). It was calculated from the linear correlation of permeate flux and applied feed water pressure at 25 °C (77 °F).

5.3.2 Contact Angle Measurement

The wetting and adhesion properties of membranes were characterized by sessile drop contact angle measurement using an NRL contact angle Goniometer-Model 100-00 (Ramé-hart, Inc. Surface Science Instrument, Landing, New Jersey); 5.0 microliters (μL) of Milli-Q water (type I) droplets were applied on the specimen surface, and the contact angle was measured immediately after the droplet deposited on the membrane. To minimize the local interference from roughness and morphology of membrane surface, at least ten droplets were applied onto the membrane specimen and the contact angle was measured from both sides of the droplet.

5.3.3 Membrane Functionality

Functional group characteristics of membrane specimens were measured using a Nicolet Nexus 870 FTIR spectrometer (Nicolet, Madison, Wisconsin). Membrane specimens were placed in close contact with a zinc selenide (ZnSe) flat-plate crystal. Using a liquid-nitrogen-cooled mercury cadmium telluride (MCT) detector, the spectra were recorded by the attenuated total reflection (ATR) method with 500 scans and a wave number resolution of 2.0 cm^{-1}. Organic

compounds absorb the infrared radiation energy corresponding to the vibrational energy of atomic bonds. Based on the unique fingerprint of the absorption spectrum of a specific compound, the functional group can be identified through FTIR spectra. In this study, the system was used to determine the functional group characteristics of the membrane surface materials and membrane foulants according to the absorption band and wave number.

5.3.4 Membrane Surface Structure and Morphology

Membrane surface structure and morphology were imaged by an environmental scanning electron microscopy (ESEM) Quanta 600 (FEI Company). ESEM operates by scanning an electron probe across a membrane specimen; high-resolution electron micrographs of the specimen morphology can be obtained at very low or very high magnifications. Membrane specimens were cut into small pieces and attached to a carbon tape on an aluminum holder. The membranes were then coated with a thin layer of gold in a Hummer VI sputtering system (Technic Inc., Providence, Rhode Island). The plasma discharge current was 20 milliampere, and the chamber vacuum was adjusted to 50–100 millitorr. Sputtering time was approximately 2 minutes. The coated membrane samples were examined with ESEM at accelerating voltage of 20–30 kV, spot size of 2.0–2.5, and working distance of 15 mm.

Membrane roughness was measured by a digital instrument atomic force microscopy (AFM) mounted in MultiMode Scanning Probe Microscopy (Digital Instruments, Santa Barbara, California) in tapping mode. The membrane mean roughness (Ra) was calculated with the offline commands of the NanoScope III program, which represented the arithmetic average of the deviation from the center plane (equation 2).

$$Ra = \frac{\sum_{i=1}^{N} \left| Zi - Z_{cp} \right|}{N} \qquad (2)$$

Where Z_{cp} = Z value of the center plane

Zi = current Z value

N = the number of points within a given area

5.3.5 Elemental Composition

Elemental composition of virgin and fouled membrane specimens were qualified by the energy dispersive spectroscopy mounted in the ESEM. Prior to

EDS analysis, the membrane specimens were coated with a thin carbon layer by Denton DV-502 Vacuum Evaporator (Moorestown, New Jersey).

5.4 Carbon Aerogel Manufacture and Characterization

The carbon aerogel was manufactured by the CDT Systems, Inc. (Dallas, Texas) using a resorcinol/formaldehyde polymerization and pyrolization process. A carbon veil was soaked with a formaldehyde/resorcinol resin in a polypropylene mold. The polymerization process was completed in a temperature-controlled oven at 85 ºC for 48 hours. The sheets were removed from the molds and solvent-washed to eliminate any impurities and retained water. The air-dried polymerized sheets were then stacked in a furnace at 1,000 °C for 72 hours in a continuous nitrogen flow environment. After pyrolization, the carbon aerogel sheets were cut to desired size, stacked, and included as electrodes in a specially machined polypropylene housing. Each carbon aerogel pair was separated by conductive carbon spacers and a nonconductive glass fiber screen to prevent short-circuiting. The distance between each pair of carbon aerogel sheets was 2.3 mm (about 90 mil). A stack of carbon aerogel sheets, spacers, and their associated electrical bus connections were pressurized in a polypropylene housing. No epoxy was used to assemble the aquacell.

The carbon aerogel had average density of 0.78 grams per cubic centimeter (g/cm^3), bulk resistivity of 20 m·ohm·cm, and specific capacitance of 2 Farad/cm^2 (Welgemoed and Schutte, 2005). The BET surface area and pore size distribution were measured using a five-point nitrogen (N_2) gas adsorption technique (ASAP 2020; Micromeritics, Norcross, Georgia). The average pore size and pore size distribution were determined from desorption of N_2 according to a theory developed by Barrett, Joyner, and Halenda (BJH) (Barrett et al., 1951). Because the carbon aerogel material was very hydrophilic (with no measurable contact angle using sessile drop method), the samples were pretreated at 250 °C in a vacuum environment for 3 hours to remove adsorbed water and carbon dioxide (CO_2) gas prior to measurement. The carbon aerogel sheet samples were characterized to have an average BET surface area of 113 square meters per gram (m^2/g), a BJH desorption pore volume of 0.177 cm^3/g, and a BJH desorption average pore size of 4.28 nm. The incremental and cumulative pore area of the carbon aerogel as a function of the pore size are shown in figure 4. About 96.2 percent of the pores in carbon aerogel had sizes between 2.65 nm and 7.69 nm, and 41.8 percent of the pores had sizes between 3.0 nm and 3.4 nm.

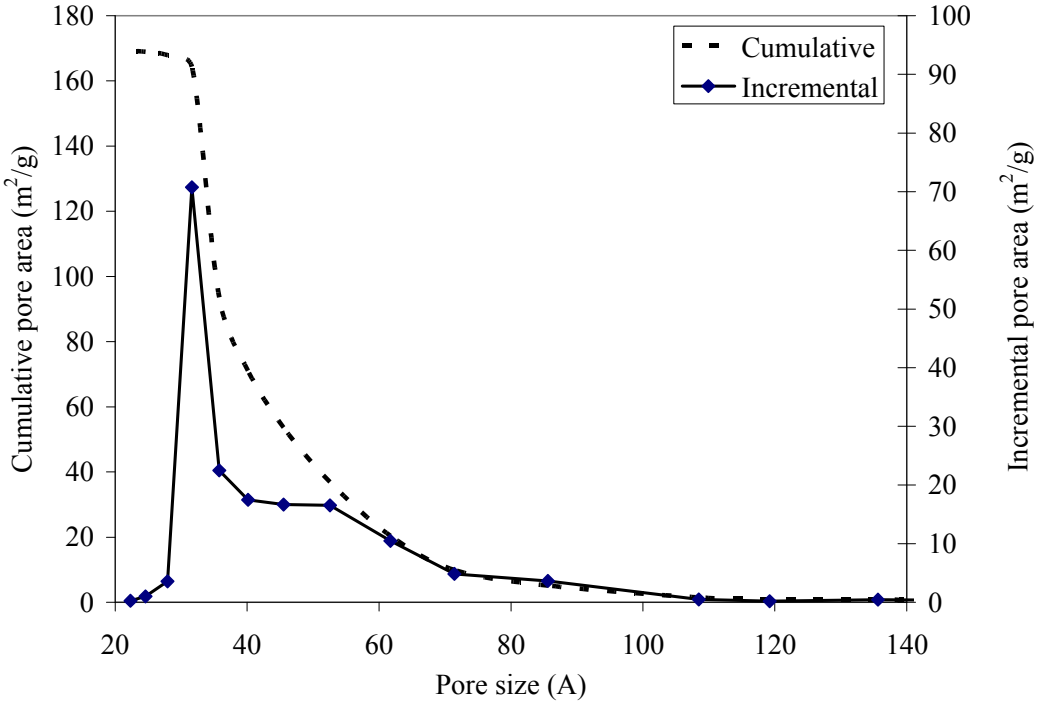

Figure 4. Pore size distribution of carbon aerogel.

5.5 Bench-Scale CDT Testing

The aquacells used in bench-scale testing were two model MK-13 units from CDT Systems, Inc. (Dallas, Texas). This model holds 1.3 liters (L) or 0.34 gallons of water and weighs 4 kilograms (kg) or 8.82 pounds (lb) dry. Each cell contains 24 sheets of carbon aerogel with about 650 grams (1.43 lb) of total aerogel. The dimensions of the sheet of MK-13 #34 AquaCell are 159 mm by 286 mm by 0.81 mm (6.25 inches by 11.25 inches by 32 mil), while the dimensions of the sheet of the MK-13 #36 AquaCell are 152 mm by 286 mm by 0.81 mm (6 inches by 11.25 inches by 32 mil).

Four pairs of graphite terminals provided connection to a power supply and measurement points to check the voltage during charging and discharging. The MK-13 #36 AquaCell was only used to test the fouling performance of produced water without addition of antiscalant solution.

The laboratory setup is shown in figure 5. Synthetic or produced water was fed into the cell by a ColeParmer Masterflex L/S pump (Barrington, Illinois). Prior to testing, the produced water fed to the units was processed through a 5 □m cartridge and a 0.45-µm filter bag (Cole-Parmer, Vernon Hills, Illinois). The required power to charge the aquacell was provided by a BK Precision 1746A DC

supply (Yorba Linda, California). The operating performance of the cells was tested at different conditions such as:

- Continuous flow mode (feed water flowing through the cell) or batch mode (product water flowing back to the feed tank for recycling).
- Different flow rate for regeneration and treatment.
- Regeneration using product water or raw water.

The effect of adding antiscalants on cell fouling was assessed using the antiscalant Hypersperse MDC700 from GE Betz (Trevose, Pennyslvania) at concentration of 3 mg/L.

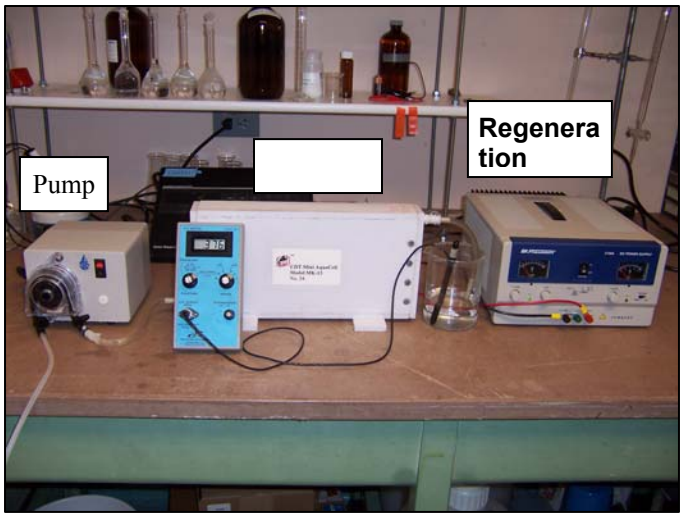

Figure 5. The CDT testing unit at CSM laboratory.

5.6 Laboratory-Scale Membrane Testing

A two-stage membrane laboratory-scale unit was employed for testing all membranes (figures 6 and 7). The membrane unit employed two single-element (4040 spiral-wound) vessels arranged in a two-stage array. A baffled stainless steel feed tank (200 liters [52.8 gallons]) was used to supply the feed water to the high-pressure pump (figure 6). For all two-stage membrane experiments, a feed water pH of 6.0-6.1 was maintained using HCl solution. Produced water used for feed water was 0.45-µm microfiltered prior to membrane experiments, and antiscalant solution was added to reach a concentration of 3 mg/L. During all two-stage membrane experiments, a vertical mixer and a tank recycle pump was used to ensure proper mixing. During operation, combined permeate and concentrate flows from the membrane unit were recycled to the stainless steel tank. The return lines were situated to maximize mixing and hydraulic retention time before returning to the system feed. A stainless steel cooling loop was used

to maintain a constant feed water temperature (about 22.5 °C [72.5 °F]) during membrane experiments.

Membrane performance was evaluated during two flow regimes: flow-through (FT) and internal-recycle (IR). For all two-stage membrane experiments, the overall feed flow was set around 34.1 liters per minute (L/min) or 9.0 gallons per minute (gpm). Flow-through mode simulates the recovery of a lead element in the first stage of a membrane treatment array, with a system recovery (percent of permeate flow rate to feed flow rate) of 15–23 percent total and a permeate flux of 0.48–0.79 cubic meters per square meter per day ($m^3/(m^2 \cdot d)$) or 12–19 gallon foot per square foot per day (gfd), that is, gallons of permeate produced per day divided by the area of membrane (ft^2).

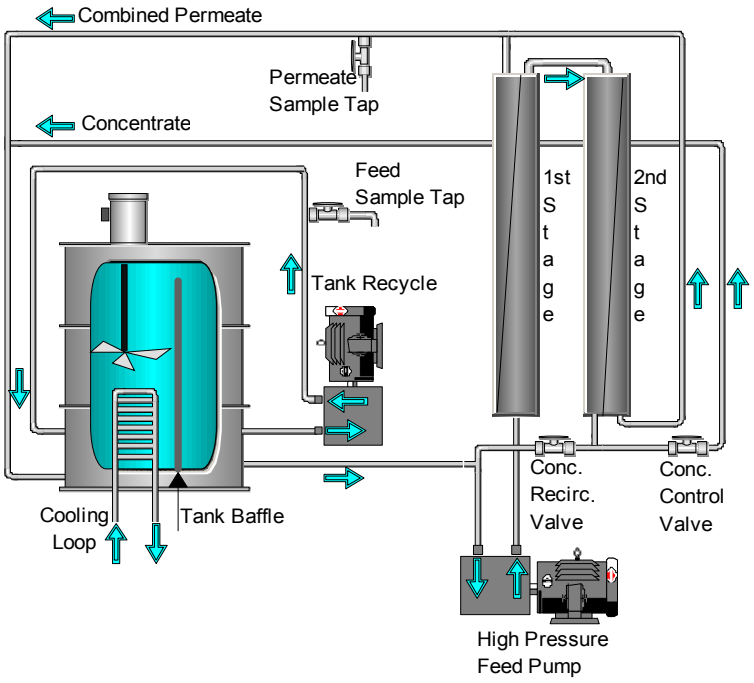

Figure 6. Schematic of the two-stage membrane testing unit using 4040 spiral-wound elements.

Figure 7. Setup of the two-stage membrane testing unit using 4040 spiral-wound elements.

During the internal-recycle mode, an internal concentrate recycle loop was used to simulate higher recoveries and bulk concentrations typically observed in the last stage of a full-scale membrane treatment array. When the internal-recycle valve was open, a portion of the combined concentrate flow was diverted to the pump inlet and the system feed flow became a combination of flow from the feed container and combined concentrate flow. By reducing the feed flow (herein raw water flow) from the feed container and maintaining the permeate flow similar to flow-through experiments, higher system recoveries could be simulated. During internal-recycle experiments, a system recovery of 50–69 percent was simulated, which resulted in a permeate flux of 0.22–0.53 $m^3/(m^2 \cdot d)$ or 5–13 gfd.

During membrane experiments, feed samples were withdrawn from the tank recycle line and permeate samples were taken from the permeate line before return to the feed tank. Membrane experiments were performed for 40 minutes in each flow regime before samples were taken for analysis. Throughout the experiments, feed flow, permeate flow, concentrate flow, feed conductivity, permeate conductivity, concentrate conductivity, feed pressure, and temperature were monitored over time to compare operational performance among candidate membranes.

In this study, the membranes were operated at different operating conditions. The rejection of a component of a feed solution is expressed as brine rejection value which is given as (3).

$$\text{Rejection (\%)} = (1 - \frac{C_p}{C_c}) \times 100 \qquad (3)$$

Where C_p = the permeate concentration

C_c = the concentrate concentration.

This value takes into account the increased concentration of a component during concentration polarization and offers a more useful comparison for two systems operated at different recoveries.

5.7 Commercial CDT Field Testing and Data Collection

The commercial CDT unit was constructed by CDT Systems Inc., in Dallas, Texas, and then transported to Havre, Montana, which is located 40 miles from the natural gas production site, and served as a base of operations during the field trial. In addition to the team from Colorado School of Mines, Paul Mendell of Mendell Energy and personnel from CDT Systems Inc., assisted in the field trial. The pilot-scale CDT cells were 10 times larger than the bench unit, containing 6.2 kg (13.67 lb) of aerogel each. Initial experiments were conducted using a single cell in order to determine the optimal flow rate through the CDT cells. The reduction in electrical conductivity (EC) achievable by connecting two cells in series was then determined. Water was initially delivered from the wellhead into feed water reservoir consisting of three 55-gallon (208-L) open drums in order to allow dissipation of methane gas prior to contact with the CDT cell and to serve as a pretreatment and short-term storage reservoir. The water was then pumped out of the reservoirs first through a 5.0-µm microfilter and then through the CDT cells to avoid contamination of the CDT cell with particles. (See flow schematic in figure 8.) After preliminary testing, the optimum treatment cycle was determined, which consisted of 80 minutes of treatment (ion removal) followed by 20 minutes of regeneration and then 10 minutes of purging prior to the next treatment stage. (See operating cycle in figure 9.) The CDT treatment unit was protected within a 10-foot by 10-foot tent. The cells were charged separately by two DC power sources at a voltage of 1.3V, with current varying from 15 to 260 amps. The exact voltage and amperage were recorded to determine power consumption. EC was measured in the influent and effluent from each cell using in-line electrodes, and EC data were logged by a laptop computer using a Labview program. (See photograph of the pilot system in figure 10.) In addition, influent and effluent samples were taken at 6-minute intervals and analyzed for iodide using an ion selective electrode and for pH, conductivity, and temperature using a conductivity meter. The samples were also shipped to the laboratory of Colorado School of Mines for further analysis including total

organic carbon (TOC), hardness, alkalinity, ultraviolet (UV) absorbance, cations, and anions.

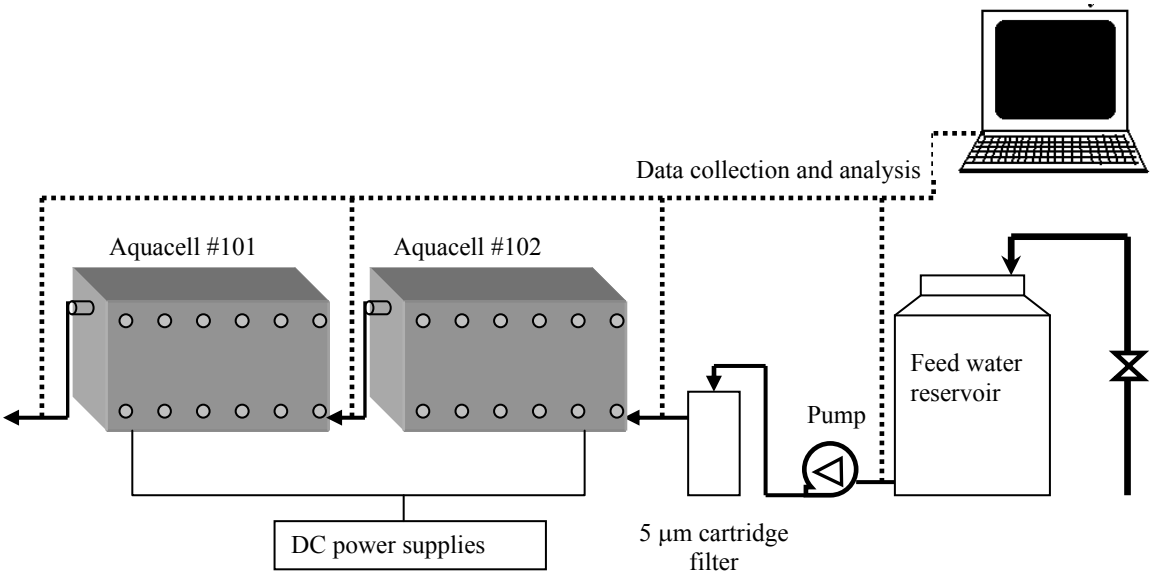

Figure 8. Flow schematic of CDT field test system.

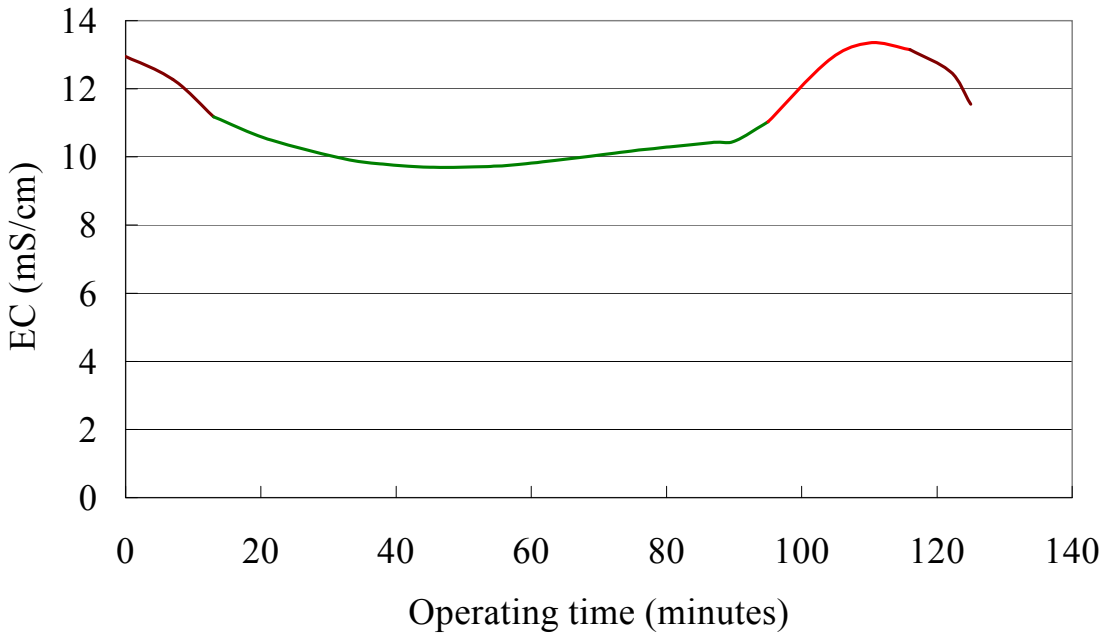

Figure 9. Operating cycle of CDT unit.

Figure 10. Field test site and equipment.

6. Analysis of Results and Commercial Viability of Projects

6.1 Water Quality Analysis

Except for hydrocarbon and BTEX analyses where composite samples were used, the results reported in table 2 represent average concentration of 22 grab samples (including 1 grab sample in 2002, 1 sample in 2003, and 19 samples over the 12 months of the project).

The water of the Jorgensen well was characterized as a brackish groundwater of sodium chloride type with a pH of 8.45±0.22. TDS concentration was quantified as 5,520±718 mg/L with a specific conductance of 10,510±9 34 µS/cm. Besides sodium and chloride, major constituents with concentrations of less than 100 mg/L were calcium, magnesium, bromide, and iodide. The well water was relatively rich in iodide with a concentration of 49.9±8.2 mg/L. The water was classified as hard (filtered water with total hardness of 124±23 mg/L as $CaCO_3$, and alkalinity of 235±20 mg/L as $CaCO_3$. Minor constituents with concentrations of less than 10 mg/L were aluminum, boron, barium, potassium, silicon, and strontium. No other inorganic constituents were detected in the well water above the detection limit of the analytical methods.

The dissolved organic carbon (DOC) concentration in the well water was 1.75±0.20 mg/L, and organics were characterized by moderate to high aromaticity (specific UV absorbance equals 4.0±0.45 liters per milligram per meter (L/mg m). Oil and grease were detected at low concentrations (1.0 and 0.4 mg/L) in the 2002 and 2003 samples, which might have been caused by contamination from piping and the pump used by the operating crew. Hydrocarbons and BTEX compounds, however, were not detected in the well water samples provided during the course of this study.

The radionuclides analysis indicated a very low level of radioactivity (combined Radium 226 and Radium 228 of 1.5 picocuries per liter (pCi/L) as compared to the criteria of maximum contaminant levels for radionuclides (combined Radium 226 and Radium 228 of 5.0 pCi/L) apply to all community water systems (CDPHE, 2004).

Although the water quality displays some variation, the minor difference in water samples should not affect membrane or CDT operation.

During silt density (SDI) measurement, even for a total elapsed time of 5 minutes, the t_f required to collect a final volume of 100 mL Jorgensen water was too long to calculate an appropriate SDI value. Therefore, SDI could not be used to

analyze the fouling tendency of the raw Jorgensen well water. Microfiltration must be employed as a pretreatment to avoid membrane fouling. Therefore, the well water sample was processed through a filtration device using a 5-μm cartridge and a 0.45-μm filter bag. The microfiltered water sample had an SDI of 19.2±0.1, which was still a very high value for membrane treatment. An SDI range of approximately 3 to 5 has been found to result in successful operation of spiral-wound RO membranes. The elevated value pointed to the fact that some precipitates would quickly build up at the membrane surface, resulting in a declining flux.

Table 2. Water quality of Jorgensen well sample

Analytes	Concentration		Method	Detection limit
	Average	Standard		
Physico-chemical				
Temperature[1]	10 °C	N.A	Std Methods 2550B	0.1 °C
pH	8.45	0.22	Std Methods 4500-HB	0.01
Conductivity	10,551 μS/cm	934 μS/cm	Std Methods 2510B	1 μS/cm
Total dissolved solids	5,520 mg/L	718 mg/L	Std Methods 2540C	1 mg/L
Total hardness	124 mg/L as $CaCO_3$	23 mg/L as $CaCO_3$	Std Methods 2320B	0.1 mg/L
Alkalinity	235 mg/L as $CaCO_3$	20 mg/L as $CaCO_3$	Std Methods 2320B	0.11 mg/L
Dissolved oxygen[2]	2.0 mg/L	N.A	Std Methods 4500 OG	0.1 mg/L
Inorganics - Cations				
Ag (Silver)	n.d.	n.d.	Std Methods 3120B	0.0035 mg/L
Al (Aluminum)	0.11 mg/L	0.21 mg/L	Std Methods 3120B	0.02 mg/L
As (Arsenic)	n.d.	n.d.	Std Methods 3114B	0.001 mg/L
B (Boron)	3.84 mg/L	0.25 mg/L	Std Methods 3120B	0.004 mg/L
Ba (Barium)	1.98 mg/L	0.47 mg/L	Std Methods 3120B	0.012 mg/L
Be (Beryllium)	n.d.	n.d.	Std Methods 3120B	0.0003 mg/L
Ca (Calcium)	29.50 mg/L	5.34 mg/L	Std Methods 3120B	0.011 mg/L
Cd (Cadmium)	n.d.	n.d.	Std Methods 3120B	0.002 mg/L
Co (Cobalt)	n.d.	n.d.	Std Methods 3120B	0.008 mg/L
Cr (Chromium)	n.d.	n.d.	Std Methods 3120B	0.005 mg/L
Cu (Copper)	n.d.	n.d.	Std Methods 3120B	0.002 mg/L
Fe (Iron)	n.d.	n.d.	Std Methods 3120B	0.002 mg/L
K (Potassium)	6.92 mg/L	1.11 mg/L	Std Methods 3120B	0.084 mg/L
Li (Lithium)	n.d.	n.d.	Std Methods 3120B	0.001 mg/L

Table 2. Water quality of Jorgensen well sample (continued)

Analytes	Concentration		Method	Detection limit
	Average	Standard		
Mg (Magnesium)	11.10 mg/L	1.88 mg/L	Std Methods 3120B	0.0002 mg/L
Mn (Manganese)	0.07 mg/L	0.03 mg/L	Std Methods 3120B	0.0007 mg/L
Mo (Molybdenium)	n.d.	n.d.	Std Methods 3120B	0.006 mg/L
Na (Sodium)	2250 mg/L	327 mg/L	Std Methods 3120B	0.02 mg/L
Ni (Nickel)	n.d.	n.d.	Std Methods 3120B	0.007 mg/L
P (Phosphorous)	n.d.	n.d.	Std Methods 3120B	0.062 mg/L
Pb (Lead)	n.d.	n.d.	Std Methods 3120B	0.023 mg/L
S (Sulfur)	n.d.	n.d.	Std Methods 3120B	0.05 mg/L
Sb (Antimony)	n.d.	n.d.	Std Methods 3120B	0.029 mg/L
Se (Selenium)	n.d.	n.d.	Std Methods 3114B	0.001 mg/L
Si (Silicon)	2.73 mg/L	0.61 mg/L	Std Methods 3120B	0.11 mg/L
Sn (Tin)	n.d.	n.d.	Std Methods 3120B	0.03 mg/L
Sr (Strontium)	2.11 mg/L	0.54 mg/L	Std Methods 3120B	0.0002 mg/L
Ti (Titanium)	n.d.	n.d.	Std Methods 3120B	0.0008 mg/L
V (Vanadium)	n.d.	n.d.	Std Methods 3120B	0.0013 mg/L
Zn (Zinc)	n.d.	n.d.	Std Methods 3120B	0.0023 mg/L
Cl^- (Chloride)	3,305.5 mg/L	853.6 mg/L	Std Methods 4110C	1.5 mg/L
Br^- (Bromide	51.3 mg/L	17 mg/L	Std Methods 4110C	1.0 mg/L
I^- (Iodide)	49.9 mg/L	8.2 mg/L	Ion selective probe	0.1 mg/L
F^- (Fluoride)	n.d.	n.d.	Std Methods 4110C	1.0 mg/L
NO_2^- (Nitrite)	n.d.	n.d.	Std Methods 4110C	1.5 mg/L
NO_3^- (Nitrate)	n.d.	n.d.	Std Methods 4110C	1.5 mg/L
SO_4^{2-} (Sulfate)	n.d.	n.d.	Std Methods 4110C	1.0 mg/L
PO_4^{3-} (o-Phosphate)	n.d.	n.d.	Std Methods 4110C	2.5 mg/L
Organics				
DOC (dissolved organic carbon)	1.75 mg/L	0.20 mg/L	Std Methods 5310C	0.06 mg/L
UV-254 absorbance	10.0 m^{-1}	4.3 m^{-1}	Std Methods 5910B	0.001 m^{-1}
Specific UV absorbance	4.0 L m^{-1} mg^{-1} [1]	0.45 m^{-1} mg^{-1}	Ratio between UV-254 and DOC	N/A
UV-272 absorbance	4.21 m^{-1}	0.26 m^{-1}	Std Methods 5910B	0.001 m^{-1}
Color (436 nm)	0.89 m^{-1}	0.55 m^{-1}	Std Methods 2120C	0.001 m^{-1}
Oil and grease	0.70 mg/L [3]	0.41 mg/L	Std Methods 5520C	0.02 mg/L
Hydrocarbons	n.d.	n.d.[4]	Std Methods 5520F	0.02 mg/L
BTEX				

Table 2. Water quality of Jorgensen well sample (continued)

Analytes	Concentration		Method	Detection limit
	Average	Standard		
Benzene	n.d.	N/A	Std Methods SW8021B	0.001 mg/L
Toluene	n.d.	N/A	Std Methods SW8021B	0.002 mg/L
Ethylbenzene	n.d.	N/A	Std Methods SW8021B	0.002 mg/L
m, p-Xylene	n.d.	N/A	Std Methods SW8021B	0.002 mg/L
o-Xylene	n.d.	N/A	Std Methods SW8021B	0.002 mg/L

n.d. – not detected
N/A – not available
[1] recorded onsite during sampling
[2] recorded upon arrival at CSM
[3] 0 mg/L and 0.4 mg/L of oil was detected in 2002 and 2003 water samples, respectively.
[4] detected by Std Methods E418.1. Detection limit: 0.1 mg/L.

6.2 Bench-Scale Membrane Selection Tests

6.2.1 Potential of Membrane Fouling During Produced Water Treatment

The SDI measurement indicated a serious fouling potential of the produced water without appropriate pretreatment. Based on the calculation of Langelier index for membrane treatment using the KOCH program ROPRO, the pH should be adjusted to below 6.5 to prevent $CaCO_3$ precipitation. Therefore, the produced water was microfiltered by a 0.45-μm filter bag and adjusted to pH 6.0–6.1 using HCl solution prior to treating by membrane. The effect of addition of antiscalants on permeate flux was assessed by bench-scale tests. The permeate flux decline of NF-90 and TMG-10 with and without addition of antiscalants is compared in figure 11. The addition of antiscalant solution resulted in significantly lower flux declines during produced water filtration for the tested membranes. As the flux decline stabilized after 48 hours with the addition of antiscalants (figure 12), the filtration time used to assess membrane performance was shortened to 75 hours in the study.

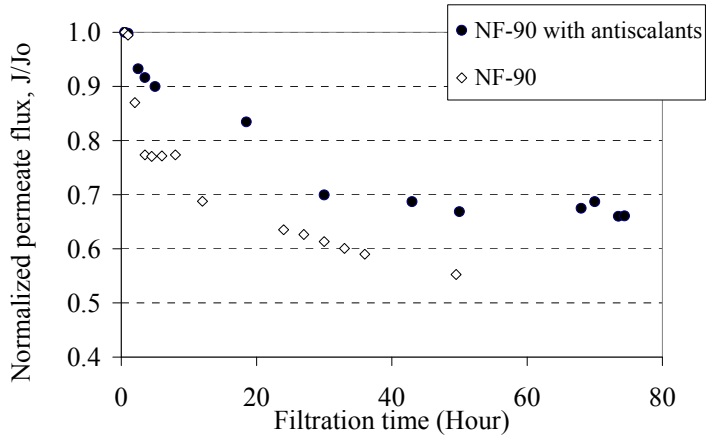

(a)

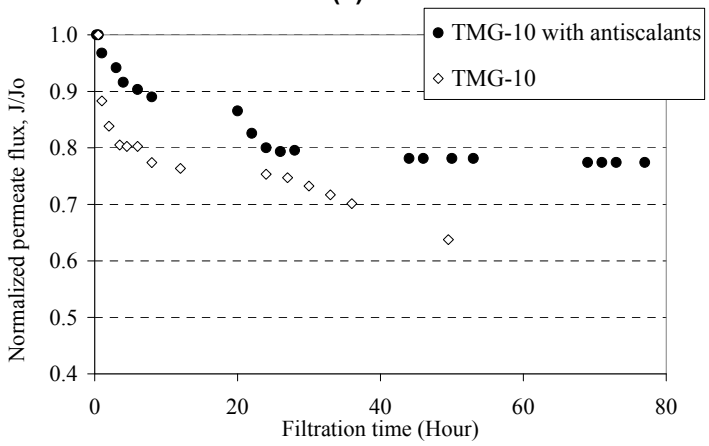

(b)

Figure 11. Reduction in permeate flux over time (a) NF-90 membrane and (b) TMG-10 membrane using 0.45-μm microfiltered produced water without and with addition of 3 mg/L antiscalants. Applied pressure 80 psi, pH 6.0, temperature 11 ± 1°C, initial recovery 0.18% (TMG-10) and 0.40% (NF-90).

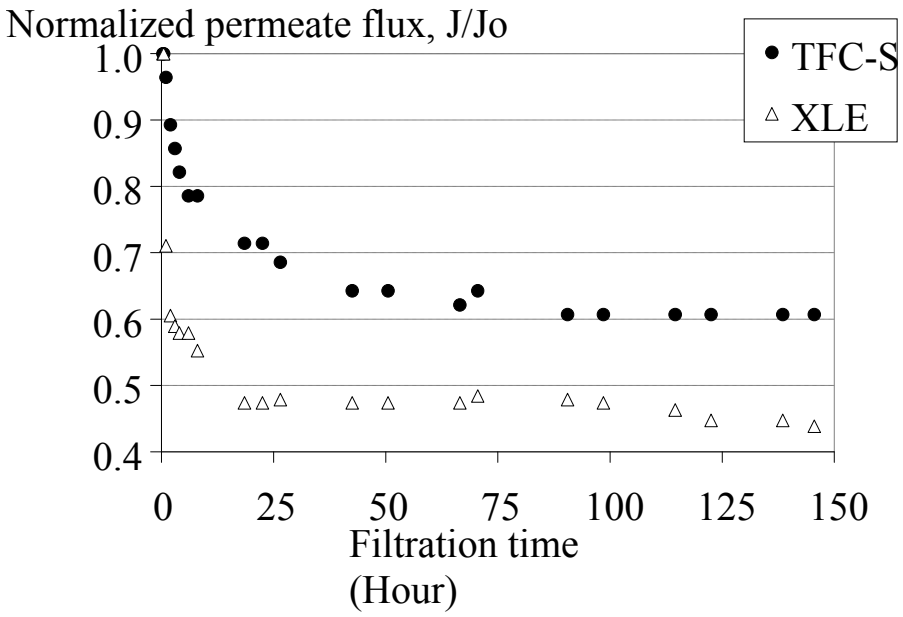

Figure 12. Reduction in permeate flux over time using 0.45-μm microfiltered produced water with addition of 3 mg/L antiscalants. Applied pressure 80 psi, pH 6.0, temperature 11±1°C, initial recovery 0.32% (TFC-S) and 0.38% (XLE).

The normalized permeate flux for all the studied membranes is shown in figure 13. The TFC-HR, TFC-ULP, TMG-10 and ESNA membranes exhibited a similar degree of fouling, resulting in a permeate flux decline of 23 percent over 75 hours. The NF-90 and TFC-S membranes showed more sensitivity to fouling in treating produced water with a permeate flux decline of 34 percent and 37 percent, respectively, over the course of the experiment. The XLE membrane was observed to have the highest sensitivity to fouling, with a permeate flux decline of 52 percent. All of the tested membranes exhibited an initial high permeate flux decline in 20 hours and reached stable flux conditions throughout the remainder of the experiments.

A comparison of the membranes during produced water treatment suggested that the flux decline was dependent on the hydrophobicity and roughness of the virgin membranes (figure 14). Hydrophilic and/or smooth membrane surfaces, such as TFC HR, TFC-ULP, ESNA, and TMG-10, exhibited a lower potential to interact with the inorganic and organic components in produced water, thus having a lower flux decline during filtration. Rough and hydrophobic membranes, such as XLE, TFC-S, and NF-90, showed a higher extent of flux decline over the course of filtration.

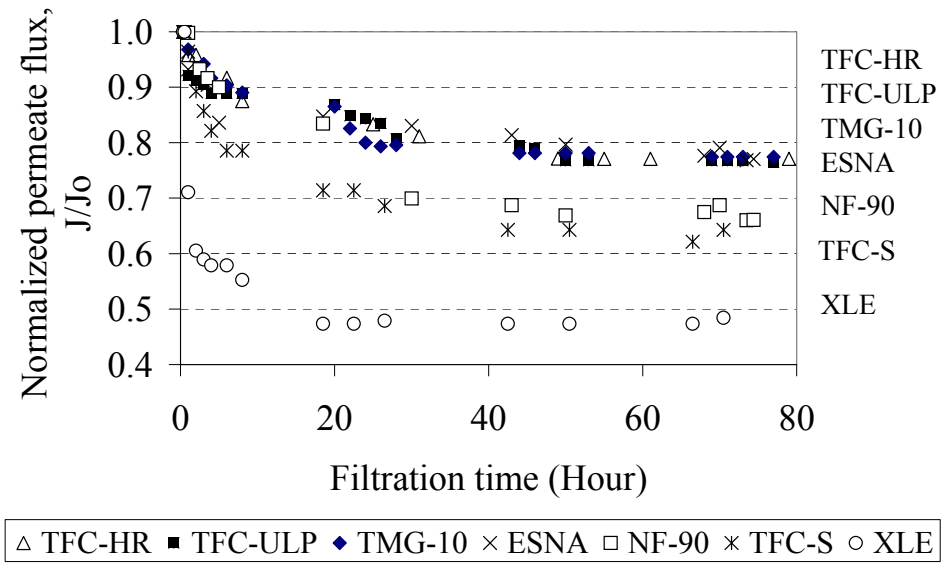

Figure 13. Reduction in permeate flux over time using 0.45-μm microfiltered produced water with addition of 3 mg/L antiscalants; applied pressure 80 psi, pH 6.0, temperature 11±1°C, initial recovery 0.14% (TFC-HR), 0.21% (TFC-ULP), 0.18% (TMG-10), 0.40% (NF-90), 0.32% (TFC-S), 0.38% (XLE), and 0.28% (ESNA).

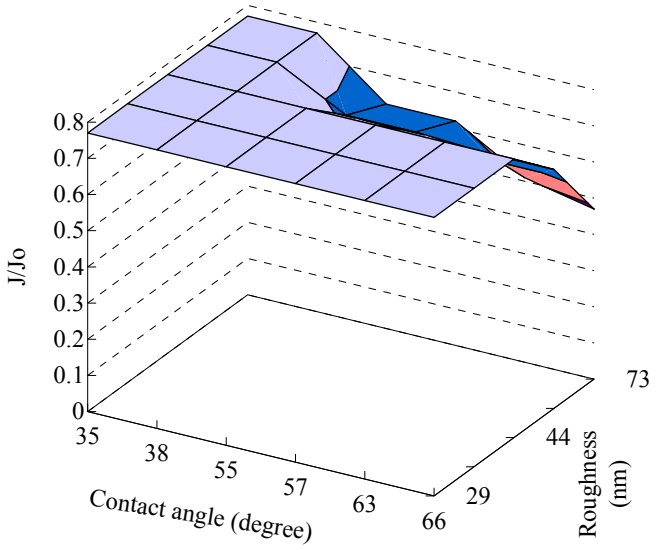

Figure 14. Correlation of normalized permeate flux/initial permeate flux (J/Jo) as a function of contact angle and surface roughness of virgin membranes.

6.2.2 Characterization of Membrane Fouling

The ESEM micrographs of the virgin NF-90 membrane specimen and NF-90 membranes fouled with and without addition of antiscalants are compared in figure 15. After 75 hours of filtration without addition of antiscalants, the NF-90 virgin membrane surface was completely covered by a gel-like fouling layer (figure 15(b)). With the addition of antiscalants, membrane fouling was significantly alleviated within the same filtration time. The ESEM graph supports that the ridge-valley surface of virgin membrane was only partially covered by the fouling layer (figure 15(c)). The ESEM micrographs of other membranes also indicated that the addition of antiscalants helped significantly in preventing precipitation of foulants on the membrane surface, and no significant foulants were observed on the membranes contacted with the produced water for 75 hours (figure 16).

The comparison of elemental composition of virgin and fouled NF-90 membrane specimens by EDS showed the presence of iron in the membrane fouled without addition of antiscalants (figure 17). With the addition of antiscalants, the EDS analysis detected no inorganic precipitation in the fouled membranes.

The functional groups of the virgin and fouled membranes were characterized by ATR-FTIR. All of the virgin and fouled membranes exhibited similar distinct and sharp absorption peaks, including the NF-90 membrane fouled without addition of antiscalants. (The spectra of NF-90 and XLE membranes are shown in figure 18.) Infrared light likely penetrated through the thin active layer (about 250 nm), resulting in detection of the polysulfone microporous support layer. Therefore, all the polyamide membranes exhibited almost the same ATR-FTIR spectra with indicative peaks at 1,650 cm-1 (amide groups), 1592 cm-1, and 1110 cm-1 (aromatic double bonded carbon), 1016 cm-1 (ester groups), 1,492 cm-1 (methyl groups), and at 1,151 cm-1 and 694 cm-1 (sulfone groups). As no additional functional groups were detected in the fouled membranes, it implied that organic fouling was not the major mechanism for the flux decline during produced water treatment.

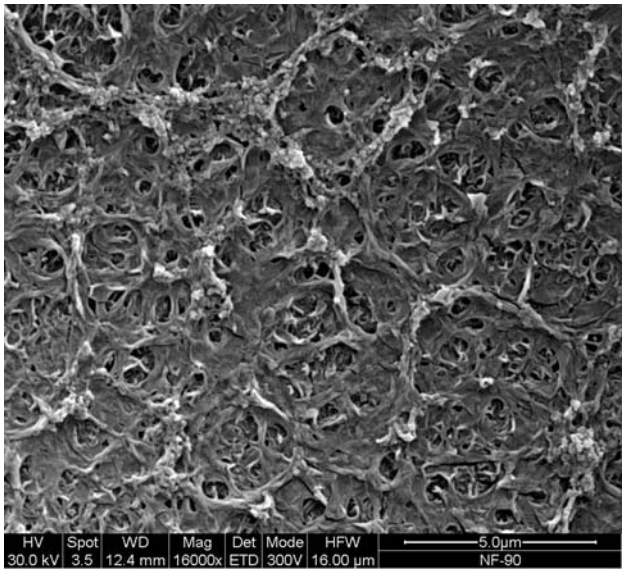

(a)

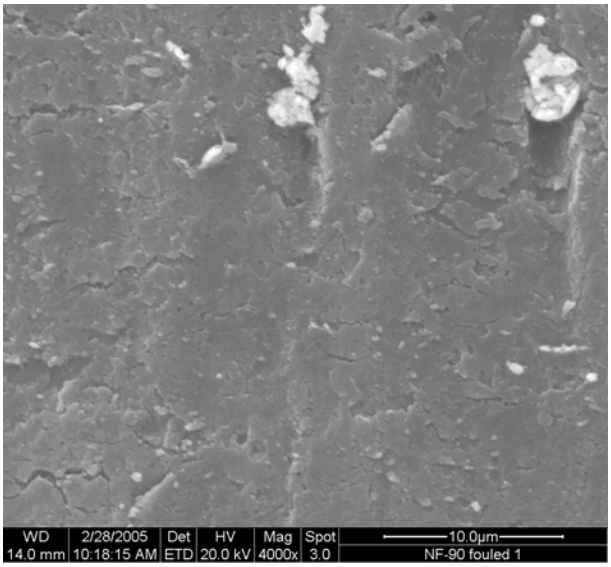

(b)

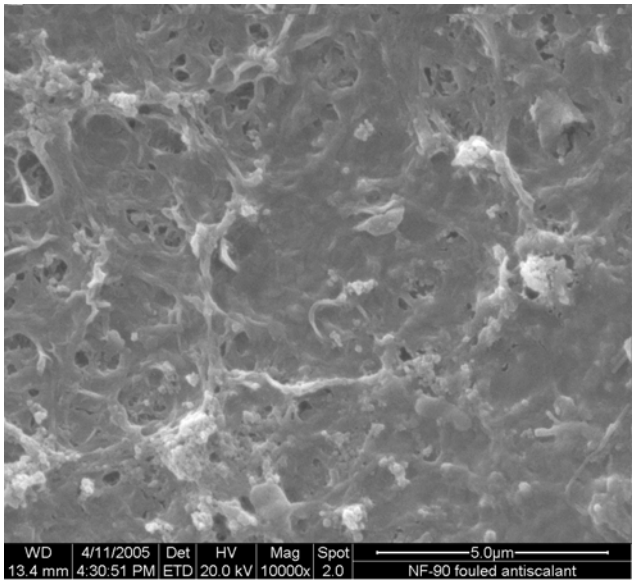

(c)

Figure 15. ESEM micrographs of (a) NF-90 virgin membrane, (b) NF-90 membranes fouled without antiscalants, and (c) NF-90 membranes fouled with antiscalants.

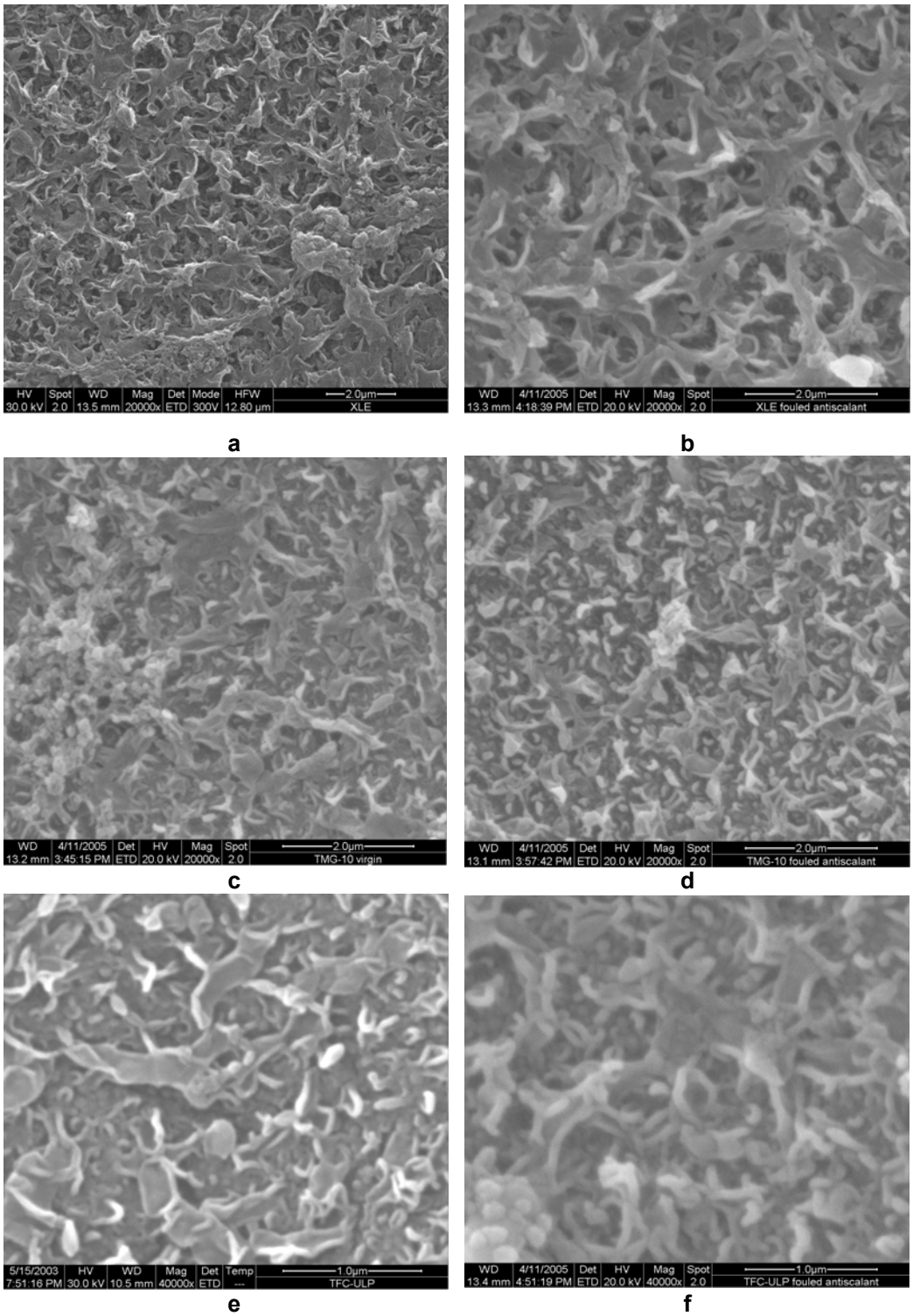

Figure 16. ESEM micrographs of virgin and fouled membranes with addition of antiscalants (a) XLE virgin (b) XLE fouled (c) TMG-10 virgin (d) TMG-10 fouled (e) TFC-ULP virgin (f) TFC-ULP fouled.

NF-90 fouled without antiscalant

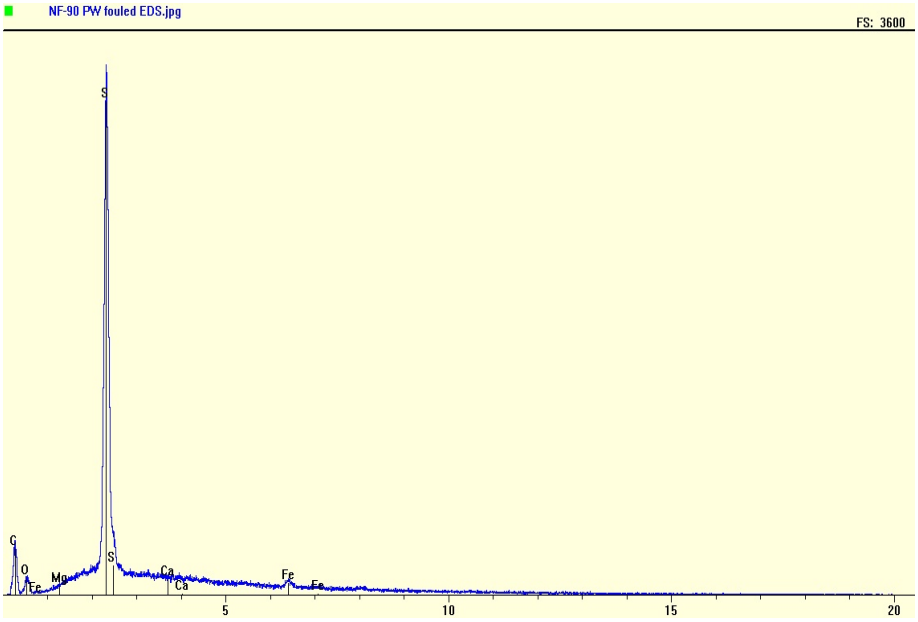

NF-90 fouled with antiscalant

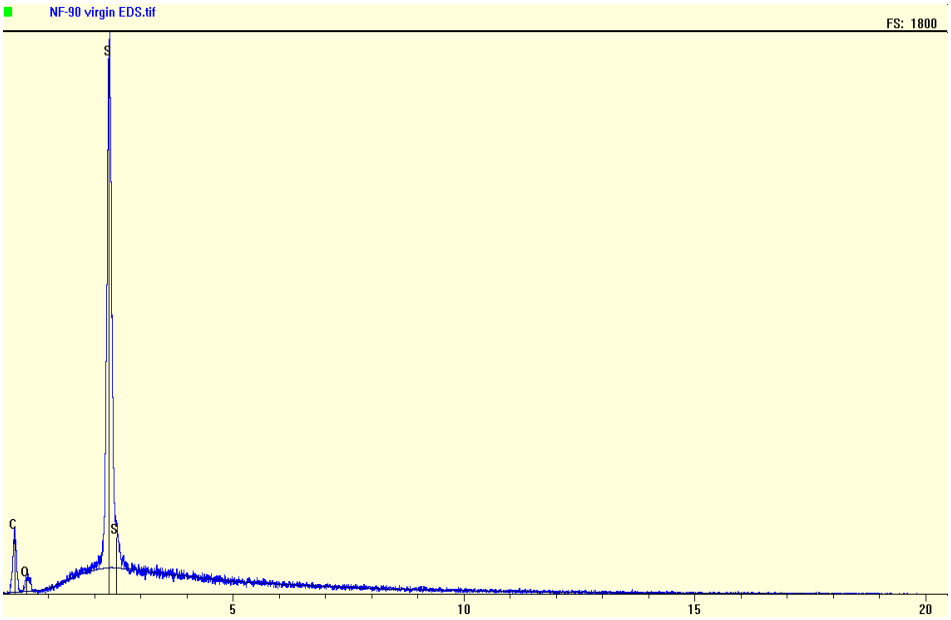

Figure 17. EDS spectra of NF-90 membrane specimens fouled with and without addition of antiscalants.

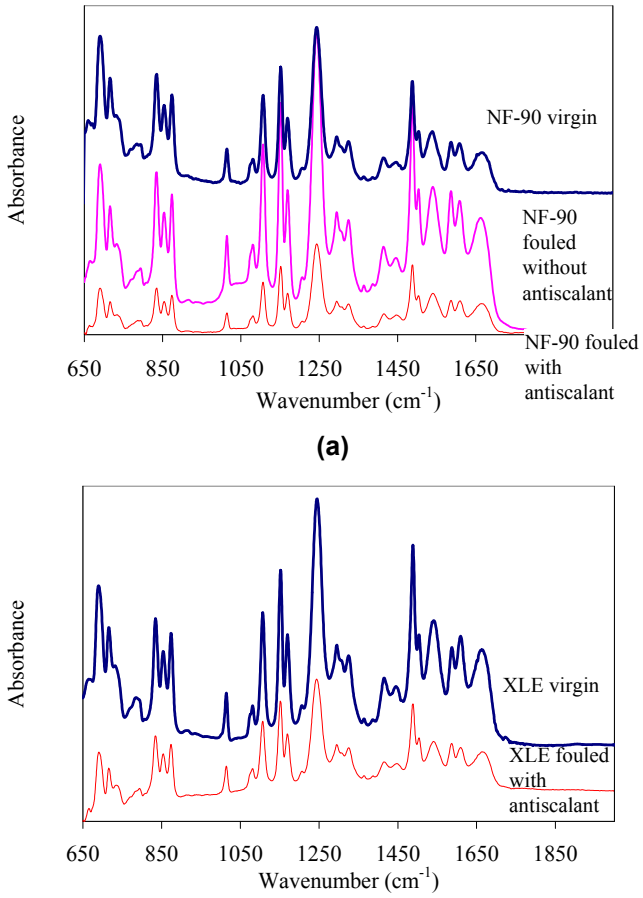

Figure 18. ATR-FTIR spectra of virgin and fouled membranes (a) NF-90 and (b) XLE.

6.2.3 Assessment of Cleaning Procedures

Different cleaning procedures were assessed to recover membrane permeate flux. Hydraulic and chemical cleaning were conducted for 10 minutes at ambient temperature. The cleaning was operated at low pressure (10 psi) with concentrate recycled back to the 10 liters of DI water or chemical cleaning solution. After chemical cleaning, the membrane was flushed with DI water for 10 minutes to remove any residual agents and to measure pure water permeability. For the membranes fouled without addition of antiscalant solution, periodic cleaning with hydraulic and a variety of chemical cleaning resulted in restoring a portion of the membrane permeability. (The variation of flux over time for TMG-10 membrane is shown in figure 19 as an example.) Cleaning by deionized water, hydrochloric acid, citric acid, and EDTA seemed less efficient in removing foulants than using NaOH and SDS solutions. The efficiency of the latter two agents and hydraulic cleaning was tested to clean the membranes fouled by produced water with addition of antiscalants. (The reduction of flux over time for NF-90 and TMG-10 membranes with the addition of antiscalants is shown in figure 20 as examples.)

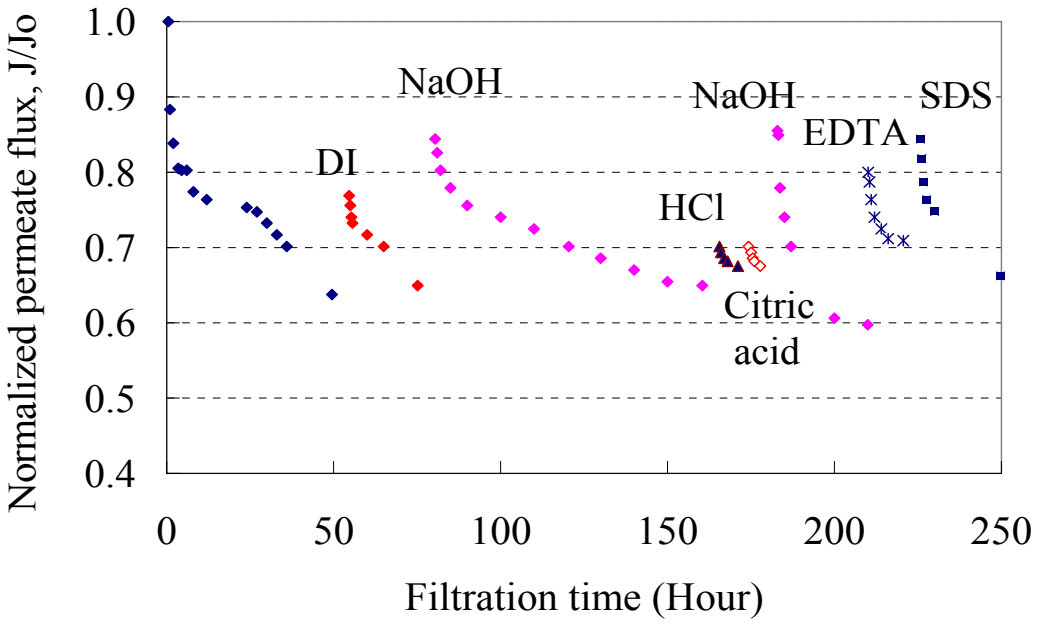

Figure 19. Permeate flux of TMG-10 membrane at different stages of fouling, hydraulic cleaning, and chemical cleaning procedures. Feedwater is 0.45-μm microfiltered produced water, applied pressure 80 psi, pH 6.0, temperature 11±1°C, initial recovery 0.18%. (a) flux after hydraulic cleaning; (b) flux after cleaning using 0.01M NaOH solution, pH 12.0; (c) flux after cleaning using 0.01M HCl solution, pH 2.1; (d) flux after cleaning using 0.01M citric acid, pH 2.6; (e) flux after cleaning using 0.01M NaOH solution, pH 12.0; (f) flux after cleaning using 0.01M EDTA solution, pH 4.6; (g) flux after cleaning using 0.01M SDS solution, pH 8.0.

Hydraulic cleaning using deionized water did not restore the membrane permeability for both NF-90 and TMG-10 membranes (figure 20). The chemical cleaning using NaOH and SDS solutions showed a high efficiency to restore the declined flux for the TMG-10 membrane, and the foulants appeared to be easily removed compared to those deposited without addition of antiscalants. The NF-90 fouled membrane, however, showed more resistance to chemical cleaning. Both caustic and surfactant cleanings could only restore 10 percent of the declined flux. The flux decline caused by the irreversible fouling on NF-90 membrane remained at 23 percent over the course of experiments.

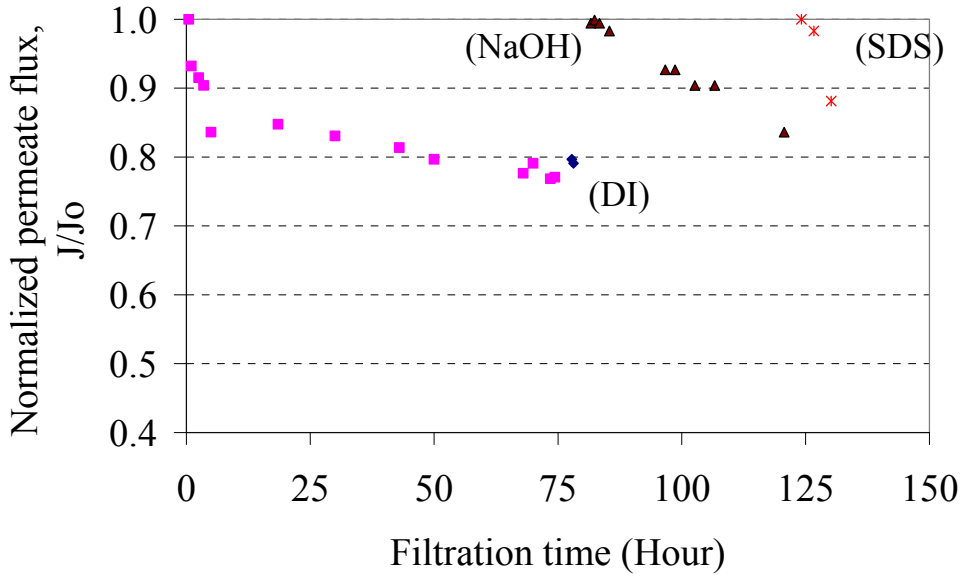

(a)

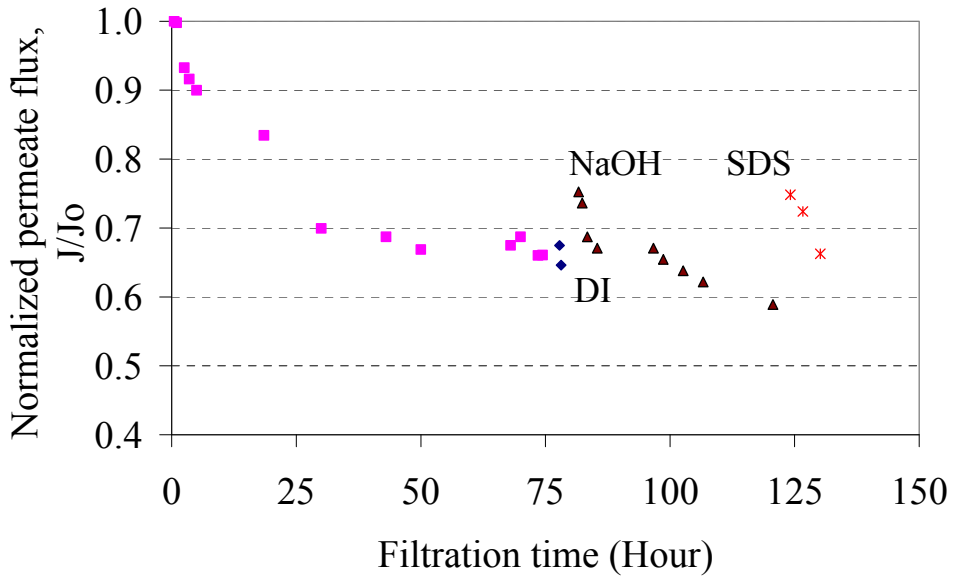

(b)

Figure 20. Permeate flux of (a) TMG-10 and (b) NF-90 membranes at different stages of fouling, hydraulic cleaning (with deionized water), and chemical cleaning procedures (with 0.01M NaOH solution, pH 12.0, and 0.01M SDS solution, pH 8.0). Feed water is 0.45-μm microfiltered produced water, applied pressure 80 psi, pH 6.0, temperature 11±1 °C, 3 mg/L antiscalants, initial recovery 0.18% (TMG-10) and 0.41% (NF-90).

6.2.4 Rejection Performance

The average rejection of iodide and bulk parameters by the tested membranes during operation is summarized in table 3. Rejection was stable during membrane filtration and not affected by fouling and cleaning over the course of the experiments. As an RO membrane, TFC-HR exhibited the highest rejection in terms of specific conductance and iodide above 91 percent and 92 percent, respectively. All tested membranes showed a low organic concentration in the permeate water samples.

Table 3. Rejection performance of the selected membranes using 0.45-μm microfiltered produced water at pH 6.0

Membrane		Rejection (%)			
		Conductivity	Iodide	TOC	UVA-254
RO	TFC-HR	91.4±0.0	92.4±0.0	80.4±3.4	87.2±0.3
ULPRO	TMG-10	78.0±1.5	87.6±0.6	79.1±4.7	87.2±3.8
	TFC-ULP	75.4±1.9	82.6±1.5	84.8±3.5	82.1±0.6
	XLE	73.1±1.7	80.1±0.8	84.3±5.6	80.8±1.3
NF	NF-90	72.7±5.4	78.3±1.3	87.6±0.6	63.8±2.1
	TFC-S	62.7±2.3	69.5±1.5	75.2±1.9	73.3±1.9
	ESNA	52.5±2.6	55.6±1.4	57.8±1.2	63.7±1.1

6.2.5 Membrane Selection

The selection criteria for evaluating candidate membranes included assessing operational performance as well as rejection of salt for beneficial water reuse and recovery of iodide. Operational performance was evaluated by considering both the specific flux and the flux decline measured during the filtration of produced water. The specific flux of nonfouled membranes related to operating pressure using the produced water and was considered the starting point for comparing membrane operational performance. The membrane-specific flux was measured at the beginning of the filtration tests using the produced water. The flux decline was related to increases in pressure needed to maintain desired recoveries with the occurrence of fouling. The flux decline was measured during the flat sheet fouling experiments and was used to correct the virgin membrane flux for potential fouling. These two terms were incorporated into a single term, termed "adjusted specific flux," in order to make a comparison among the candidate membranes. The adjusted specific flux is defined as the difference between the specific flux and the flux lost due to fouling (equation 4). Although the fouling experiments did not simulate actual filtration time or pressure conditions (75 hours and 80 psi) typical for full-scale systems, the membranes were tested

under the same conditions, and it is assumed that the measured flux decline is relative, allowing the use of this data for comparison of the target membranes.

Adjusted Specific Flux = Specific Flux*normalized permeate flux J/Jo (4)

The adjusted specific flux [L/(m^2•day•kPa)] of the candidate membranes ranks as: NF-90 (0.252) > ESNA (0.214) > TFC-ULP (0.191) > TFC-S (0.189) > TMG-10 (0.187) > XLE (0.168) > TFC-HR (0.090). The NF membranes NF-90 and ESNA displayed a high adjusted flux due to their large specific flux and low fouling potential. Although the XLE membrane showed a high initial specific flux, the adjusted flux was low as a result of membrane fouling. The RO membrane TFC-HR exhibited the lowest adjusted specific flux, as the initial specific flux was the smallest. The TFC-ULP, TFC-S, and TMG-10 membranes exhibited similar adjusted specific fluxes.

The candidate membranes are also ranked according to the rejection of salt and recovery of iodide as: the iodide and salt rejections by the ULPRO and NF membranes rank as TFC-HR > TMG-10 > TFC-ULP > XLE > NF-90 > TFC-S > ESNA.

In summary, based on the membrane performance with regard to adjusted specific flux and rejection of salt and iodide, THC-HR, TMG-10, TFC-ULP, and NF-90 membranes were selected for laboratory-scale testing using 4040 spiral-wound elements in a two-stage testing unit configured as a 1:1 array.

6.3 Laboratory-Scale Membrane Tests

6.3.1 Membrane Operation

The operational conditions for the four membranes employed during this study in both flow-through and internal-recycle flow regimes are summarized in table 4. Due to the high TDS concentration present in the Jorgenson well water, the feed pressure required to produce the desired membrane flux was relatively high (approximately 1,292–1,467 kPa (185-210 psi)) for NF and ULPRO membranes. The desired flux and recovery, however, were not tested for the conventional RO membrane (TFC-HR) since the maximum pressure rating of the membrane testing unit was exceeded.

Table 4. Membrane Experiment Operational Conditions

Flow Regime	Pressure (psi)	Feed Cond. (µS/cm)	Perm Cond. (µS/cm)	Conc. Cond (µS/cm)	Perm Flow (gpm)	Feed Flow (gpm)	Conc. Flow (gpm)	Recovery (%)	Flux (gfd)	Specific Flux (gfd/psi)	Cond. Rej. (%)
TFC-HR											
FT	200±0	11230±60	170±0	12330±0.05	1.3±0.01	8.80±0.17	7.51±0.16	14.7±0.2	11.8±0.1	0.06	98.50±0.03
IR	207.5±3.8	9990±90	980±160	27800±0	0.60±0.02	8.87±0.02	0.27±0.01	69.3±0.8	5.3±0.2	0.03	96.48±0.57
TFC-ULP											
FT	200±0	10650±60	276±5	13140±0.03	2.00±0.01	8.75±0.02	6.75±0.03	22.8±0.1	18.2±0.1	0.09	97.42±0.03
IR	195.7±1.9	10470±40	548±2	16880±0.12	1.46±0.03	8.93±0.04	1.48±0.01	49.8±0..3	12.8±0.2	0.07	96.75±0.02
TMG-10											
FT	180.0±0	10890±50	217±7	12660±0.04	2.15±0.21	8.47±0.04	6.66±0.03	21.4±0.1	16.5±0.1	0.09	98.0±0.1
IR	210±1.88	9750±90	525±21	22560±0.00	1.48±0.06	8.46±0.16	0.78±0.17	65.5±6.3	11.3±0.5	0.06	97.7±0.1
NF-90											
FT	185.7±9.8	11430±80	700±30	13810±0	2.15±0.21	9.2±0.03	7.05±0.23	23.4±2.4	18.9±1.9	0.1	93.85±0.28
IR	210±1.0	11100±270	1650±330	14590±0	1.48±0.06	9.36±0.19	2.76±1.30	68.3±0.1	13.0±0.5	0.07	88.70±2.25

Of the membranes tested during flow-through experiments (15–23 percent recovery), the TFC-HR required the highest feed pressure of 1,397 kPa (200 psi) and displayed the lowest specific permeate flux value of 0.34 L/(m^2·day·kPa) (i.e., 0.06 gfd/psi). The NF-90 had a significantly higher specific flux of 0.59 L/(m^2·day·kPa) (i.e., 0.1 gfd/psi) while operating at a similar pressure as the TMG10 between 1,260 and 1,290 kPa (180 to 185 psi). The two ULPRO membranes TFC-ULP and TMG10 provided a similar specific flux 0.53 L/(m^2·day·kPa) (0.09 gfd/psi) while the TMG10 operated at a lower pressure than the TFC-HR and the TFC-ULP. In the internal-recycle regime, the specific flux was much lower than in the flow-through regime, simulating low recoveries due to the high osmotic pressure as a result of higher feed concentrations. The operating performance of the tested membranes during simulation of higher recoveries followed a similar trend as observed during the flow-through regime (table 4). The TFC-ULP exhibited a higher specific flux and lower pressure than the TMG10, due to the lower recovery of the TFC-ULP (50 percent versus 69 percent of the TMG10).

As an RO membrane, the TFC-HR exhibited the greatest salt rejection (96.5–98.6 percent) followed by TMG10 (97.7-98.3 percent) and TFC-ULP (96.8–97.9 percent). The NF-90, however, displayed the lowest salt rejection (85.3–94.9 percent). The tested membranes all displayed higher rejection in terms of conductivity at low recovery during flow-through experiments than at high recovery during internal-recycle (table 4).

6.3.2 Rejection Performance

During membrane experiments in flow-through and internal-recycle flow regimes, samples were collected for TOC, iodide, UV absorbance, cation, and anion analyses. The concentrations in feed, permeate, and concentrate streams are summarized in the appendix. The rejections for select constituents above the detection limits and at relatively high concentrations are shown in figure 21.

For flow-through regime, rejection was calculated using the feed and permeate concentration, i.e., rejection (%) = (1-permeate concentration/feed concentration)*100. For internal-recycle regime, rejection was calculated using the concentration of the constituent in the concentrate flow of membrane, since this value was more indicative of the concentration at the membrane surface.

TOC concentration in permeate streams was below 200 µg/L for all four membranes at different recoveries, with the TFC-ULP and TMG-10 exhibiting slightly higher rejection of TOC than TFC-HR and NF-90 (figure 21). The rejection of aromatic organics in terms of UV absorbance at 254 nm, however, was higher by TFC-HR than other three membranes during flow-through and internal-recycle experiments (figure 21).

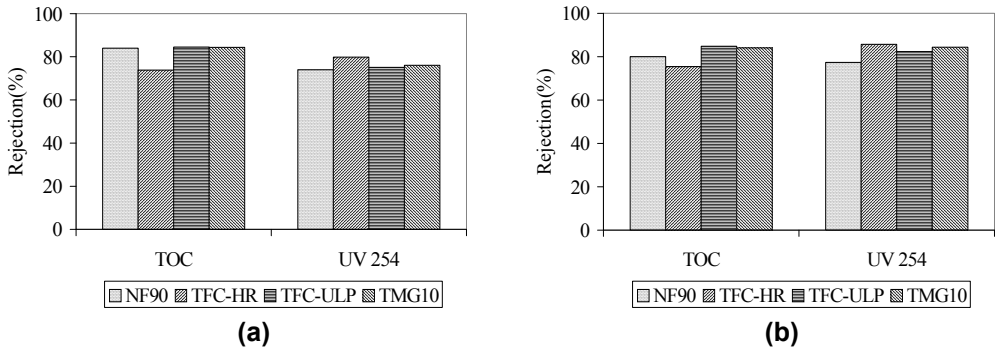

Figure 21. Rejection of TOC and aromatic substances (in terms of UV absorbance at 254 nm) in (a) FT and (b) IR flow regimes.

The divalent cations, such as Ba, Ca, and Mg, exhibited very high rejection by the tested membranes, above 99.3, 98.5, 99.5, and 99.5 percent by the TFC-HR, NF-90, TFC-ULP, and TMG-10, respectively, during flow-through and internal-recycle regimes (figure 22). Silica was also well rejected, with rejection above 96.6, 96.2, 98.1, and 98.3 percent by the TFC-HR, NF-90, TFC-ULP, and TMG-10, respectively, during flow-through and internal-recycle regimes. The TFC-HR, TFC-ULP, and TMG-10 observed a higher rejection of sodium than the NF-90 (>96.0 percent vs. 91.1–93.3 percent), during flow-through and internal-recycle regimes. Boron showed the lowest rejection among the detected components for all the tested membranes: 36.0–58.4 percent during flow-through regime and 30.4–55.6 percent during internal recycling regime.

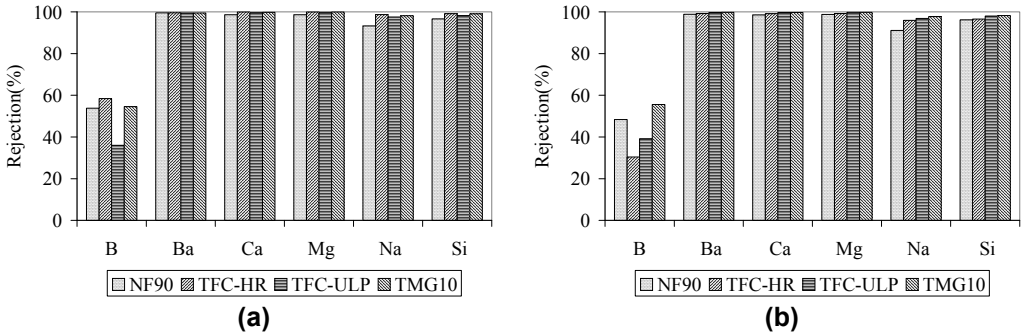

Figure 22. Rejection of boron, barium, calcium, magnesium, sodium and silicon in (a) FT and (b) IR flow regimes.

Iodide exhibited a much lower rejection (62.7–82.6 percent) by the four membranes compared to chloride (93.1–99.6 percent) and bromide (90.7–100 percent), while the NF-90 exhibited the lowest rejection among the tested membranes (figure 23).

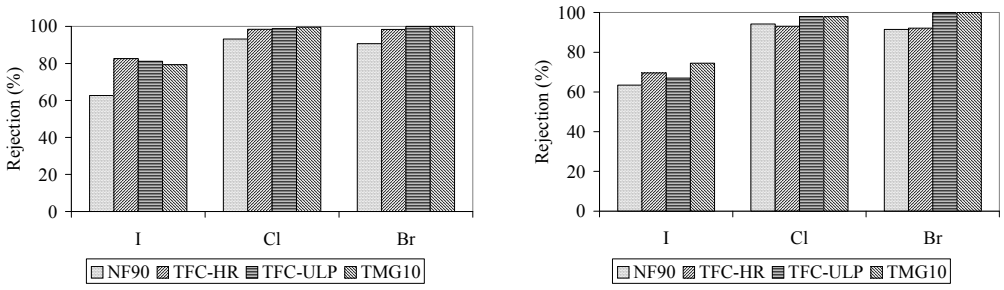

Figure 23. Rejection of chloride, bromide, and iodide in (a) FT and (b) IR flow regimes.

6.3.3 Membrane Product Water Quality

A potential beneficial use of membrane-treated produced water is to augment potable water sources. Table 5 compares the key constituents of interest in membrane product water with U.S. Environmental Protection Agency's (EPA) National Primary and Secondary Drinking Water Regulations (primary standards and secondary standards). The constituents not listed in the table are those concentrations in the produced water below the detection limit or the drinking water standards. No trace pollutants of concern (such as arsenic, selenium, etc.) were detected in membrane-treated water. The product water quality listed in table 5 is the average value of permeates from flow-through and internal-recycle regimes simulating a composite final product quality.

Table 5. Comparison of membrane final product water with water standards

Contaminant	Primary MCLs	Secondary MCLs	Average concentration (mg/L)			
			TFC-HR	TFC-ULP	TMG10	NF-90
Barium	2 mg/L		0.01	0.03	0.01	0.02
Boron			2.5	1.9	1.9	2.6
Bromide			7.0	1.2	1.4	14.0
Chloride		250 mg/L	190	74	78	372
Iodide			14.9	16.6	17.0	22.9
TDS		500 mg/L	325	176	172	566
TOC			0.13	0.20	0.20	0.08

The quality of the final product water from the RO and ULPRO membranes can meet EPA primary and secondary drinking water standards. The permeate of the NF-90 could not meet EPA secondary standards for chloride and TDS.

Boron is another concern for applying treated produced water for beneficial use. On February 23, 2005, EPA included boron in the second Drinking Water

Contaminant Candidate List (CCL). Due to possible, despite controversial and inconclusive, toxic effects that impair growth in animals and cause nerve damage, the European Union regulates a 1 mg/L value for boron in the *Drinking Water Directive* (Weinthal et al., 2005). In 1993, the World Health Association (WHO) guidelines for drinking water quality proposed a 0.3 mg/L (later revised to 0.5 mg/L) standard for boron, while the United Kingdom had a standard of 2 mg/L for drinking water.

Boron is a naturally occurring element, usually prevalent in seawater and brackish ground water. The maximum concentration found in 1,546 samples of river and lake waters from various parts of the United States was 5.0 mg/L; the mean value was 0.1 mg/L (EPA, 1986). Ground waters could contain substantially higher concentrations at certain places. The concentration in seawater is reported as 4–5 mg/L. Although boron is an essential element for growth of plants, sensitive crops have shown toxic effects at 1.0 mg/L or less of boron. While the criterion of 750 μg/L is thought to protect sensitive crops such as citrus during long-term irrigation (EPA, 1986), most grasses are relatively tolerant at 2.0 to 10 mg/L of boron (Rowe and Abdel-Magid, 1995).

Boron often exists in the form of boric acid in aqueous solutions, which is a weak acid with a pKa of 9.2. Within the experimental pH range (6.0–6.1), boric acid exists primarily as the undissociated state (H_3BO_3), which resulted in the low rejection by RO and NF membranes. In this study, feed water concentration of boron was 3.84 mg/L and all the tested membrane exhibited a low rejection with the boron concentration of 1.9–2.5 mg/L in the final product water. Several options are available to achieve additional boron removal from the RO/NF product water.

1. Increasing pH to above 9.5 (optimal at 10.5), boron can be effectively removed by most thin-film composite membranes. Membrane scaling, however, will be severe, and frequent acid cleaning will be required, which will increase membrane operating cost and shorten membrane life time.
2. Two-pass membrane system. The permeate from the first membrane system flows into the second system with or without pH adjustment to remove boron. Membrane scaling associated with high pH operation is avoided and the operating pressure is low due to purer feed water quality. Currently, this is the most common practice to meet boron water quality specifications (Kabay et al., 2004; Nadav, 1999, Pastor et al., 2001, Wilf and Bartels, 2005).
3. Using new commercial RO membranes that are effective for boron removal, such as Hydranautics SWC4 RO membrane. These membranes can meet the WHO requirement in a single pass, but these are generally very tight membranes and reject boron by size exclusion (Redondo et al.,

2003; Taniguchi et al., 2004). Membranes are operated at very high pressure, and scaling is an issue due to concentration polarization effects. Moreover, these techniques have not yet been adequately developed at the present time and will result in additional cost.

4. Using post-treatment by ion-exchange resin, which is reported to be expensive (Bick and Oron, 2005).

5. Blending with other water with low boron concentration.

Bromide and iodide are also of concern as the primary precursors to the formation of disinfection byproducts (DBPs) in drinking water. Although not regulated individually, CALFED, the California State and Federal coalition that governs California Bay-Delta water use, has the goal of achieving an average TOC concentration of 3 mg/L and bromide concentration of 50 µg/L or equivalent level of public health protection in its Drinking Water Quality Program. Despite the relatively high concentration of bromide and iodide in the final product water (1.2–14 mg/L and 15–23 mg/L, respectively), the formation of DBPs is not problematic due to the low concentration of TOC (<200 µg/L). The effective removal of TOC by the RO and NF membranes significantly reduced the potential formation of DBPs.

The potential application of the membrane-treated water for agricultural irrigation needs to consider the TDS level of the product water and the concentration of sodium, calcium, and magnesium ions. All of the tested membranes were capable of achieving an acceptable TDS concentration for irrigation (1,000 mg/L TDS). However, due to the greater rejection of divalent ions than mono-valent ions, the final product water after membranes treatment displayed a high sodium to calcium and magnesium ratio. High sodium concentrations not only reduce the clay-bearing soil's permeability but also affect the soil structure. To estimate the degree to which sodium will be adsorbed by a soil from a given water, the sodium adsorption ratio (SAR) has been developed (5).

$$SAR = \frac{Na^{+}(meq/L)}{\sqrt{\frac{(Ca^{2+} + Mg^{2+})(meq/L)}{2}}} \qquad (5)$$

For sensitive fruits, the tolerance limit of SAR value for irrigation water is about 4. For general crops, a limit of 8 to 18 is generally considered within a usable range (Rowe and Abdel-Magid, 1995). Therefore, without addition of calcium, the membrane permeates would not be suitable for crop irrigation. Due to the low TDS of the product water, addition of a calcium source (e.g., calcium carbonate, gypsum, calcium chloride) can decrease SAR effectively. Compared to calcium carbonate and gypsum, the addition of calcium chloride will result in higher

concentrations of soluble calcium and should be the most effective way to lower irrigation water SAR. However, calcium chloride is considerably more expensive than calcium carbonate and calcium sulfate (gypsum).

6.4 Bench-Scale CDT Tests

As an emerging desalination technology, capacitive deionization needs substantial effort in investigating desalination efficacy and optimizing operation performance. Bench-scale experiments were focused on understanding and optimization of CDT performance with regard to desalting efficiency, operational modes, fouling behavior of electrodes and regeneration effectiveness during the treatment of synthetic solutions and produced water from the Jorgensen well.

6.4.1 The Effect of Flow Rate and Initial NaCl Concentration on NaCl Removal Rate in Continuous Flow Mode

Synthetic solutions were prepared at 265, 500, and 1,000 mg/L NaCl using Milli-Q water (type I). The flow was set at 50 or 250 mL/min (19 or 95 gallons per day [gpd]). The cell was first equilibrated with the feed water by flushing the cell at the prescribed flow rate until the effluent electrical conductivity was equal to the EC of the influent. Once equilibration was achieved, a voltage of 1.30V was applied to the cell and the effluent collected in 5 minute intervals for EC measurement. In these early experiments, the cell was discharged by connecting a shorting wire until the voltage difference between opposite terminals was less than 0.10V, usually requiring 45 minutes to 1 hour. The cell was then thoroughly rinsed with the feed water for the next experiment to remove salts released during regeneration. When initiating a new test, the polarity of the electrodes was reversed. For each combination of initial NaCl concentration and flow rate studied, the rate of NaCl retention during the first hour was calculated by a mass balance equation (6):

$$\text{mg NaCl retained} = \sum Q\Delta t \{(EC_i - EC_t)/EC_i\}[NaCl]_I \quad (6)$$

Where:

Q = the flow rate (L/min)

Δt = the time increment (5 minutes)

EC_i = the electrical conductivity of the influent (µS/cm)

EC_t = the EC for the specific time interval (µS/cm)

$[NaCl]_I$ = the concentration of NaCl in the influent (mg/L).

An example of the results obtained for continuous flow experiments at low-to-moderate NaCl concentrations is shown in figure 24 for a flow rate of 250 mL/min and initial NaCl concentration of 500 mg/L. The rate of retention of NaCl was calculated based on data collected during the first hour of treatment. Duplicate treatments of 265 mg/L NaCl produced a minimum EC in the effluent of 364 and 376 µS/cm (table 6). Doubling the concentration of NaCl doubled the retention rate. Increasing the flow rate from 50 mL/min (19 gpd) to 250 mL/min (95 gpd) also resulted in a five-fold increase in retention rate. Increasing flow rate from 50 to 250 mL/min at a concentration of NaCl of 500 mg/L resulted in approximately the same minimum EC in the effluent (table 6). Based on these results, a flow rate of 250 mL/min was used for all subsequent experiments.

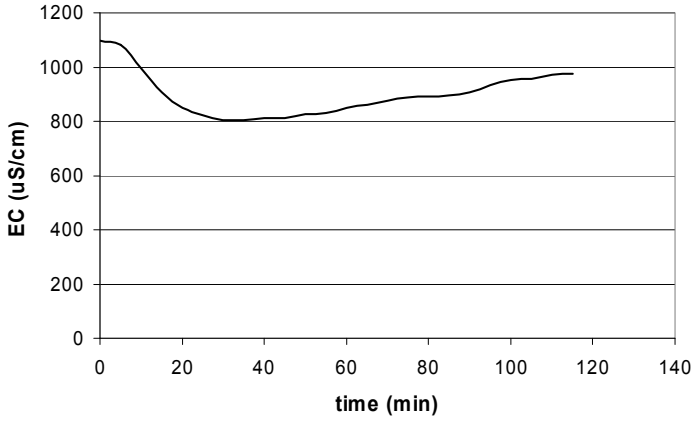

Figure 24. EC of CDT effluent during treatment of 500 mg/L NaCl at a flow rate of 250 mL/min.

Table 6. Dependence of NaCl removal rate on NaCl concentration and flow rate in continuous flow mode

Flow rate mL/min	NaCl mg/L	Feed EC µS/cm	Minimum EC µS/cm	Retention rate mg NaCl/ (g aerogel·min)
50	265	520	376	0.0045
50	265	512	364	0.0042
50	500	1,030	728	0.0080
250	500	1,090	805	0.0395
250	1,000	1,930	1,447	0.0677

6.4.2 Comparison of Removal of NaCl in Batch Mode

To assess the efficiency of NaCl removal in batch mode, feed water with a concentration of 500, 1,000, or 2,000 mg/L NaCl was prepared. Two liters of

each solution were pumped through the cell MK-13 #34 at a flow rate of 250 mL/min in batch mode. The EC was measured in 5-minute intervals, and the total amount of NaCl adsorbed per gram of aerogel was calculated based on the final EC observed.

The final EC obtained for treated water in batch mode (table 7) was significantly less than for continuous flow mode (table 6). This is due to the repeated treatment of the same limited volume of water in batch mode. Batch experiments provided a simple and accurate method for determining adsorption capacity. The highest value observed for adsorption capacity was 6.98 mg NaCl/g aerogel (table 7), for a 3 hour treatment period.

Table 7. Removal of NaCl from 2.0 L of batch water in batch (recycling) experiments at a flow rate of 250 mL/min

NaCl (mg/L)	Feed EC (µS/cm)	Final EC (µS/cm)	Total NaCl adsorbed mg NaCl/g aerogel	Time of treatment (minutes)
500	1,045	79	2.42	200
1,000	1,888	294	3.69	110
2,000	4003	976	6.98	170

6.4.3 Retention and Recovery of NaCl for a Regeneration Time Period of 1 Hour vs. 16 Hours

The experiments were initiated after the cell MK-13 #34 had been unused for a period of at least 16 hours, and then thoroughly equilibrated with feed water in order to minimize the influence of previous charge cycles on ion removal. NaCl solutions were prepared at concentrations of 2,000 and 5,000 mg/L. The cell was pre-charged for 10 minutes with the pump off. The treatment stage consisted of 1 hour at an applied voltage of 1.30V and a flow rate of 250 mL/minute. A total of 15 L of water was treated for each concentration. The 1-hour regeneration was accomplished by applying reverse polarity for 15–18 minutes to discharge the cell, with 2.0 L of fresh feed water flushed through the cell for 1 hour. The EC after 1 hour of regeneration was measured, then the cell was allowed to stand for 16 hours with no applied potential, after which it was flushed with the same regenerant water and EC was measured again. The amount of NaCl removed during treatment and the amounts of NaCl recovered during both the 1-hour and 16-hour regeneration periods were calculated based on mass balance.

The amount of NaCl recovered after 1 hour of regeneration was 78 percent and 81 percent for the initial NaCl concentrations of 2,000 mg/L and 5,000 mg/L (table 8). After continuing the regeneration for 16 hours, recovery increased to

98 percent and 100 percent. The increase in recovery between 1 and 16 hours may be due to the diffusion of ions out of micropores within the aerogel sheets.

Table 8. Recovery of NaCl achieved after 1-hour vs. 16-hour regeneration period

Initial NaCl concen-tration (mg/L)	Initial EC (milli-siemens per centimeter) (mS/cm)	NaCl removed (mg)	Total NaCl adsorption mg NaCl/g aerogel	1-h NaCl recovery (mg)	16-h NaCl recovery (mg)
2,000	4.24	3,672	5.65	2,879	3,585
5,000	9.86	3,867	5.95	3,131	3,937

6.4.4 Removal and Recovery of NaCl and Iodide in Successive Cycles

The experiments were conducted with a feed water containing 5,000 mg/L NaCl and 50 mg/L iodide added as KI. A 50-minute treatment stage was used consisting of 12.5 L (3.3 gallons) of water. After the regeneration step of each cycle, the cell was rinsed for 10 minutes with feed water at the same flow rate (2.5 L of water), to bring the EC in the cell to near that of the feed water. The cell was then precharged to begin the next cycle. The procedure is illustrated in figure 25. A total of five cycles were completed in succession. Mass balance of NaCl was based on measurements of EC at 5-minute intervals during the treatment stage, in the final solution for the regeneration step, and in the combined solution from the rinse stage of each cycle. The concentrations of both iodide and iodine gas (I_2) were measured in 15-minute intervals for the effluent from the treatment stage, in the final solution from the regeneration stage, and the combined solution from the rinse stage.

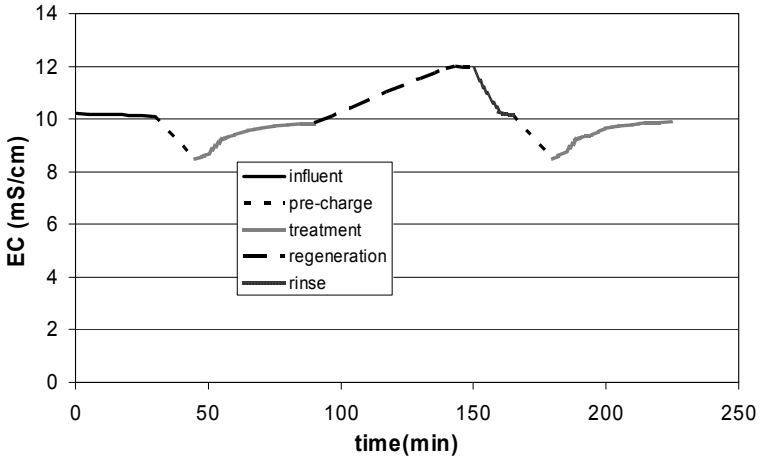

Figure 25. Treatment procedure of one cycle.

The average NaCl concentration in the effluent increased, and the amount of NaCl removed decreased between the first and fifth cycles (table 9 and figure 26). Accumulation of NaCl in the cell occurred over the five cycles, which was recovered nearly completely after overnight (16-hour) regeneration. The concentration of NaCl in the effluent at the end of the rinse step slightly increased during the five stages (figure 26), indicating that salts released during regeneration were not completely rinsed from the cell before the next cycle was started. However, the duration of the rinse step was left at 10 minutes for remaining experiments because the production of large volumes of rinse water decreases the efficiency of the treatment process.

Table 9. Removal and recovery of NaCl in five successive cycles

Cycle	Minimum NaCl (effluent) (mg/L)	Average NaCl (effluent) (mg/L)	NaCl removed (mg)	NaCl recovered (mg)	NaCl recovery deficit (mg)	Overnight recovery (mg)
1	4,213	4,674	3,911	2,689		
2	4,223	4,706	3,524	2,956		
3	4,307	4,698	3,474	3,255		
4	4,307	4,732	3,086	3,097		
5	4,332	4,747	2,910	2,511		
Sum			16,905	14,508	2,397	1,999

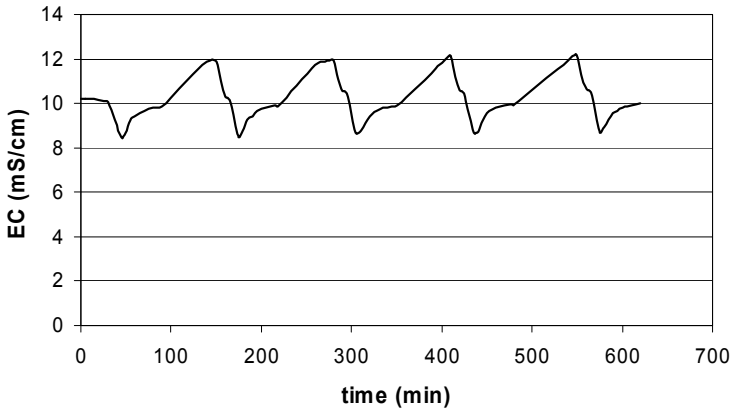

Figure 26. Reduction in EC achieved after successive treatment of 10 mS/cm water.

Iodide concentration was decreased from an initial concentration in the influent of 50 mg/L to 17–25 mg/L in the effluent (table 10). This corresponds to at least

50-percent removal of iodide by the cell, compared to only 5–6 percent removal of NaCl (table 9). The average concentration of I_2 gas generated in the effluent was as high as 5.7 mg/L, observed during cycle 3. Given the half-cell potential of I_2/2I- 0.54V, iodide can be reduced to iodine at the applied potential of 1.3V during CDT treatment. Iodine gas production was greater for cycles 1 and 3, where the electrodes were connected in opposite polarity than for cycles 2, 4, and 5. However, the final recovery of iodide in the regenerant water was only slightly less for cycles 1 and 3. The final concentration of iodide in the regenerant water was between 71 and 89 mg/L.

Table 10. Iodide concentration and recovery in five successive cycles

Cycle	Average iodide (effluent) (mg/L)	Average I_2 (mg/L)	Iodide removed (mg)	Iodide Recovered (mg)	Iodide in concentrate (mg)
1	20.6	4.8	367	286	71
2	24.8	1.1	316	340	89
3	17.4	5.7	405	315	82
4	22.6	2.6	342	332	85
5	23.1	2.1	353		

6.4.5 Simulation of Treatment of Saline Produced Water with 10 Millisiemens per Centimeter Water as Rinse

To improve the recovery of the CDT cell, feed water with an EC of 10 miillisiemens per centimeter (mS/cm) (equal to the feed water EC) was recycled and used for rinsing. Reducing the EC of 6.25 L (1.65 gallons) of water from an initial value of 10 mS/cm required nine cycles to reach an EC of 5.40 mS/cm (figure 27). The incremental reduction in EC decreased from 1.04 mS/cm for the first cycle to 0.22 mS/cm by the ninth cycle (table 11). Improvements in the increment of EC reduction were observed after overnight regeneration, which occurred between the fourth and fifth and the ninth and tenth cycles, respectively. After the tenth cycle, the EC of the treated water was decreased in steps to approximately 4.0, 3.0, and 2.0 mS/cm in order to accelerate completion of the experiments. This procedure was deemed acceptable because the iodide concentration in the treated water had stabilized at approximately 10–13 mg/L, and iodide concentration in the regenerant water was near 50 mg/L. Treatment of the 2.0 mS/cm water yielded a very low value for the increment of EC reduction of only 0.08 mS/cm. Consequently, with the given experimental setup, at least 10 cycles would be required to decrease EC from 2.0 mS/cm to 1.0 mS/cm. Because the regenerant water was reused, the EC in the regenerant stage reached values as high as 13.33 mS/cm. However, after the treated water EC was below

5.0 mS/cm, EC in the regenerant water tended to remain near a value of 10.0 mS/cm. This is probably due to carryover of relatively low EC water remaining in the cell after the treatment step.

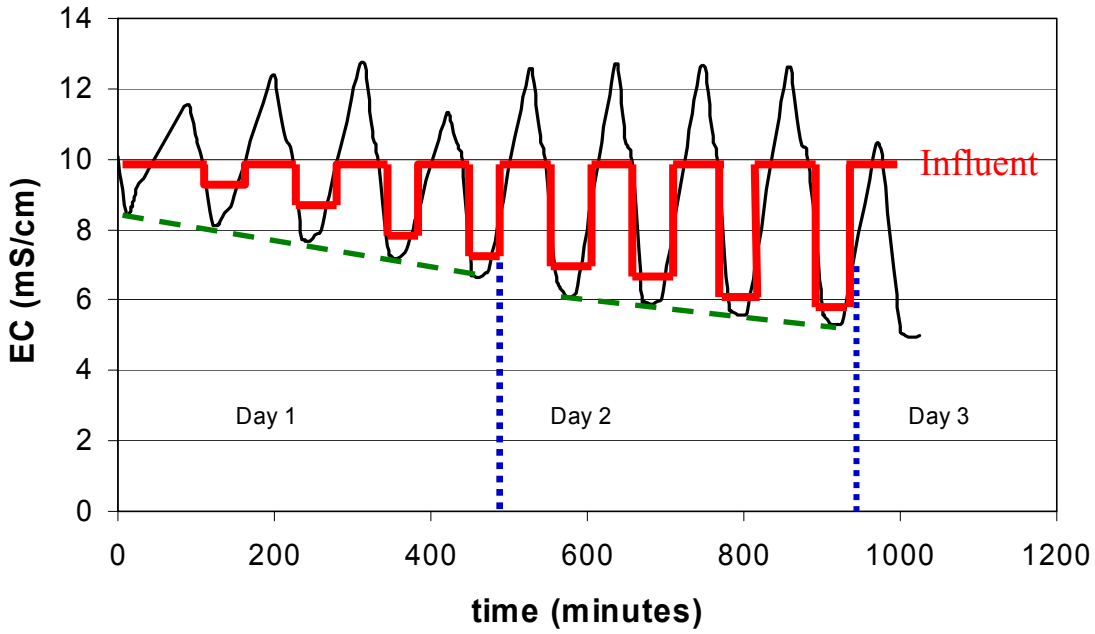

Figure 27. Treatment of high salinity water using 10 mS/cm water for rinsing.

Iodide concentration in the regenerant water was 74.4 mg/L after the first cycle, and then gradually decreased during the first day to 66.4 mg/L at the end of the fourth cycle. Iodide concentration in the regenerant then increased to 89.9 mg/L after the overnight regeneration.

In order to estimate the effect of carryover from regeneration on the treatment of water in the following cycle, the reduction in adsorption capacity was calculated. The maximum adsorption capacity available was calculated as 5.54 milligrams per gram (mg/g) aerogel based on the results from the first cycle. The residual concentration of NaCl in the cell after the rinse stage was slightly above 5,000 mg/L (EC = 10.0 mS/cm) throughout the entire range of initial EC values. After draining the cell following the end of the rinse step, at least 800 milliliters (ml) of this water remained in the cell. Therefore, the adsorption capacity needed to reduce the EC of the residual water in the cell from 10.0 mS/cm to match the EC of the treated water at a given stage of treatment was calculated as:

$$mgreq = \frac{.80L(5000 - C_i)}{650g} \quad (7)$$

Where:

mgreq = the mg of adsorption capacity per g aerogel lost due to carry-over

C_i = the initial concentration of NaCl in mg/L at a given stage of the treatment process.

The percentage of the adsorption capacity available for treating water at a given initial NaCl concentration is then:

$$capavail = \frac{5.54 - mgreq}{5.54} 100\% \quad (8)$$

These calculations suggest that the percentage of available adsorption capacity decreases from 100 percent at initial EC of 10.0 mS/cm to only 11 percent for an initial EC of 2 mS/cm (figure 28). This predicted 10-fold decrease in available adsorption capacity is consistent with the experimentally measured reduction in EC increment from approximately 1 mS/cm at an initial EC of 10 mS/cm to 0.08 mS/cm at an initial EC of 2 mS/cm (table 11). The very low increments of EC reduction at low initial EC levels can be accounted for based on consideration of the carryover of ions from regeneration.

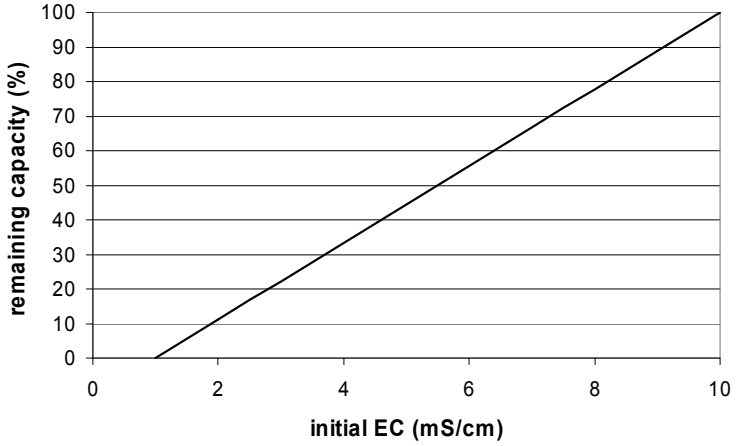

Figure 28. Percentage of adsorption capacity available after reduction of EC achieved after various stages of treatment for a feed water quality of 10 mS/cm.

Table 11. Treatment of 10.0 mS/cm water (5,000 mg/L NaCl plus 50 mg/L I) using 10 mS/cm water to rinse cell between treatment cycles

Cycle	Treatment Stage			Regeneration	
	EC (mS/cm)	Increment (mS/cm)	Iodide (mg/L)	EC (mS/cm)	Iodide (mg/L)
0	10.0		50.0		
1	8.96	1.04	32.4	11.53	74.4
2	8.32	0.64	24	12.38	71.6
3	7.77	0.55	17.7	12.72	70.3
4	7.29	0.48	14.4	11.67	66.4
5	6.72	0.57	14.9	12.59	89.9
6	6.22	0.50	14	12.72	56
7	5.93	0.29	14.1	12.62	56.1
8	5.62	0.31	13.1	12.62	49.1
9	5.40	0.22	10.6	13.33	53
10	4.98	0.42	13.6	10.25	
11	4.00>3.88	0.12	(10.0)	—	
12	3.03>2.88	0.15		10.64	
13	2.08>2.00	0.08		10.3	

6.4.6 Simulation of Treatment of Saline Produced Water with 1 mS/cm Water as Rinse

The use of 1.0 mS/cm water in the rinse step produced greater increments of reduction in EC for each cycle (table 12). The EC of the rinse water was increased from 1.0 to 3.5 mS/cm, indicating that the rinse water could be reused when treating water in the early stages of the process. Iodide recovery was poor due to rinsing the cell with low-iodide (I = 10 mg/L) treated water before the first cycle.

Table 12. Treatment of 10.0 mS/cm water (5,000 mg/L NaCl plus 50 mg/L I) using 1.0 mS/cm water to rinse cell between treatment cycles

Cycle	EC (mS/cm)	Increment (1 mS rinse) (mS/cm)	Increment (10 mS rinse) (mS/cm)
1	10.06>8.70	1.36	1.04
2	7.10>6.16	0.94	0.57
3	5.12>4.46	0.66	0.42
4	3.00>2.63	0.37	0.15

6.4.7 Simulation of Treatment of Saline Produced Water with 10 mS/cm Water as Rinse in Batch Mode

The increments of EC reduction obtained in batch mode were very similar to those obtained using repeated continuous flow (table 13). This result indicates that a 25-minute treatment step in continuous mode was sufficient to achieve the full potential salt removal for the relevant conditions. The effluent EC stabilized after only 20–25 minutes in the batch experiments. Iodide recovery in the batch experiments was inferior, probably due to increased contact time of the solution with the charged electrodes resulting in increased generation of I_2 gas.

Table 13. Recycle mode (batch) treatment of 10.0 mS/cm water (5,000 mg/L NaCl Plus 50 mg/L I) using 10.0 mS/cm water to rinse cell between treatment cycles

Cycle	Treatment stage			Regeneration	
	EC (mS/cm)	Increment (mS/cm)	Iodide (mg/L)	EC (mS/cm)	Iodide (mg/L)
0	9.99		50.0		
1	8.89	1.10	36.3	11.35	61.6
2	8.16	0.73	15.8	12.68	48.2
3	7.61	0.55	15.7	10.93	
4	7.09	0.52	12.4	11.68	42.2
5	6.51	0.58	11.3	12.48	33.7
6	6.08	0.43	15.2	12.72	
7	5.80	0.28	14.1		

6.4.8 Effect of Treating Produced Water on Cell Performance Over Multiple Cycles

Unlike membrane operation, scaling was not considered an issue for CDT process during produced water treatment. Antiscalant solution was added during treatment of produced water to observe the effect of the addition of antiscalant on CDT performance. The increments of reduction in EC for the produced water with antiscalant added (table 14) were very similar to those achieved for treatment of synthetic solutions of NaCl (tables 12, 13) using the same cell (CDT unit #34). Iodide concentrations in the treated water were 79–91 mg/L, similar to the results obtained in the previous experiments with synthetic solutions. The decrease in the increment of removal observed between cycles 1 and 5 of approximately 20 percent was similar to studies with the synthetic solutions. The formation of scale within the cell was a major concern because the initial pH of the produced water was 8.40. However, pH of the effluent actually decreased during treatment, and pH was even lower in the regenerant water (table 14).

This phenomenon is likely due to the different hydrated radius of H+ and OH-. Gabelich et al. (2002) found that the ions with small hydrated radii were preferentially removed from solution. The hydrated radius of OH- is 3.5 angstrom (Å), much smaller than that of H+ 9.0 Å (Dean, 1992), resulting in a higher sorption capacity of OH- onto carbon aerogel electrodes than H+. This effect is likely causing the decrease of pH in the product water.

Table 14. Results of the produced water treatment of cell #34 with addition of antiscalant. Initial EC = 12.56 mS/cm; initial iodide = 48 mg/L

Cycle	Final effluent EC (mS/cm)	EC increment (mS/cm)	Effluent iodide (mg/L)	Regenerant iodide (mg/L)	Effluent pH	Regenerant pH
1	11.53	1.03	24.2	87.4	7.83	6.93
2	11.52	1.04	30.4	78.5	7.53	6.95
3	11.66	0.90	26.1	90.9	7.56	7.06
4	11.66	0.90	29.9	79.9	7.49	n.d.
5	11.73	0.83				

*Terminals connected the same for cycles 1, 3, and 5

The increment of EC reduction without antiscalant added did not diminish dramatically between the first and fifth cycle (table 15). The adsorption capacity of cell #36 appears to be 10–20 percent less than for cell #34. This was also observed for treatment of synthetic water with cell #34 before the produced water was treated. Iodide concentration in the regenerant was low for the first two cycles, probably because the cell was not fully equilibrated with iodide before initiation of the first cycle. Although the effluent iodide concentration was very close to the influent concentration before the experiments began, iodide was apparently not equilibrated with micropores within the aerogel. As for the experiments with the antiscalant added, the pH of the produced water decreased both after treatment and regeneration.

Although these initial experiments on the effect of scaling did not indicate a reduction in cell performance, a relatively small volume of water was passed through each cell. Additional studies need to be conducted to reveal the potential for scaling with this water during long-term operation.

Table 15. Results of the produced water treatment of cell #36 without addition of antiscalant. Initial EC = 12.40 mS/cm; initial iodide = 44 mg/L

Cycle	Final effluent EC (mS/cm)	EC increment (mS/cm)	Effluent iodide (mg/L)	Regen-erant iodide (mg/L)	Effluent pH	Regen-erant pH
1	11.61	0.79	12.3	56.2	7.66	6.88
2	11.53	0.87	17.6	76.4	7.25	7.10
3	11.62	0.78	24.2	83.2	7.60	7.13
4	11.62	0.78	23.4	97.3	7.60	n.d.
5	11.69	0.71				

*terminals connected the same for cycles 1, 3, and 5

6.4.9 Estimated Scale-Up of CDT Performance

Treatment of 10 mS Water Using 10 mS Water as Rinse

Based on the number of cycles required to reduce the EC of the water from 10.0 mS/cm to 5.0 mS/cm (10 cycles) and the increments observed for reductions in EC from initial EC values of 4.0, 3.0, and 2.0, it was estimated that a total of 35 cycles would be required to treat 6.2 L of water (1.64 gallons) to a final EC of 1 mS/cm. Assuming that five cycles per day could be completed followed by overnight regeneration, a total of 7 days would be needed to complete the treatment. The pilot-scale CDT system is designed to contain approximately 80 times more aerogel than the bench unit. If the sheets of aerogel in the industrial sized bricks are arranged in parallel mirroring the design of the bench-scale unit, it can be expected to treat 80 × 1.64 = 131 gallons in seven days (= 18.7 gpd).

Treatment of 10 mS Water Using 1 mS Water as Rinse

Based on the improved increments in EC reduction obtained with rinsing the cell with 1 mS/cm water, the number of cycles required for treatment was estimated to be 16 cycles, requiring a period of 3 days. However, a total of 20 L of rinse water would be required over the entire treatment process, which represents a net water production of negative 13.8 L. Since the EC of the rinse water increased by 2.5 mS/cm (data not shown), the rinse water could be used a total of 4 times. Therefore, the total production of water could be increased to 4 × 6.2 L = 24.8 L (6.55 gallons), requiring 12 days. This would yield a net production of 4.8 L of clean water in 12 days, which is a loss in performance compared to the 6.2 L treated in 7 days for the system rinsed with feed water. Although rinsing with treated water requires fewer cycles to treat the 6.2 L of water, net production is actually decreased with a recovery of 19.4 percent.

6.4.10 Effect of Temperature on Cell Performance

Cell #36 was employed to examine the effect of temperature variations in CDT performance. A total volume of 150 L of produced water was pre-filtered prior to CDT treatment. The cell was equilibrated with the filtered produced water at a rate of 250 mL/min (95 gpd) without power applied until both the EC and the iodide concentration of the effluent were within 1 percent difference of the feed water. This required approximately 20 L for equilibration of EC, but 60 L for equilibration of iodide. Batch treatment was then conducted at both 23 °C (73.4 °F) (ambient room temperature) and 12 °C (53.6 °F). At each temperature, four treatment cycles were completed. The applied voltage was set at 1.3V for all experiments. During the treatment step, 6.25 L of produced water was re-circulated at a flow rate of 250 mL/min for a period of 50 minutes. Regeneration was achieved using 2.0 L of fresh feed water at the same flow rate for 50 minutes, with electrode discharge accomplished by charge reversal (requiring approximately 15–18 minutes). Following the regeneration step, the cell was rinsed for 10 minutes with fresh feed water at 250 mL/min. The EC, pH, and iodide concentrations were measured immediately after each treatment and regeneration step was completed. Samples were also collected after each treatment and regeneration step in addition to the initial feed water. These samples were analyzed for multiple elements by ICP analysis as well as TOC and absorbance at 254-nm, 272-nm, and 436-nm measurements.

For the experiments conducted at 12.5 °C, produced water was chilled by using a cooling coil placed in the 55-gallon plastic drum containing the produced water. The water used for chilling was at 12.2 °C. During both the treatment and regeneration steps when water was contained in a 5-gallon bucket, the bucket was placed in a shallow ice bath to prevent warming. The temperature of the water discharged from the CDT cell was checked periodically and ranged from 11.6 to 13.2 °C.

During CDT treatment, reduction in EC at 23 °C was very similar to that achieved at 12.5 °C and resulted in reduction between 6.7 to 7.0 percent (figure 29). Iodide reductions in both the treated water and regenerant water were also similar at the two temperatures examined and varied between 66 to 69 percent, with iodide concentrations close to 15 mg/L in the treated water and close to 90–100 mg/L in the regenerant solution. Divalent cations, such as Ca, Mg, and strontium (Sr), exhibited between 21.7 and 22.5 percent removal on average at 23 °C and between 16.3 and 18.0 percent removal at 12.5 °C, respectively. The removal of sodium, however, was higher at 12.5 °C than at room temperature (13.3 percent versus 8.2 percent on average). The removal of potassium was similar to the divalent cations: 21.3 and 15.7 percent removal at 23 °C and 12 °C, respectively. The carbon aerogel did not remove any silica and boron from the produced water, likely due to the undissociated state of these constituents within the operating pH

range (8.3–8.5). If the pH is increased to above 9.5, boron will dissociate and could be removed by the CDT® process, potentially meeting water quality standards for beneficial use such as irrigation.

TOC concentrations were actually greater in the treated effluent than the regenerant solution (table 16). Adsorption of TOC to the aerogel material apparently occurred when the cell was uncharged, and the lower volume of solution being recirculated through the cell during regeneration (2.0 L) might provide a greater opportunity for reduction in initial TOC concentrations than during the treatment stage (6.25 L). The increased removal of TOC during regeneration was also consistent with partitioning of non-ionic organic solutes, which is maximized when the adsorbant is neutrally charged (which occurs during regeneration when the cell is discharged). UV absorbance measurements were consistent with the expected adsorption of anions during treatment followed by their release during regeneration. These results suggest that organic acids might behave similarly to what is expected for inorganic anions.

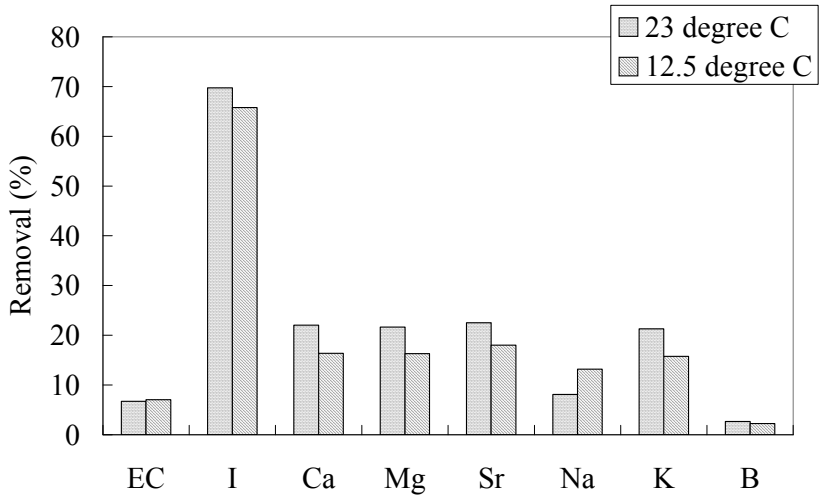

Figure 29. Effect of temperature on removal of different constituents from produced water (Batch recycling operation using laboratory bench-scale unit.)

Table 16. Organic parameters during temperature experiments (T = treatment stage, R = regeneration stage)

	TOC mg/L	Abs(254) (/cm)	Abs(272) (/cm)	Abs(436) (/cm)
Influent	0.88	0.115	0.0308	0.0035
23 °C				
Cycle 3-T	0.88	0.083	0.0354	0.0064
Cycle 3-R	0.35	0.181	0.0163	0.0012
Cycle 4-T	0.80	0.088	0.0369	0.0059
Cycle 4-R	0.39	0.207	0.0205	0.0032
12 °C				
Cycle 3-T	0.70	0.069	0.0162	0.0014
Cycle 3-R	0.29	0.160	0.0076	0
Cycle 4-T	0.66	0.077	0.0240	0.0046
Cycle 4-R	0.34	0.192	0.0101	0

6.4.11 Ion Selectivity of Carbon Aerogel

The amount of adsorbed ions by carbon aerogel (in mol/g aerogel) in treating produced water increased in the order of Na (7.9×10^{-5}) >> Ca (1.6×10^{-6}) > Mg (9.7×10^{-7}) > K (4.6×10^{-7}) for cations, and Cl (7.7×10^{-5}) >> Br (3.6×10^{-6}) > I (2.6×10^{-6}) for anions.

Previous studies suggested that, for ion species having similar initial solution concentration (in terms of molarity), the hydrated radius might control their sorption capacity of carbon aerogel electrodes (Gabelich et al., 2002; Ying et al., 2002). Monovalent ions such as sodium with smaller hydrated radii were preferentially removed from solution over multivalent ions (such as calcium) on a percent or molar basis. There was also evidence that the counter ion present could play an important role in an individual ion's sorption capacity (Gabelich et al., 2002; Ying et al., 2002). In this study, it was observed that, in a competitive multi-ionic solution, feed concentration seemed to play a more important role in ion uptake than the ionic hydrated radius. For instance, potassium has an effective ionic radius of 3.31 Å in aqueous solution, much smaller than sodium (3.58 Å), calcium (4.12 Å), or magnesium (4.28 Å). Therefore, it is expected that the sorption capacity of potassium should be higher than sodium, calcium, and magnesium based on hydrated radius. The experimental results, however, showed that the mass of adsorbed ions was dependent on the feedwater concentration (in terms of molarity) rather than the hydrated radius, and followed the order of Na>Ca>Mg>K. A similar conclusion can be drawn for anions. Ying et al. (2002) reported that the sorption capacity of anions followed the trend of Br>Cl

considering similar feed concentrations (in terms of molarity). This study observed the opposite trend of sorption capacity, which corresponded to the initial feed concentration (in terms of molarity) of Cl>Br (table 16).

The removal of iodide in the produced water reached 69 percent, much higher than other ions (table 17). Ying et al. (2002) attributed high sorption capacity of iodide to its higher partial charge-transfer coefficient than chloride and bromide. The partial charge-transfer coefficient is an indicator of how many electrons can be released from the adsorbate to an adsorbent. In this study, a concentration between 1.1 and 5.7 mg/L of iodine was detected in the CDT effluent during produced water treatment. Besides electrostatic adsorption, iodide and iodine can have complex intermolecular interactions with the carbon aerogel material. Iodide and iodine can react with various carbon groups of the aerogel, such as carbonyl and phenolic functional groups, resulting in higher sorption capacity.

Table 17. Ion sorption and hydrated area of the carbon aerogel electrodes in treating produced water. (Batch recycling operation using laboratory bench-scale unit at 23°C.)

Ions	Hydrated radius* (Å)	Feed concentration (millimoles [mM]/liter)	Sorption capacity ($\times 10^{-5}$ mol/g aerogel)	Removal (%)	Hydrated area (m^2/g aerogel)
Na	3.58	97.83	7.9	8.1	19.15
K	3.31	0.18	0.046	21.3	0.10
Ca	4.12	0.74	0.16	22	0.51
Mg	4.28	0.46	0.097	21.7	0.34
Cl-	3.32	93.26	7.7	7.6	16.05
Br-	3.3	0.63	0.36	50	0.74
I-	3.31	0.39	0.26	69.7	0.54
Total cations			8.20		20.09
Total anions			8.32		17.33

Note: * Reference: Nightingale, 1959.

To further investigate the effective surface area of the carbon aerogel in produced water treatment, the amount of aerogel surface area covered by each ion specie (m^2/g aerogel) was calculated by multiplying the molar sorption capacity of the ions (mol/g aerogel) by Avogadro's number (6.022 × 1023) and the two-dimensional area based on the hydrated radius (m^2):

$$Hydrated\ \ Area = Sorption\ Capacity \times Avogadro's\ number \times \pi \times hydrated\ \ radius^2 \quad (9)$$

The carbon aerogel exhibited similar sorption capacities of total cations and anions, 8.07×10^{-5} versus 8.32×10^{-5} equivalents per gram aerogel (table 17). Based on the hydrated radius, cations and anions covered similar surface areas of the carbon aerogel, about 20 and 17 m^2/g aerogel, respectively. The utilized surface area was low, about 33 percent of the total surface area as compared to the measured BET surface area of 113 m^2/g aerogel. Given the average pore size of the aerogel in the range of 4 nm, the solutes could not effectively diffuse into the inner micropores and resulted in lower effective surface area for sorption. Gabelich et al. (2002) reported that only 10 percent of the carbon aerogel was available for sorption.

6.5 CDT System Field Tests

A pilot-scale CDT system was tested to treat produced water at a gas production site in Montana to verify findings derived from laboratory bench-scale experiments. The field tests were focused on examination of the performance of CDT at a larger scale under "real" operational conditions. The results from bench- and pilot-scale testing with regard to design, manufacture, and operation would be used to compare CDT process against membrane treatment based on technical and economic criteria.

During the field testing, the effect of some operational parameters on CDT performance could not be tested due to the equipment limitations, including flow rate and applied current. These operational parameters were further examined using synthetic water after the aquacells were shipped back to CDT Systems Inc., in Dallas, Texas. The experimental results from the field tests and the tests conducted in the laboratory of the CDT Systems Inc. are presented and discussed in the following section.

6.5.1 Effect of Flow Rate on CDT Performance

The effects of flow rate and initial feed concentration on electrosorption performance were investigated using synthetic sodium chloride solutions at a single-pass continuous flow regime (figure 30). At the feed flow rate of 250 mL/min using the bench-scale testing unit, the increase of dissolved salts in feed stream resulted in an initially linear increase of operational sorption capacity (figure 30(a)). After the feed concentration was greater than 2,000 mg/L, the operational sorption capacity of the electrodes leveled off, reaching 6 mg TDS per gram of carbon aerogel. The average sorption rate followed the same trend: increasing initially and stabilizing at 0.1 mg TDS per gram of carbon aerogel per minute of treatment time (figure 30(a)).

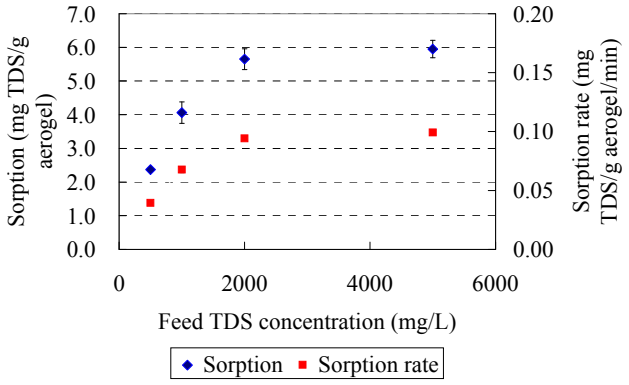

(a)

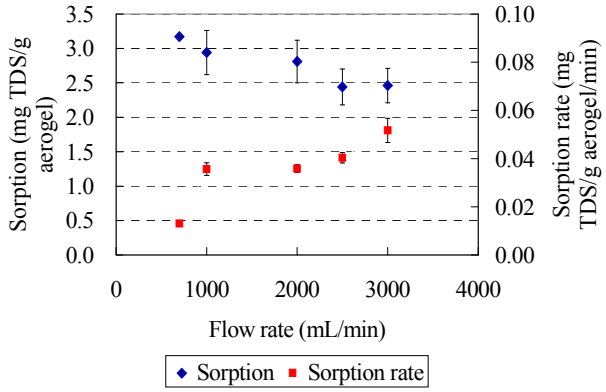

(b)

Figure 30. Effect of flow rate and feed concentration on operational sorption capacity and average sorption rate of the carbon aerogels using synthetic water. The error bars represent the standard deviation of 3 to 5 runs of each testing condition. (a) Feed flow rate 250 mL/min using laboratory bench-scale unit; (b) Feed TDS 500 mg/L using pilot-scale testing unit.

The effect of flow rate on electrosorption of CDI was examined using the pilot-scale testing unit treating synthetic sodium chloride solutions. As compared to the feed concentration, the increase in feed flow rate exhibited a limited effect on the electrosorption performance of the electrodes (figure 30(b)). At the feed concentration of 500 mg/L, the operational sorption capacity of the electrodes decreased from 3.2 to 2.5 mg TDS per gram of carbon aerogel when the flow rate increased from 700 to 3,000 mL/min. The average sorption rate, however, increased from 0.013 to 0.052 mg TDS per gram carbon aerogel per minute g/(g aerogel•min) with the increase of flow rate. This result implies that high flow rate should be employed for industrial CDI process design and operation

since fewer CDI modules will be required to produce the same amount and quality of desalinated water than at low flow rate.

To better understand the effect of feed flow rate and concentration on electrosorption performance of the electrodes, the experimental results were plotted as a function of TDS loading - mass of TDS loaded per gram of aerogel per minute during the sorption stage (i.e., feed flow rate × feed concentration / mass of the electrodes) (figure 31). At lower feed concentrations (i.e., lower TDS loading) the sorption rate increased linearly. When TDS loading exceeded 0.55 g/(g aerogel•min), the sorption rate leveled off at approximately 0.09 mg TDS/(g aerogel•min).

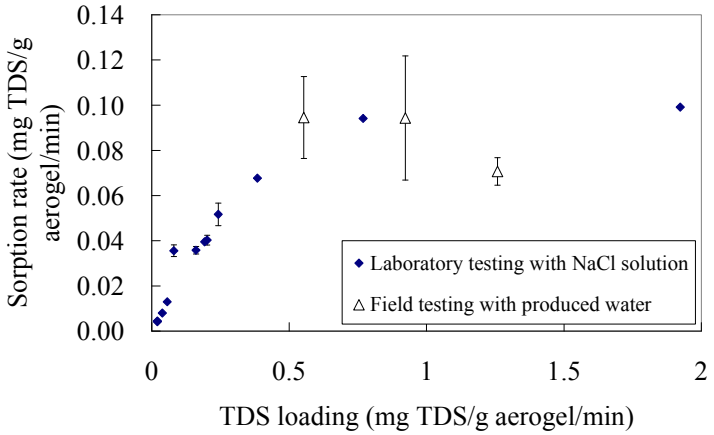

Figure 31. Effect of TDS loading on sorption rate of carbon aerogel. The error bars represent the standard deviation of 3 to 5 runs of each testing condition.

Previous studies have demonstrated that the adsorption capacity of the carbon aerogels is mainly affected by electrical double-layer capacity due to the electrostatic attractive force between the ions and the electrode (Yang et al., 2001; Gabelich et al., 2002; Ying et al., 2002). In porous electrodes such as carbon aerogel, the electrical double layers are formed inside the pores instead of adjacent to the electrode surface. The pores can greatly increase the effective surface area of the porous electrodes as well as the electrical capacity. However, when the magnitude of the pore size is similar to the thickness of the electrical double layer, the electrical double layer inside the pores overlaps; this results in a loss of electrical capacity (Yang et al., 2001). This overlapping effect exists in microporous (<2 nm) and part of mesoporous (2–50 nm) regions. Given the microporous structure of the carbon aerogel (figure 1), this overlapping effect likely prevents ions from entering the micropores, resulting in lower electrosorption capacity (Yang et al., 2001; Gabelich et al., 2002). The electrical

double-layer thickness is primarily affected by ion solution concentration and applied voltage. Farmer et al. (1996) reported that the electrical double-layer thicknesses were 1 and 20 nm for 0.1 and 10-4 moles/liter (**M)** electrolytes solutions, respectively. This study confirmed that increasing electrolytes loading to the electrode surfaces through increasing feed concentration could reduce electrical double-layer thickness and, consequently, improve electrical capacity of the carbon aerogel. However, the mass transfer limitations may still be in effect due to micropores overlapping and monolayer sorption behavior of carbon aerogel electrodes. These effects may explain the observed trend that the sorption rate increased with initially increasing electrolytes loading but leveled off after the loading rate reached 0.55 g TDS/(g aerogel•min), as illustrated in figure 31.

No significant correlation between iodide sorption and flow rate was observed during produced water treatment. Within the tested flow rate ranging from 600 to 1,500 mL/min, the retained iodide in the carbon aerogel electrodes varied between 0.13 and 0.15 mg I/g aerogel and the sorption rate varied in the range of 0.004 to 0.006 mg I/(g aerogel•min).

6.5.2 Treatment of Various Constituents in Produced Water by 1-Stage Aquacell

The retention of various constituents in the produced water by the 1-stage aquacell is presented in figure 32. The sorption and regeneration trend of each studied parameter during field tests is consistent with laboratory bench-scale results. The sorption capacity of carbon aerogel (in mmol/g aerogel) in treating the produced water was found following the order of Na>>Ca>Mg>K for cations, and Cl>>Br>I for anions during field tests. The percentage removal of each constituent, however, was higher during the field tests, likely due to a lower hydraulic loading rate of the carbon aerogel electrodes. The maximum removal followed the order of organic acids (in terms of UVA at 254 nm, 83.3%) > iodide (77%) > Br (62.5%) > Ca (40.7%) > alkalinity (in terms of $CaCO_3$, 40.0 %) > Mg (34.3%) > Na (18.4%)> Cl (16.0%).

TOC concentrations were actually lower in the regenerant solution than in the treated effluent (figure 32(a)). Adsorption of TOC to the aerogel material during regeneration when the cell is uncharged could result in potential electrode fouling by organic matter by clogging the pores of carbon aerogel material. UV absorbance measurements are consistent with the expected adsorption of anions during treatment followed by their release during regeneration (figure 32(a)). These results suggest that organic acids behave similarly to inorganic anions. Carbon aerogel showed a preferential sorption of iodide from produced water with regard to the degree of removal. Moreover, the iodide adsorbed onto the electrodes exhibited incomplete desorption during regeneration in comparison to chloride and bromide (figure 32(b)). Calcium, magnesium, and sodium had the

same sorption and desorption trend during produced water treatment (figure 32(c)). The carbon aerogel did not remove any silica and retained very little boron from produced water due to the undissociated state within the operating pH range (figure 32(d)). The maximum removal of boron was about 16.9 percent during the first-stage treatment, and the boron concentration in the effluent of the third stage was still exceeding 3 mg/L. pH varied between 7.5 and 9.1 during sorption and regeneration cycles due to the different sorption capacity of H+ and OH- ions onto carbon aerogel electrodes (figure 32(d)). The carbon aerogel also exhibited a high retention of alkalinity during produced water treatment (figure 32(d)).

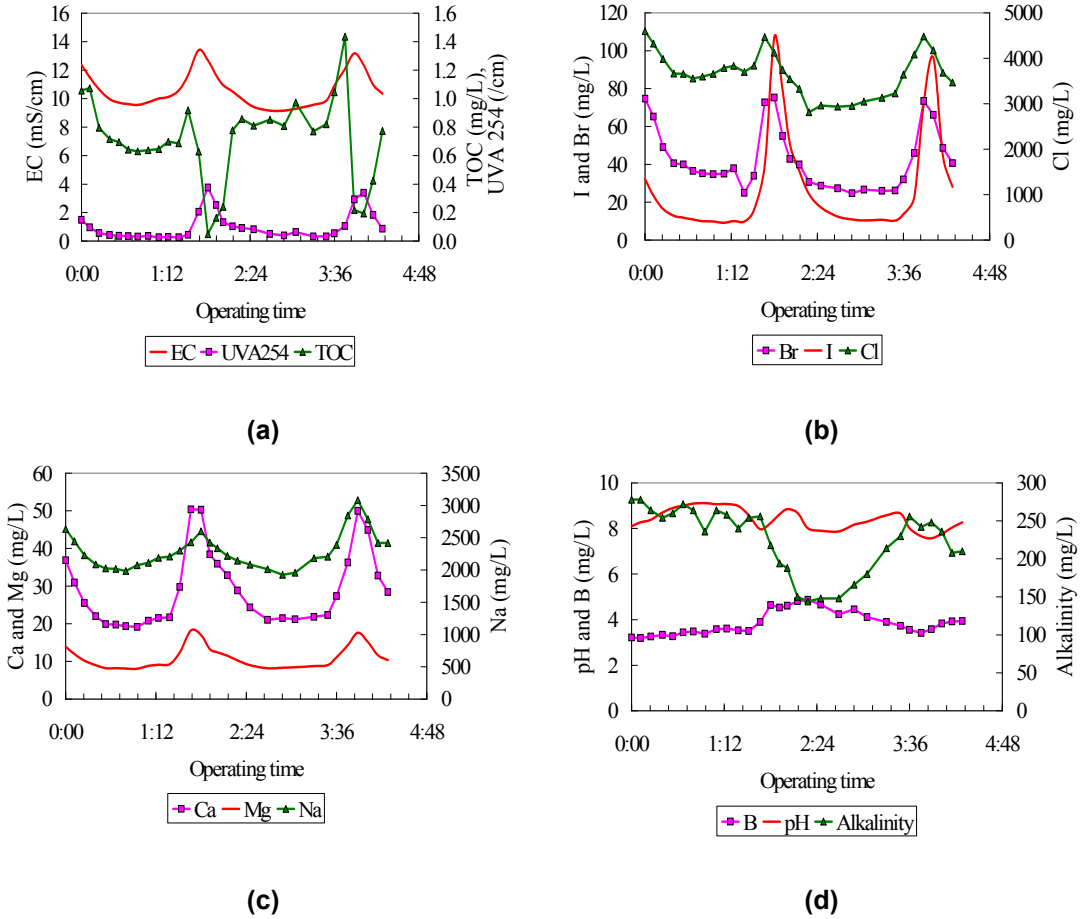

Figure 32. Treatment of various constituents in the produced water using (once—through two CDT aquacells in series)a flow rate of 560 mL/min and regeneration rate of 1,900 mL/min.

With a high flow rate during regeneration, the regeneration time was shortened to one-third of the production time. More than 80 percent of adsorbed ions were desorbed from the electrodes during regeneration. However, a rather high

volume of brine was produced, for instance, at least the same amount of product water for the first-stage treatment.

6.5.3 Treatment Efficiency by Two-stage and Three-stage Aquacells

To simulate the treatment efficiency of multiple CDT stages, the product water (effluent) from the previous stage was collected and used as influent of the subsequent stage. Figures 33 and 34 present results of the sorption and regeneration cycles by two-stage and three-stage aquacells at a flow rate of 550 mL/min. The cells were regenerated with filtered well water at a flow rate of 1700 mL/min. As compared to a single stage, the treatment efficiency of salts was constant over the multiple stages with 2.8–2.9 mg TDS/g aerogel (table 18). Iodide recovery during the regeneration step was effective, with iodide concentrations increasing from 45 mg/L in the influent to values in excess of 120 mg/L during the regeneration of the first stage, and to in excess of 80 mg/L during the regeneration of the second stage. This was similar and even better than the results obtained with the bench-scale unit. The CDT cell was highly selective for iodide as compared to other salts, with 65 percent of the iodide removed from the influent in the first cell as compared to 8 percent of the total salts, as measured by overall EC reduction. Using original well water for regeneration, the iodide concentration in the regenerant of a third stage could be lower than the influent as a result of dilution effect. During the CDT treatment, pH increased from 8.1 to 9.36 with the decrease of iodide concentration from 30 mg/L to 10 mg/L in the effluent. The half-cell potential of iodide/iodine is 0.536V; the following reaction occurred at the applied electrical field of 1.3V and 1.6V: 2HI → H2 + I2, which resulted in depletion of H+ ions.

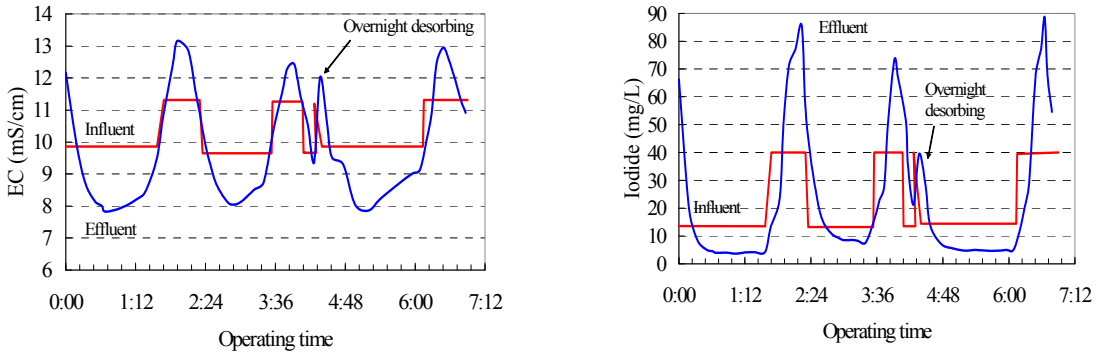

(a) (b)

Figure 33. Multiple sorption and regeneration cycles of once-through operation by two-stage aquacells (two cells in series). (a) conductivity; (b) iodide.

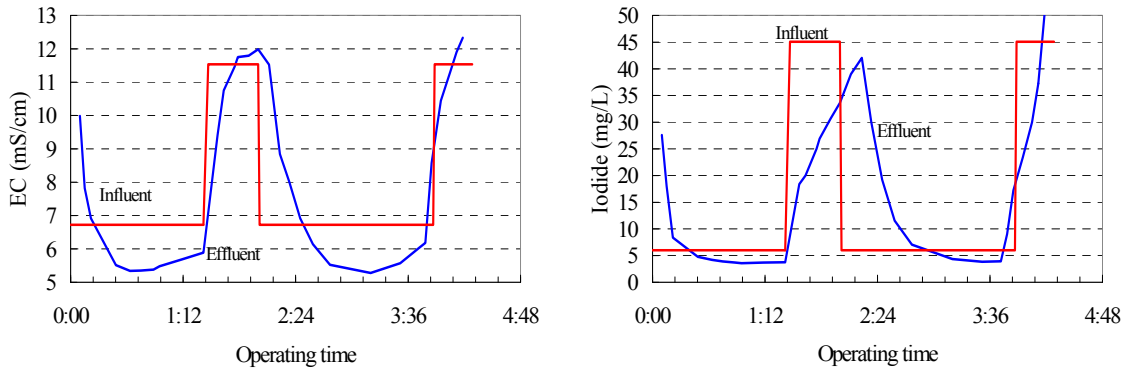

(a) (b)

Figure 34. Multiple sorption and regeneration cycles of once-through operation by three-stage aquacells (two cells in series). (a) conductivity; (b) iodide.

Table 18. Comparison of salts and iodide removal by one-, two-, and three-stage treatments

Stage	Conductivity (mS/cm)			Iodide (mg/L)			
	Infl.	Effl. Min.	Sorption (mg/g aerogel)	Infl.	Effl. Min.	Regenerant (max.)	Sorption (mg/g aerogel)
1	11.68	9.15	2.9	45.0	10.0	123	0.10
2	9.86	7.83	2.8	13.5	3.7	85	0.03
3	6.70	5.33	2.8	6.0	3.5	42–50	0.005

6.5.4 Energy Consumption During Produced Water Treatment

During the field tests, the applied voltage was kept between 1.3 and 1.6 volts and the current between 60 and 70 amps. The effect of applied current on energy utilization efficiency during produced water treatment was examined using synthetic water with NaCl concentration between 500 and 1,500 mg/L. The tested current was in the range of 15 to 260 amps for sorption and regeneration. The consumed energy (in terms of per gram of removed salts and per kgal [1,000 gallons] of produced water with TDS 500 mg/L) increased exponentially with the applied energy (figure 35). The minimum energy consumption was 0.00021 kilowatthour per gram (kWh/g) salts removed (i.e., 3.35 kWh/kgal product water) at applied current of 15 amps for both sorption and regeneration. Although applying high current could shorten the time for electrodes charging and discharging, power consumption is getting excessively high with regard to gram of removed salts.

Summary

Capacitive deionization technology proved to be a potential alternative for onsite treatment of produced saline water from the Jorgensen well. The performance of

the CDT system was maintained at a consistent level throughout the duration of the field trial, indicating that scaling or fouling of the aerogel electrodes was not a problem when treating this water source. Although the system as configured did not reduce TDS to the extent needed to meet the water quality standards, the scale at which the test was conducted allowed an extrapolation to determine the number of cells and configuration needed to meet the desired standards. Capacitive deionization technology is especially promising for iodide recovery from produced water at this site as well as other sources that contain iodide. The efficiency and production capacity of the system needs to be improved before CDT will become economically feasible to treat water of this level of salinity. However, the results of the field test allowed identifying critical equipment parameters and operational conditions which merit further improvement.

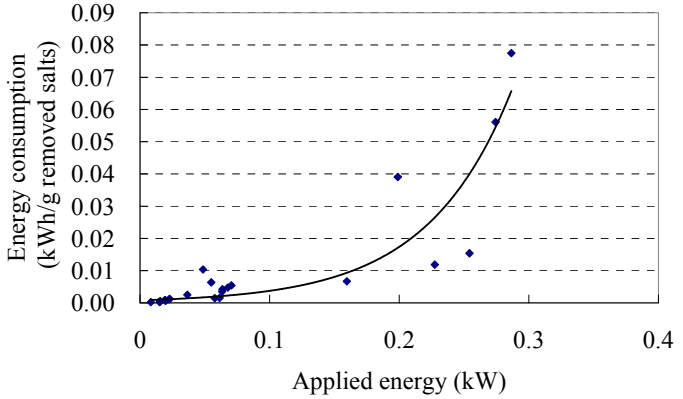

(a)

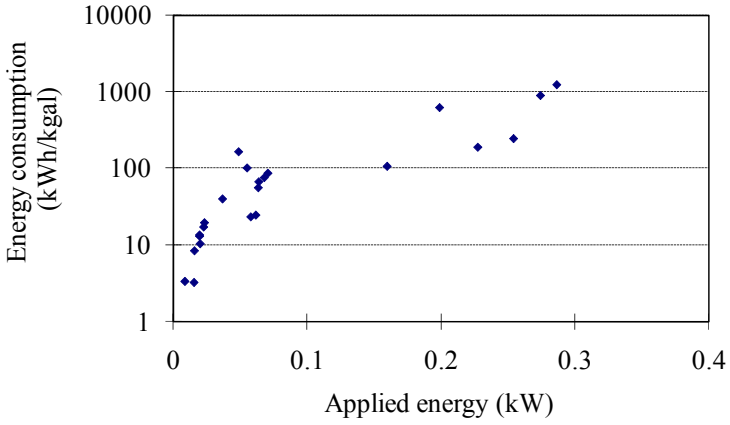

(b)

Figure 35. Correlation between energy consumption and applied current. (a) kWh per gram of salt removed; (b) kWh per 1,000 gallons of product water with TDS 500 mg/L.

6.6 Technical-Economic Assessment of Membrane and CDT Technologies

6.6.1 Cost Analysis for Membrane Technology

Water Quality Modeling and Cost Analysis for the Koch HR-400 and ULP-400 Membranes

Water quality modeling was performed with the ROPRO program, distributed by Koch, using the Koch TFC-HR-400 and TFC-ULP-400 membranes. It was assumed that the water quality simulation and cost analysis would be the same for the TMG-10 and the TFC-ULP because these two ULPRO membranes performed similarly during the laboratory tests. Water quality parameters for a worse-case scenario were taken from the 2003 analysis of the Jorgensen well water, which contained the greatest levels of TDS and alkalinity. Analysis was also performed for the average analytical measurements of multiple samples of the water. Water quality input parameters for the ROPRO program are given in table 19. All calculations were based on producing 1 million gallon per day (MGD) or 3,785 cubic meters per day (m^3/d) of product assuming that the produced water was generated from a cluster of wells. Treatment to both the drinking water standard and the irrigation water standard was evaluated. Blending with untreated water was considered to reduce the final product TDS to a goal of 450 mg/L for the drinking water standard or 900 mg/L for the irrigation water standard. This provides a safety factor of 10 percent under the regulations. Blending also increases the pH of the product water. Permeate recovery was fixed at 75 percent for all calculations. Iodide and boron were added to the ROPRO database by including rejection values measured experimentally for the two specific membranes. Two-stage trains were configured by setting the flux at 16 gfd ($0.65\ m^3/m^2 \bullet d$)). Cost analysis was done using the COSTPRO programs, using parameters listed in table 20. The cost analysis was only used to compare the economic aspects of the tested membranes and the CDT on a same cost basis. It should not be used to estimate the "real" costs of a produced water treatment plant because varied costs on labors, energy, chemicals, and financing, etc.

Water Quality Modeling and Cost Analysis for the Dow NF-90 Membrane

Water quality analysis for the Dow NF-90 membrane was simulated using the ROSA program. The NF-90 membrane was evaluated for meeting the irrigation water standard only because the permeate water quality for both the 2003 water and the average water composition exceeded the drinking water level of 500 mg/L. Cost analysis was performed using the COSTPRO program, to be consistent with cost analysis of the other two membranes. The feed pressure, acid dosage, and number of elements required for the cost analysis were taken from the ROSA program output.

Table 19. Water quality input parameters for the ROPRO and ROSA models (mg/L except as noted)

Parameter	2003 water	Average (over 4 years) composition water	Standard deviation
Temperature	10 °C	10 °C	N.A.
pH	7.85	8.45	0.22
TDS[£]	6,350	5,520	718
Sum of ions[‡]	6,460	5,901	
Alkalinity (as $CaCO_3$)	380	235	20
Ca^{2+}	34.2	29.5	5.34
Mg^{2+}	13.8	11.1	1.88
Na^{+}	2,368	2,200[†]	155.0
K^{+}	6.84	6.92	1.11
Sr^{2+}	2.60	2.11	0.54
Ba^{2+}	2.34	1.98	0.47
Mn^{2+}	--	0.07	0.03
Si	14.3	2.73	0.61
Cl^{-}	3,502	3,306	853.6
B	6.51	3.84	0.25
I^{-} (*)	46.6	49.9	8.2

[£] Analytical TDS by evaporation at 105 ^{o}C
[‡] Sum of ions calculated by ROPRO
[†] Sodium concentration adjusted to provide charge balance. Analytical Na = 1,713 mg/L.
* Iodide was not modeled by the ROSA program

Table 20. Values and sources of cost parameters

Parameter	Basis	Value	Source
Plant life		20 years	Filteau, 1997
Interest rate		10%	
Capacity	Permeate	1 mgd	
Flux	Permeate	16 gfd	Filteau, 1997
Remaining capital (In addition to initial membrane investment)	Permeate flow	$549/mgd permeate	Filteau, 1997
Membrane replacement	7 year membrane lifetime	$795/element (HR) $901 (TFC-ULP) $900 (Dow NF-90)	Company software and vendor
Energy cost	Purchased from off-site	$0.06/kWh	Paul Mendell (Nov 2005)
Pump efficiency	Overall efficiency	0.77	Hydranautics IMS Design
Acid dose	37% HCl, including transportation to site	$0.12/lb	DOW sales rep
Antiscalant dose	Concentration used in bench experiments	3.0 mg/L	
Antiscalant cost	Bulk cost for 270 gallons including transportation	$3.18/lb	GE Betz sales rep
Labor	1 mgd product	$38,400/year	Filteau, 1997

Determination of Membrane Configurations

For the NF-90 membrane treating both water types and for the Koch ULP-400 membrane treating both water types to the drinking water standard, a two-stage 18/8 array with six elements per vessel provided the desired permeate flux near 16 gfd (0.65 $m^3/(m^2 \cdot d)$). This represents a total of 156 8040 membranes for each system. For the other combinations, which included the ULP membrane treating to the irrigation water standard and the HR membrane treating to both standards, a 16/8 array using 144 elements fit the criteria. In these cases, the larger amount of water used for blending resulted in less feed water required.

Calculation of Required Antiscalant and Acid Dosages

Initial modeling showed that calcium sulfate ($CaSO_4$) and $CaCO_3$ scaling would occur in treating the produced water. Based on the bench-scale testing results, 3 mg/L of antiscalant would be used to prevent $CaSO_4$ scaling. Acid dose requirements were calculated by the ROPRO program using a target pH which

was determined to be 0.2 pH units less than the pH value at which the Langelier index was greater than zero. Acid dosage was affected by membrane rejection; higher rejection corresponds to higher accumulation of ions in the concentrate, causing a high value for the Langelier index. For a membrane with lower rejection, precipitation of $CaCO_3$ can be avoided at a higher feed water pH (table 21). Acid dosages are independent of the water quality standard to be met.

Table 21. Target pH and acid dosage required to avoid calcium carbonate precipitation

Water type	Membrane type	Target pH	Acid dosage (mg/L 37% HCl)
Average	TFC-HR	6.3	273
	TFC-ULP	6.4	247
	NF-90	6.6	186
2003	TFC-HR	6.1	515
	TFC-ULP	6.2	475
	NF-90	6.4	356

Neutralization of Acid in Product Water

Product water pH is neutralized by two processes: carbon dioxide stripping and blending of raw feed water with the permeate. Permeate pH values before stripping or blending range from 4.85 to 5.34. After carbon dioxide stripping and blending, product water pH is increased to acceptable values, ranging between 6.88 and 7.34. Further acid neutralization of the product water with either caustic or lime should not be necessary.

Results of Water Quality Modeling

The permeate TDS increased in the order TFC-HR< TFC-ULP < NF-90 (table 22). This allowed a greater blending flow rate to be used for the TFC-HR membranes, with the least blending flow allowed for the NF-90. The NF-90 membrane system did not meet the drinking water standard for TDS, even without blending. Iodide concentration reached the greatest values with the TFC-HR membrane. Iodide rejection was not modeled for the NF-90 system. Boron concentrations were in excess of the WHO recommendation of 0.5 mg/L in both the permeate and product water for both water types treated to either the drinking or irrigation water standards (table 22). Although blending caused the boron concentrations to be greater in the product than the permeate, permeate boron levels did not meet the water quality standards in any case.

Table 22. Results of water quality modeling of the membrane systems

System	Flux (avg) (gfd)	Blend flow (gpm)	Feed pressure (psi)	Permeate TDS (mg/L)	Product TDS (mg/L)	Conc. I^- (mg/L)	Permeate B (mg/L)	Product B (mg/L)
Average water composition treating to the drinking water standard								
HR	16.4	37	383	153	452	140	2.78	2.83
ULP	15.7	15	294	331	448	116	3.59	3.59
2003 water treating to the drinking water standard								
HR	16.6	32	399	172	451	129	4.75	4.83
ULP	15.8	9	309	373	449	107	6.09	6.10
Average water composition treating to the irrigation water standard								
HR	15.1	92	363	163	904	136	2.85	3.84
ULP	15.6	72	294	334	896	116	3.58	3.61
NF-90	15.6	25	294	767	913	------	-------	5.32
2003 water treating to the irrigation water standard								
HR	15.3	83	380	182	904	126	4.85	5.05
ULP	15.8	62	310	373	895	107	6.08	6.12
NF-90	15.8	11	311	816	910	-------	-------	5.32

Results of Cost Analysis

In comparing the costs associated with using the three different membranes, several cost advantages were apparent for both high- and low-salt rejection membranes. High rejection of salt led to increased blending flow. This results in a lesser flow rate of feed water to be pumped, and less water that must be treated with HCl and antiscalant. The feed flow rate factor which contributes to energy costs is also reduced. Low rejection of salt has the advantage of lower acid dosage (table 21). The ULP membrane array requires less pressure to operate than the HR system, but the NF-90 system requires very similar feed pressure to the ULP.

The Koch ULP membrane system provides the lowest overall cost of treating produced water from the Jorgensen well to the drinking water standards (table 23). The ULP and NF-90 provided an identical cost for treating the average composition water to the irrigation water standard. The NF-90 system provides the lowest cost for treating the water to the irrigation water standards.

Table 23. Results of cost analysis for the membrane systems of 1-mgd production (3,785 m^3/d)

System	Initial Capital ($ per year)	Replace Membranes ($ per year)	Chemical ($ per year)	Labor ($ per year)	Energy ($ per year)	Total Costs ($ per year)	Total costs ($ per 1,000 gallons)
Average water composition treating to the drinking water standard							
HR	55,026	16,354	162,761	38,400	99,632	372,174	1.02
ULP	59,445	20,079	155,644	38,400	78,974	352,542	0.97
2003 water treating to the drinking water standard							
HR	55,344	16,354	276,151	38,400	104,531	490,780	1.34
ULP	59,826	20,079	266,890	38,400	83,697	468,893	1.28
Average water composition treating to the irrigation water standard							
HR	51,530	16,354	149,136	38,400	86,467	341,886	0.94
ULP	54,569	18,535	142,578	38,400	72,384	326,465	0.89
NF-90	59,236	20,057	128,224	38,400	79,988	325,905	0.89
2003 water treating to the irrigation water standard							
HR	52,102	16,354	254,877	38,400	91,829	453,561	1.24
ULP	55,205	18,535	246,241	38,400	77,533	435,913	1.19
NF-90	59,681	20,057	211,473	38,400	85,075	414,686	1.14

Substitution of Sulfuric Acid for Hydrochloric Acid for Feed Water Acidification

A high proportion of the cost of treatment is due to acidification with HCl. Treatment of the produced water to the drinking water standard with the TFC-ULP membrane and using sulfuric acid was tested as an alternative. The dosage of 93 percent sulfuric acid required to decrease pH to 6.2 is 254 mg/L. The cost per pound of sulfuric acid, including transportation, was assumed to be $0.105. The total cost of treatment using acidification with sulfuric acid was $0.95 per 1,000 gallons of product ($0.25/$m^3$), less than the $1.28 per 1,000 gallons using HCl. However, barium sulfate is supersaturated by a factor of 162 in the concentrate flow stream with sulfuric acid.

A similar comparison of using sulfuric vs. hydrochloric acid was completed using the Hydranautics program for the NF-90 membrane system treating the produced water to the drinking water standard. Use of sulfuric acid resulted in supersaturation of barium sulfate by a factor of 190.

6.6.2 Cost Analysis for Capacitive Deionization

Acquisition of Required Data

Removal of TDS by capacitive deionization was estimated based on laboratory experiments by CDT Inc. (Dallas, Texas) during fall 2005 and the field demonstration at the Jorgensen well site during summer 2005 for the commercial subcells containing 6.2 kg of carbon each. Cost analysis was completed for flow rates of 0.7 L/min (0.18 gal/min) and 3.0 L/min (0.79 gal/min). Increments of TDS reduction obtained at TDS levels between the initial TDS of 6,350 mg/L and the irrigation water quality goal of 1,000 mg/L were used in the analysis (table 24). The TDS reduction achieved at an initial TDS of near 500 mg/L was very similar for the two flow rates. For estimation of TDS removal, it was assumed that the TDS reduction would be similar at the two flow rates across the range of TDS. The average TDS reduction across the range of TDS during treatment of 1,000–6,350 mg/L was calculated by assuming that a linear increase in TDS reduction with respect to initial TDS would be observed. This yields an average TDS reduction of 361 mg/L for each subcell. Power consumption was determined at each flow rate by integrating the product of applied voltage and current vs. time for both the treatment and regeneration stages and normalizing based on the gram of TDS removed.

Table 24. Data used for cost analysis using capacitive deionization

Flow (L/min)	Initial EC (µS/cm)	Initial TDS† (mg/L)	Δ EC (µS/cm)	Δ TDS (mg/L)	Regeneration period (minutes)	Power usage (kWh/g TDS)
0.7‡	11,200	6,400	850	486		
0.7	1,053	527	280	140	51	0.00021
3.0	1,041	521	285	143	20.0	0.0045
3.0	1,926	963	472	236	21.4	0.007
3.0	3,100	1,550	503	252	16.7	0.039

† For conversion of EC to TDS, a calibration factor of 2.0 was used for laboratory data and 1.75 for field data.

‡Data from field demonstration. All other data is from laboratory experiments.

Configuration of the CDT Module Trains

For the 2003 water with an initial TDS of 6350, 14.8 cells arranged in series would be required to reduce the TDS of the effluent to 1000 mg/L:

$$Cells = \frac{(6350 - 1000)\ mg/L}{361\ mg/L} = 14.8 \qquad (10)$$

A train of four modules containing a total of 16 subcells was selected for design. The actual final TDS for this configuration treating the 2003 water would be 700 mg/L. This calculation accounts for the lower TDS reduction observed below TDS of 1,000 mg/L (table 24). For treatment of the average water composition with an initial TDS of 5520 mg/L, a final TDS of 436 mg/L would be achieved.

Simulation of Treatment at 700 mL/min

In order to provide a continuous flow of treated water from each train, a rotating system was chosen. Based on the maximum observed adsorption capacity of 4.10 mg TDS per gram of carbon from the fall 2005 experiments, each cell can spend a total of 100 minutes in the treatment stage before regeneration is necessary:

$$treatment\ time = \frac{4{,}100\ mg\ TDS}{kg\ carbon}\ \frac{24.8\ kg\ carbon}{\text{mod}ule}\ \frac{1\ subcell}{361\ mg\ TDS}\ \frac{1\ \text{mod}ule}{4\ subcells}\ \frac{1\ \text{min}}{0.7\ L} = 100\ \text{min} \quad (11)$$

With four modules in treatment mode, the position of each module in the train must be rotated every 25 minutes. If one cell is regeneration mode for each 25-minute time segment, a fifth cell must be added to the train. A regeneration period of 50 minutes was needed at 700 mL/min for a single subcell (table 24). It is anticipated that at least 50 minutes will be needed to regenerate a module containing four subcells. Considering that the volume of water rinsed through the cell is 35 L and each cell holds 29.5 L of water, 1.2 pore volumes of water was used to rinse the individual subcell during regeneration in the laboratory experiment performed at 700 mL/min. Even with minimal mixing, it is anticipated that a minimum of 1 pore volume is needed to effectively rinse excess salts from the cell following regeneration. It is not expected that the same volume of water used to rinse a single subcell will be adequate to rinse more than a single module containing four subcells during the regeneration of a module. It is apparent that the regeneration period for a flow rate of 700 mL/min must be at least 50 minutes in duration. Therefore, a second module is placed in regeneration mode, giving a total of six modules per train with a revolving cycle using 25 minutes per step (figure 36). This system provides a recovery of 33 percent.

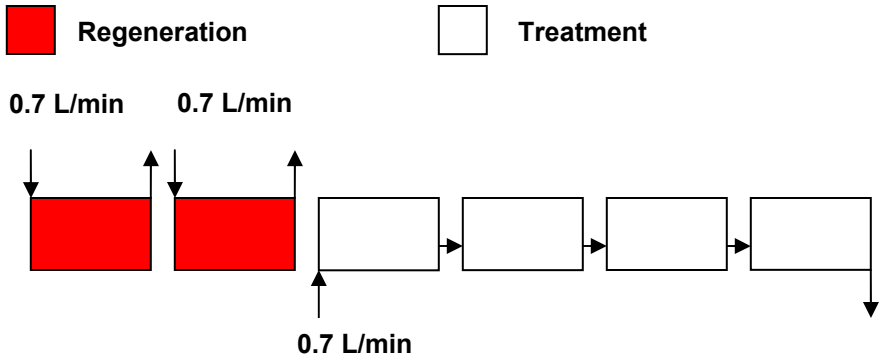

Figure 36. CDT module train for a flow rate of 0.7 L/min.

Simulation of Treatment at 3L/minute

Assuming that the TDS reduction at a flow rate of 3 L/min is the same as at 700 mL/min, the number of modules required in the treatment stage and the final water quality should be the same as at 700 mL per minute. At 3 L/min, the total time that each cell is in the treatment stage is 24 minutes. This provides only 6 minutes for regeneration for a fifth cell. The data from laboratory experiments at 3 L/min suggests that a minimum regeneration period of 18 minutes is required (table 24), which represents 1.8 pore volumes of water rinsed through an individual subcell. Again, it is anticipated that at least this volume of water will be required to rinse an individual module. Based on a minimum of 18 minutes required for regeneration at 3 L/min, three modules will be placed in regeneration mode. Each train requires seven modules with 6 minutes per step (figure 37). The recovery for this system is 25 percent.

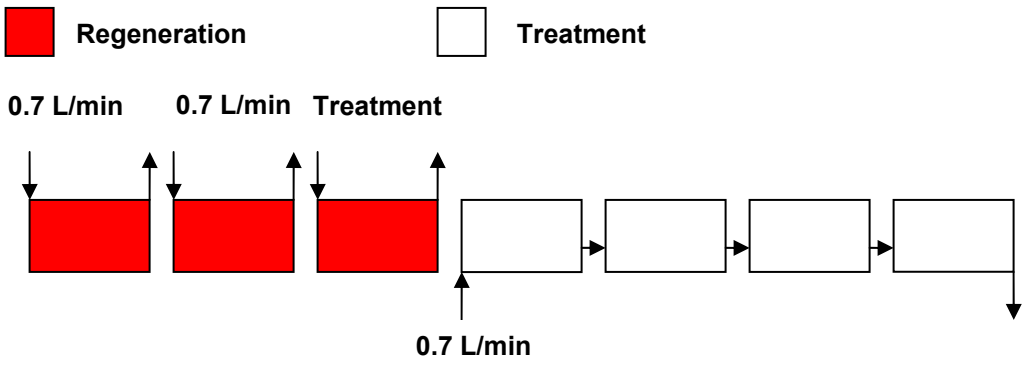

Figure 37. CDT module train for a flow rate of 3.0 L/min.

Scale-Up to 1 MGD

At a flow rate of 0.7 L/min, each train is producing 266 gpd (1 m^3/d) product. A total of 3,760 trains and 22,556 modules will be required to produce 1 MGD product (3,785 m^3/d). At a flow rate of 3 L/min (0.79 gal/min), each train is producing 1,140 gpd of product. A total of 876 and 6,132 modules will be required to produce 1 MGD product at 3 L/min.

Estimation of Cost of Water Treatment using Capacitive Deionization

Power Costs.—The cost of power required per 1000 gallons of product water when treating water of the average composition to the irrigation water quality goal was calculated as:

$$\frac{\$}{1000\ gallons} = \frac{3,785\ L}{1000\ gallons}\ \frac{(5520-1000)\ mg}{L}\ \frac{x\ kWh}{g\ TDS}\ \frac{1\ g}{1000\ mg}\ \frac{\$0.06}{kWh} \quad (12)$$

Where "x" indicates the power consumption at the relevant flow rate in kWh/g TDS removed.

At a flow rate of 0.7 L/min, the power consumption is 0.00021 kWh/g (table 24). The corresponding energy cost is $0.21 per 1,000 gallons of product. These values were obtained using an applied current of 30 Å during treatment and a limiting current of 30 Å during regeneration, with an initial TDS of 521 mg/L. A higher current may be required for treatment at higher TDS.

At a flow rate of 3 L/min, the power consumption was 0.0045 kWh/g TDS when using an applied current of 60 amps for treatment and a limiting current of 60 Å for regeneration. The values from table 24 for a flow rate of 3 L/min indicating a greater power consumption were calculated from experiments using a maximum current of 260 Å for either regeneration or treatment. Adopting the power consumption of 0.0045 kWh/g TDS results in an energy cost of $4.62 per 1,000 gallons.

Other Costs.—Costs for the CDT modules are $1,000 per module, which includes 30 percent for supporting equipment (Welgemoed and Schutte, 2005) (table 25). The lifetime of the CDT modules is assumed to be 10 years. A plant life of 20 years was applied to match the RO analysis. The COSTPRO program was used to determine all costs other than power (including amortization).

Table 25. Values and sources of cost parameters for capacitive deionization treatment

Parameter	Basis	Value	Source
Plant life	Matching RO analysis	20 years	
Interest rate	Matching RO analysis	10%	
Capacity	Product	1.0 MGD	
Capital	Including initial module cost plus supporting equipment	$1,000/module	Welgemoed and Schutte, 2005
Module replacement	10 year module lifetime	$770/module	Estimated lifetime
Energy cost	Purchased from off-site	$0.06/kwh	Paul Mendell (Nov 2005)

Results of Cost Analysis for Capacitive Deionization Treatment

The total cost of treatment was $9.85 per 1,000 gallons of product ($2.6/m^3) at a flow rate of 0.7 L/min and $7.32 at a flow rate of 3.0 L/min (table 26). If the lifetime of the modules is assumed to extend through the plant lifetime of 20 years, the total cost of treatment is reduced to $7.47 per 1,000 gallons at a flow rate of 0.7 L/min, and $6.67 per 1,000 gallons at a flow rate of 3.0 L/min.

Table 26. Cost of treatment of the Jorgensen water using capacitive deionization

Flow rate (L/min)	Initial capital ($ per year)	Replace modules ($ per year)	Labor ($ per year)	Energy ($ per year)	Total costs ($ per year)	Total costs ($ per 1,000 gallons)
0.7	2,612,044	868,406	38,400	76,650	2,595,500	9.85
3.0	710,102	236,082	38,400	1,686,300	2,670,884	7.32

Increasing Recovery for the CDT system

Several attempts were made to design configurations yielding greater recovery with the capacitive deionization system. One option is to treat the water produced from regenerating the modules. Considering the 0.7 L/min system, two cells are in regeneration mode, each producing 0.7 L/min of rinse water. The TDS of this rinse water will be 9,300 mg/L, based on the amount of TDS retained in the module and the amount of water rinsed through the cell during regeneration. Treating water of this initial TDS to the irrigation water quality standard will require 23 subcells, or 6 modules. The time step within which modules must be cycled becomes 17 minutes. For the second stage, three modules will need to be

in regeneration mode at any time, in order to provide a 50-minute regeneration period for each module (figure 38). The recovery for this two-stage system is determined by dividing the amount of product water (3 lines of 0.7 L/min each) by the total feed plus regeneration water (1 line feed plus 8 lines regeneration = 9 lines at 0.7 L/min each). The system recovery remains at 33 percent.

Another option for increasing recovery is to use water from the regeneration lines as feed water for the first stage (figure 39). As before, the increased TDS of the rinse water requires two additional modules for treatment and one additional module for regeneration. The recovery of this single stage system with recycle is also 33 percent. Again, this system is less efficient than the single-pass one-stage system in that a greater number of modules are required per train to produce the same recovery and product flow rate.

Similar attempts were made at increasing recovery at a flow rate of 3.0 L/min. Neither dual-stage systems nor recycling rinse water increased recovery. As with the 0.7 L/min systems, treating rinse water from regeneration required an increased number of modules in regeneration per train, which cancels out the water savings from recycling.

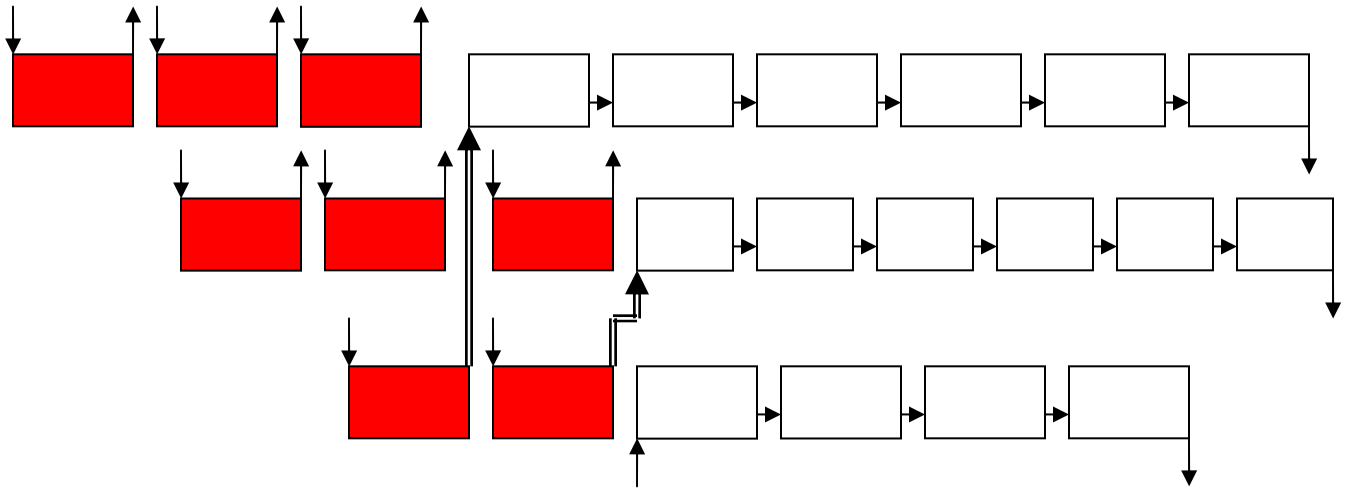

Figure 38. Dual-stage treatment system for a flow rate of 0.7 L/min. Bottom row is the first stage; middle and top rows are the second stage. Double lines indicate recycled rinse water.

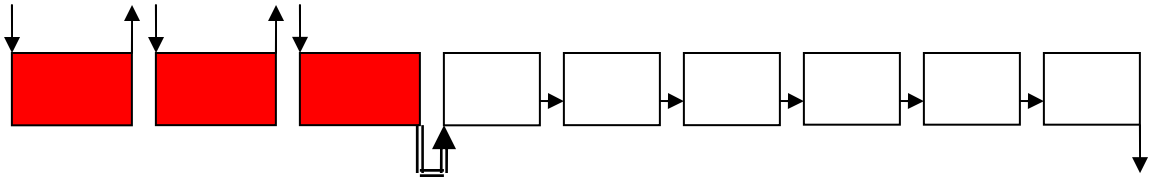

Figure 39. Single-stage system with the use of rinse water for feed at a flow rate of 0.7 L/min.

Analysis of Recovery Limitations

The maximum recovery attainable at a given flow rate can be calculated as:

$$Maximum\ \text{Recovery} = \frac{V_T}{V_R}(100\%) \qquad (13)$$

V_T = volume of water treated to the water quality goal by an individual module

V_R = minimum volume of water required to rinse an individual module during regeneration at the given flow rate

The volume of water treated to the water quality standard is expressed as:

$$V_T = \frac{Q_{TDS}\ M_C}{TDS_i - TDS_f} \qquad (14)$$

Q_{TDS} = adsorption capacity = 4,100 mg TDS/kg C

M_C = mass of carbon in each module= 24.8 kg

TDS_i = initial TDS in feed water (6,350 mg/L)

TDS_f = effluent TDS goal (1,000 mg/L)

This equation indicates that the maximum attainable recovery will decrease as initial TDS of the feed water becomes greater. Synthesis of carbon aerogel with a greater adsorption capacity would increase the maximum recovery. The volume of water required for regeneration is determined experimentally. If it is assumed that the water needed to rinse a module is similar to the volume required to rinse an individual subcell in laboratory experiments (table 26), then:

V_T = 54 L at 3.0 L/min

V_T = 35 L at 0.7 /min

Using these values, the calculated maximum recoveries are 26 percent at a flow rate of 3.0 L/minute, and 35.2 percent at a flow rate of 0.7 L/minute. These values are very similar to the recoveries achieved for the one-stage, single-pass configurations at both flow rates. Unless a lower volume of rinse water can be used for regeneration of a module, recovery will be limited to these values regardless of the configuration used. If a greater volume of water than the values adopted for this analysis is actually required to rinse the modules, then recoveries will be less. Further data regarding the minimum time and volume of water required to rinse a module or train of several modules in series is required for accurate calculations of recovery.

6.6.3 Assessment of Membrane Technologies vs. CDT

The technical-economic criteria used to assess membrane technologies and CDT include production efficiency (water recovery) and concentrate management, product water quality and iodide recovery, operation and design considerations, energy consumption, chemical consumption, life cycle, overall water costs, and pre- and post-treatment.

Production Efficiency and Concentrate Management

The recovery of membrane systems for brackish water desalination ranges from 60 to 85 percent depending on levels of silica and sparingly soluble salts (i.e., those formed by calcium-, barium-, and strontium sulfate and calcium carbonate) in the feed water. In this study, the maximum recovery tested during laboratory experiments was 70 percent. The permeate recovery was fixed at 75 percent for all of the membrane systems modeled; this resulted in overall system recoveries of 75–77.8 percent, depending on the amount of blend water used. The recovery of CDT process is much lower for produced water treatment due to water used for electrode regeneration and rinsing. To meet irrigation standards, the projected product recovery is about 25 33 percent, the simulated CDT systems, therefore, generate a greater volume of brine. The CDT system at a flow rate of 0.7 L/min (0.18 gal/min) through each train will generate 2 MGD (7,570 m3/d) of brine for each 1 MGD of product water. The CDT system at a flow rate of 3.0 L/min will generate 3 MGD of brine for each 1 MGD of product water. By comparison, the membrane systems will produce 0.23 MGD brine for each 1 MGD of product. The TDS content in the membrane brines, however, is much higher than in the CDT brine (20-22 g/L vs 7-7.8 g/L on average). The differences in quality and quantity of brine will lead to different measures for concentrate management, handling, and disposal.

Product Water Quality and Iodide Recovery

Both technologies can meet TDS standards for water reuse. Membrane can recover 60–80 percent iodide from the produced water, resulting in iodide concentration in the concentrate exceeding 100 mg/L at 75 percent recovery. The carbon aerogel electrodes can remove a maximum of 45–77 percent iodide from the produced water. By collecting the fraction of regenerant with high iodide concentration in the first and second stages of CDT process, the iodide concentration can exceed 80 mg/L in the regenerant solution. The CDT is only effective to remove salts from water, while membrane treatment is effective to remove silica, organic matters, and pathogens. Membrane technology can produce an overall better water quality than CDT.

Neither technology could meet irrigation and drinking water standards for boron under the tested conditions. By increasing pH to above 9.5, boron can be removed by the CDT process and might eventually meet the water quality standards. There are several options for boron removal by membrane process, such as two-pass RO or ion exchange post-treatment.

Operation, Design, and Construction Considerations

Both processes are compact and modular systems. Membrane technologies require more advanced operation and construction considerations for high-pressure pumps and clean-in-place systems. The CDT process operates at ambient conditions, and there are no requirements for high-pressure pumps and heaters, etc. Membrane fouling/scaling is an issue for produced water treatment, while CDT has much less fouling and scaling problems.

Energy Consumption

Energy consumption is similar between the two technologies—about 4 kWh per 1,000 gallons of water treated—although ULPRO consumes slightly less energy than NF, RO and CDT (at 0.7 mL/min flow rate). The energy consumption of CDT designed for 3 L/min system is significantly higher as a result of applied high current to electrodes. Future design of the CDT treatment system will likely incorporate recapturing energy during electrode discharge, which will decrease energy consumption considerably when used in place of powered cell discharge. The drawback to this approach is that a longer period of time will be required for regeneration with this arrangement.

Chemical Consumption

Membrane process needs acid, caustic, and detergent for membrane cleaning; and antiscalant, acid, and disinfectant for control of fouling and scaling. CDT process uses electrostatic regeneration and requires minimal or no chemicals for electrode fouling and scaling controls.

Life Cycle

The life cycle of membrane treatment plant is about 20 years. Major replacement needs include membrane replacement about every 7 years, sometimes shortened to 3 to 5 years. As the CDT technology is relatively new compared to membrane processes, no long-term operational data is available for industrial-size systems. The electrode lifetime is conservatively estimated to last at least 10 years by LLNL (Welgemoed and Schutte, 2005).

Overall Cost

It is difficult to compare the costs of treatment using membrane technologies and CDT, because the recoveries obtained by CDT were much less. The total cost of the most efficient CDT system which was found at a flow rate of 3.0 L/min for each train is \$7.32 per 1,000 gallons (\$1.93/m^3), much higher than any of the membrane systems tested (\$0.89–\$ 1.34 per 1,000 gallons). The major cost components for CDT process are the capital costs of CDT modules and replacement (\$710,102–\$2,612,044 per year for initial capital cost and \$236,082–\$868,406 per year for modules replacement), while the initial capital costs of membrane process and membrane replacement are in the range of \$51,530–\$59,826 per year and \$16,354–\$20,079 per year, respectively. Although MF pretreatment for membrane process will increase the overall cost by \$0.79 per 1,000 gallons of product water (Jurenka et al., 2001), the total cost of membrane process in treating this source of produced water is significantly lower than CDT.

In addition, the costs of disposal of brine by deep-well injection or other alternatives also need to be considered when evaluating the total cost of treatment for both technologies.

Pre- and Post-Treatment

Membrane process needs pretreatment to prevent membrane fouling, including pH adjustment, addition of antiscalant and disinfectant (optional), and microfiltration. The post-treatment needs degasification and alkalinity adjustment for corrosion control (optional). The CDT needs a simple cartridge filtration as pretreatment for desalination. However, as discussed previously, CDT might need complex pre- and post-treatment to remove organic matters.

In summary, membrane technologies provide an overall better treatment performance and cost-effectiveness than CDT in produced water treatment. ULPRO membranes, notably TMG-10, demonstrated competitive treatment efficiency as RO and operated at low cost. NF membrane can only meet the TDS standard for irrigation. None of the membranes tested can meet irrigation standards for boron. Either pH adjustment or dual-membrane system is recommended for boron removal by membrane treatment.

References

ALL Consulting, 2003. *Handbook on Coal Bed Methane Produced Water: Management and Beneficial Use Alternatives*. Tulsa, Oklahoma. http://www.all-llc.com/CBM/pdf/CBMBU/CBM%20BU%20Screen.pdf.

American Public Health Association (APHA), American Water Works Association (AWWA), and Water Environment Federation (WEF), 2005. *Standards Methods for the Examination of Water and Wastewater*, 21st Edition.

Andelman, M.D., and G.S. Walker, U.S. Patent 6,709,560, 2004.

Barrett, E.P., L.G. Joyner, and P.P. Halenda, 1951. "The Determination of Pore Volume and Area Distributions in Porous Substances, I. Computations from Nitrogen isotherms." *J. Am. Chem. Soc*. 73, 373.

Beagle, 2006. "Countercurrent Ion Exchange Applied to CBM Produced Water Treatment in the PRB." In the Proceedings of the Rocky Mountain Unconventional Gas Conference, South Dakota School of Mines and Technology, October 13, 2006.

Bellona, C., and J.E. Drewes, 2006. "Reuse of Produced Water Using Nanofiltration and Ultra-low Pressure Reverse Osmosis to Meet Future Water Demands." In the Proceedings of 2002 GWPC Produced Water Conference, Colorado Spring, Colorado, October 16-17, 2002.

Bick, A., and G. Oron, 2005. "Post-Treatment Design of Seawater Reverse Osmosis Plants: Boron Removal Technology Selection for Potable Water Production and Environmental Control." *Desalination* 178(1-3), 233-246.

Bordjiba, T., M. Mohamedi, and L.H. Dao, 2007. "Synthesis and Electrochemical Capacitance of Binderless Nanocomposite Electrodes Formed by Dispersion of Carbon Nanotubes and carbon aerogels," *Journal of Power Sources* 172 (2), 991-998.

CDPHE, 2004. Colorado Department of Public Health and Environment, Colorado State Board of Health 5 CCR 1003-1 - Colorado Primary Drinking Water Regulations.

CDT Systems, Inc., 2003. *CDT – Activated Water – Emergency Response System*, Technical Report, CDT Systems, Dallas, Texas.

Dean, J.A., 1992. *Lange's Handbook of Chemistry*, 5th Edition, McGraw-Hill Handbooks.

D4189-95, 2002. *Standard Test Method for Silt Density Index (SDI) of Water*, ASTM International.

Desalination and Water Purification Technology Roadmap, 2003. Discussion facilitated by Sandia National Laboratories and the Bureau of Reclamation. Desalination & Water Purification Research & Development Program Report #95.

EPA, 1986. *The Gold Book, Quality Criteria for Water 1986*. http://www.epa.gov/waterscience/criteria/goldbook.pdf.

Farmer, J.C., D.V. Fix, G.V. Mack, R.W. Pekala, and J.F. Poco, 1996. "Capacitive deionization of NH4ClO4 solutions with carbon aerogel electrodes," *J. Appl. Electrochem*. 26, 1007-1018.

Filteau, G., and P. Moss, 1997. "Ultra-low pressure RO membranes:an analysis of performance and cost," *Desalination* 113, 147-152.

Funston, R., R. Ganesh, and L.Y.C. Leong, 2002. "Evaluation of technical and economic feasibility of treating oilfield produced water to create a "New" water resource." In the Proceedings of 2002 GWPC Produced Water Conference, Colorado Springs, Colorado, October 16-17, 2002.

Gabelich, C.J., T.D. Tran, and I.H.M. Suffet, 2002. "Electrosorption of inorganic salts from aqueous solution using carbon aerogels." *Env. Sci. Tech*. 36, 3010-3019.

Hayes, T., and D. Arthur, 2004. Overview of Emerging Produced Water Treatment Technologies, Proceedings of the 11th Annual International Petroleum Environmental Conference, Albuquerque, New Mexico., October 12-15, 2004.

Hou, C-H., C. Liang, S. Yiacoumi, S. Dai, and C. Tsouris, 2006. "Electrosorption capacitance of nanostructured carbon-based materials." *Journal of Colloid and Interface Science* 302, 54-61.

Jurenka, R., S. Martella, and R. Rodriguez, 2001. *Water treatment primer for communities in need, Advanced Water Treatment Research Program Report #68*, Bureau of Reclamation.

Kabay, N., I., Yilmaz, S. Yamac, M. Yuksel, U. Yuksel, N. Yildirim, O. Aydogdu, T. Iwanaga, and K. Hirowatari, 2004. "Removal and recovery of

boron from geothermal wastewater by selective ion-exchange resins - II." Field tests. *Desalination* 167, 427-438.

IOGCC/ALL Consulting, 2006. *A Guide to Practical Management of Produced Water from Onshore Oil and Gas Operations in the United States*. A final report prepared for U.S. Department of Energy, Tulsa, Oklahoma. http://www.all-llc.com/iogcc/prodwtr/ProjInfo.htm

Larson, L.E., 1999. *Water and Wastewater Technology Demonstration Projects*. Consultant Report for California Energy Commission.

Lee, R., R. Seright, M. Hightower, A. Sattler, M. Cather, B. McPherson, L. Wrotenbery, D. Martin, and M. Whitworth, 2002. "Strategies for produced water handling in New Mexico." 2002 Produced Water Meeting, Groundwater Protection Council.

Matthews, M., 2007. *Coalbed methane producers have some new options*. McGraw-Hill Construction/ENR 258, 19.

Morales, G., and M. Barrufet, 2002. *Desalination of Produced Water Using Reverse Osmosis*. http://tamu.edu/

Nadav, N., 1999. "Boron Removal from Seawater Reverse Osmosis Permeate Utilizing Selective Ion Exchange Resin." *Desalination* 124, 131-135.

Nicolaisen, B., 2003. "Developments in Membrane Technology for Water Treatment." *Desalination* 153(1-3), 355-360.

Nicolaisen, B., 2002. "Membrane Filtration of Oil and Gas Field Produced Water." GE Osmonics Report.

Nightingale, E.R., Jr., 1959. "Phenomenological Theory of Ion Salvation: Effective Radii of Hydrated Ions. *J. Phys. Chem*. 63, 1381-1387.

Oh, H-J., J-H., Lee, H-J Ahn,, Y, Joeng, Y-J Kim, and C-S Chi, 2006. "Nanoporous Activated Carbon Cloth for Capacitive Deionization of Aqueous Solution." *Thin Solid Films* 515 (1), 220-225.

Pastor, M. R., A.F. Ruiz, M.F. Chillon, and D.P. Rico, 2001. "Influence of pH in the Elimination of Boron by Means of Reverse Osmosis," *Desalination* 140, 145-152.

Pekala, R.W., J.C. Farmer, C.V. Alviso, T.D. Tran, S.T. Mayer, J.M. Miller, and B. Dunn, 1998. "Carbon Aerogels for Electrochemical Applications." *J. Non-Cryst Solids* 225, 74-80.

Redondo, J., M. Busch, and J.P. De Witte, 2003. "Boron Removal from Seawater Using FILMTEC (TM) High Rejection SWRO Membranes." *Desalination* 156, 229-238.

Roskill Report, 2002. *The Economics of Iodine*, 8th ed.

Rowe, D.R., and I.M. Abdel-Magid, 1995. *Handbook of Wastewater Reclamation and Reuse*. CRC Press, Inc.

Ryoo M-W., J-H Kim, and G. Seo, G., 2003. "Role of Titania Incorporated on Activated Carbon Cloth for Capacitive Deionization of NaCl Solution." *Journal of Colloid and Interface Science* 264, 414-419.

Shiue, L-B., W-T Hung, G-N Chou, S-Y Wang, and I-C Chiu, 2005. "Energy-Effective Desalination with Online Sterilization Using Capacitors," Proceedings of IDA World Congress, Singapore, September 2005.

Spiegel, E.F., and Y.M. El-Sayed, 2001. "The Energetics of Desalination Processes. *Desalination* 134, 109-28.

Spitz, L.R., 2003. "Advanced Mobile Water Treatment Systems for Treating Coal Bed Methane Produced Water." Paper presented at the 2003 Ground Water Protection Council Meeting.

Taniguchi, M., Y. Fusaoka, T. Nishikawa, and M. Kurihara, 2004. "Boron Removal in RO Seawater Desalination. *Desalination* 167, 419-426.

Tran, T.D., J.C. Farmer, and R.W. Pekala, 2003. "Carbon Aerogels and Their Applications in Supercapacitors and Electrosorption Processes." http://www.vacets.org/vtic97/tdtran.htm.

Veil, J., M. Puder, and D. Elcock, 2004. "A White Paper Describing Produced Water from Production of Crude Oil, Natural Gas, and Coal Bed Methane," a final report prepared for U.S. Department of Energy. Argonne National Laboratory, Chicago, Illinois. http://www.netl.doe.gov/publications/oil_pubs/prodwaterpaper.pdf

Welgemoed, T.J., and C.F. Schutte, 2005, "Capacitive Deionization Technology: An Alternative Desalination Solution. *Desalination* 183(1-3), 327-340.

Visvanathan, C., P. Svenstrup, and AP. riyamethee, 2000. "Volume Reduction of Produced Water Generated from Natural Gas Production Process Using Membrane Technology," *Water Science & Technology* 41(10-11), 117-123.

Weinthal, E., Y, Parag, A. Vengosh, A. Muti, and W. Kloppman, 2005. *European Environment*, 15, 1-12.

Wiesner, M.R., and P. Aptel, 1996. Chapter 4, "Mass Transport and Permeate Flux and Fouling in Pressure Driven Processes," *Water Treatment Membrane Processes*, Editors, J. Mallevialle, P. Odendaal, and M.R. Wiesner, McGraw-Hill.

Wilf, M., and C. Bartels, 2005. "Optimization of Seawater RO Systems Design," *Desalination* 173, 1-12.

Xu, P., and J.E. Drewes, 2006. "Viability of Nanofiltration and Ultra Low Pressure Reverse Osmosis Membranes for Multi-Beneficial Use of Methane Produced Water," *Separation & Purification Technology* 52, 67-76.

Xu, P., J.E. Drewes, and D. Heil, 2008. "Beneficial Use of Co-Produced Water through Membrane Treatment: Technical-Economic Assessment. *Desalination* (in press).

Yang, K-L., T-Y Ying, S. Yiacoumi, C. Tsouris, and E.S. Vittoratos, 2001. "Electrosorption of Ions from Aqueous Solutions by Carbon Aerogel: An Electrical Double Layer Model," *Langmuir* 17, 1961-1969.

Yang, C-Y., W-H Choi, B-K Na, B.W. Cho, and W.I. Cho, 2005. Capacitive Deionizaton of NaCl Solution with Carbon Aerogel-Silica Gel Composite Electrodes," *Desalination* 174, 125-133.

Ying, T-Y., K-L Yang , S. Yiacoumi, and C. Tsouris, 2002. "Electrosorption of Ions from Aqueous Solutions by Nanostructured Carbon Aerogel," *Journal of Colloids and Interface Science* 250, 18-27.

Zhang, D., L. Shi, J. Fang, K. Dai, and X. Li, 2006. "Preparation and Desalination Performance of Multiwall Carbon Nanotunes," *Materials Chemistry and Physics* 97, 415-419.

Abstract

Large volumes of produced water are generated during natural gas production. Beneficial use of produced water has become an attractive solution to produced water management by providing additional and reliable water supplies and reducing the cost for disposal. The produced water extracted from a sandstone aquifer in eastern Montana was characterized as brackish groundwater of sodium chloride type with total dissolved solids (TDS) concentration of 5,520±718 mg/L, absence of hydrocarbons, and elevated iodide with a concentration of 49.9±8.2 mg/L. As an important industrial product, recovering iodide from the brine will bring additional economic benefits to produced water treatment besides water reuse and reduced disposal volume.

The advent of ultra-low pressure RO (ULPRO) membranes and nanofiltration (NF) membranes with high desalting degree could offer a viable option for produced water treatment because they can be as effective as RO in removing certain solutes from water while requiring considerably less feed pressure. Capacitive deionization technology (CDT) with carbon-aerogel electrodes represents an attractive novel process in desalination of brackish source water due to its low fouling potential, ambient operational conditions, electrostatic regeneration, and low voltages.

The treatment objective of this study was to compare NF/ULPRO membranes with CDT in treating produced water to provide a water quality that meets (1) irrigation water quality standards (TDS of 500–1,000 mg/L), (2) potable water quality standards (primary and secondary MCLs), and (3) allows an economical way to recover iodide. The study was designed for a period of 12 months with four main tasks. The study included: (1) comprehensive water quality analysis to identify constituents in produced water critical for membrane and CDT treatment; (2) bench-scale membrane tests to select membranes with high salt and iodide rejection and low fouling potential; and (3) laboratory-scale membrane testing with focus on recoveries and rejection of the produced water by the selected ULPRO and NF membranes. The tests allow transfer of research results to full-scale applications; (4) bench-scale CDT tests with focus on operational parameters, fouling behavior of electrodes, regeneration effectiveness, and desalting efficiency; (5) CDT field-scale tests to identify key operational parameters and performance; and (6) technical-economic assessment of the proposed technologies based on a variety of technical-economic criteria derived from laboratory and field tests, water quality modeling, and cost analysis.

The studied candidate membranes included one conventional RO membrane (TFC-HR, Koch Membrane Systems), three ULPRO membranes XLE (Dow/Filmtec), TFC-ULP (Koch) and TMG-10 (Toray America), and three NF

membranes NF-90 (Dow/Filmtec), TFC-S (Koch), and ESNA (Hydranautics). Bench-scale, cross-flow, flat-sheet test units were employed to assess the candidate membranes using the produced water with focus on fouling potential, iodide recovery, and general salt rejection. The degree of flux decline was found to be dependent upon the physico-chemical properties of the membranes. Hydrophobic and rough membranes exhibited a higher flux decline and lower chemical cleaning efficiency than smooth and/or hydrophilic membranes. Flux decline experiments, in-situ microscopic techniques, and analysis of elemental composition and functional groups revealed that the pretreatment, including microfiltration, pH adjustment, and addition of antiscalants could alleviate membrane fouling significantly. Chemical cleaning using caustic and anionic surfactant solutions restored membrane permeability more efficiently than hydraulic cleaning or using acids and metal chelating agents.

Based on the membrane performance with regard to adjusted specific flux and rejection of salts and iodide, the TMG-10, TFC-ULP, and NF-90 membranes were selected for further testing and compared to the RO membrane TFC-HR using a two-stage laboratory-scale membrane unit. The nanofiltration membrane NF-90 required a low pressure to produce a high permeate flux. The rejection of the NF-90, however, was much lower in comparison to the TFC-HR, TFC-ULP, and TMG-10, especially regarding the intended iodide recovery. The permeate quality of the NF-90 could not meet the drinking water standard for TDS. The two ULPRO membranes exhibited a high permeate flux while displaying a competitive rejection in comparison to the conventional RO membrane TFC-HR, notably the TMG-10, which showed a very stable rejection at low and high recoveries (flow-through and internal recycling regimes). In comparison to the RO membrane, cost analysis showed that an ULPRO membrane system provided lower overall cost while meeting the drinking water standards ($0.97–$1.28 vs. $1.02–$1.34 per 1,000 gallons of product water). The ULPRO and NF membranes provided an identical cost ($0.89 per 1,000 gallons of product water) for treating produced water to irrigation water standards. Iodide recovery was higher in the concentrate stream from the RO system than ULPRO (>126 mg/L vs. >107 mg/L). All the tested membranes exhibited a low rejection of boron, which would require further treatment, such as two-pass RO in order to meet water quality standards for either irrigation or potable use.

The performance of the CDT system was consistent throughout the bench-scale experiments and duration of the field test, indicating that scaling of the aerogel electrodes was not a problem when treating this water source. The sorption capacity of carbon aerogel (in mol/g aerogel) in treating the produced water was found following the order of Na>>Ca>Mg>K for cations, and Cl>>Br>I for anions. The maximum percentage removal, however, followed a different trend in the order of organic acids (in terms of UVA at 254 nm, 83.3%) > iodide (77%)

> Br (62.5%) > Ca (40.7%) > alkalinity (in terms of CaCO3, 40.0 %) > Mg (34.3%) > Na (18.4%)> Cl (16.0%). Adsorption of organic matter into the aerogel material occurred during regeneration when the cell was uncharged, which might result in potential electrode fouling by clogging the interstitial pores. The boron removal rate was very low within the operating pH range; however, the rate could be improved by increasing the pH of the feed water above 9.5. The consumed energy per gram of removed salts increased exponentially with the applied energy. The minimum energy consumption was 0.00021 kWh/g salts removed at applied current of 15 or 30 amps for both sorption and regeneration. The treatment efficiency of CDT maintained a constant level over the multiple stages with sorption about 2.8–3.2 mg TDS/g aerogel. Iodide could be recovered in the first and second stages of the process by collecting the fraction of regenerant with high iodide concentration.

Membrane technologies provided a better overall performance in terms of product water quality and iodide recovery. Water cost of CDT process was much higher than all membrane products tested due to the low product water recovery (25–33 percent vs. 75 percent) and high capital cost. Unlike membrane process, electrode fouling was not observed throughout the laboratory and field tests. Capacitive deionization exhibited an alternative to desalination technologies. The efficiency and production capacity of the system needs to be improved before CDT will become economically feasible to treat water of this level of salinity (TDS > 5,000 mg/L).

The partners of the project included:

- CDT Systems, Inc., providing CDT testing units and technical support.
- Mendell Energy, Inc., assisting in field test and data analysis.

The outreach of the project includes:

Peer-reviewed papers:

1. Xu, P., Drewes, J.E., Heil, D. and Wang, G. (2008) Treatment of brackish produced water using carbon aerogel based capacitive deionization technology. Water Research, in press.

2. Xu, P., Drewes, J.E., and Heil, D (2008). Beneficial use of co-produced water through membrane treatment: technical-economic assessment. Desalination, in press.

3. Xu, P., Drewes, J.E. (2006) Viability of Nanofiltration and Ultra Low Pressure Reverse Osmosis Membranes for Multi-Beneficial Use of Methane Produced Water. Separation & Purification Technology, 52, 67-76.

Conference presentations:

1. Xu, P. and Drewes, J. E. (2006). Multi-beneficial use of produced water through high-pressure membranes and capacitive deionization technology. Produced Water Workshop. April 4-5, 2006, Fort Collins, Colorado.

2. Xu, P. and Drewes, J. E. (2006) Multi-beneficial use of co-produced water through high-pressure membrane treatment. AMTA Biennial Conference "Desalination Comes of Age – The Answer for New Supplies" July 30 – August 2, 2006, Anaheim, California.

3. Xu, P., Drewes, P.E., Wang, G. and Heil, D. (2006). Field study on capacitive deionization for produced water reuse. 2006 Water Quality Technology Conference (WQTC), Denver, Colorado, November 5-9, 2006.

4. Xu, P., Heil, D. and Drewes, J. E. (2005) Viability of capacitive deionzation technology (CDT) in water reuse and desalination. 20th Annual Watereuse Symposium on Water reuse & desalination, Denver, Colorado. September 18-21, 2005.

5. Drewes, J.E., and Xu, P. (2004) Multi-beneficial use of co-produced water through high-pressure membrane treatment and capacitive deionzation technology. EUWP Conference, Golden, Colorado. June 22, 2005.

Education:

Two 3-credit hour independent studies of graduate students.

SI Metric Conversion Table

English Unit	Convert to SI unit	Multiply by
Temperature		
F	C	(F-32)*5/9
Volume		
gallons	L	3.7854
Flow		
gpd	m^3/d	$3.785*10^{-3}$
mgd	m^3/d	$3.785*10^{3}$
gpm	m^3/s	$6.308*10^{-5}$
gph	m^3/h	$3.785*10^{-3}$
Flux		
gpd/ft^2 (gfd)	m/d	0.0407
Area		
in^2	cm^2	6.4518
ft^2	m^2	0.092903
Length		
in	mm	25.4
ft	m	0.3048
Pressure		
psi	kPa	6.9848
Weight		
lb	g	453.6

Appendix 1: Raw Data for Figures

Figure 4. Pore size distribution of carbon aerogel

Pore Diameter Range (Å)	Average Diameter (Å)	Incremental Pore Volume (cm^3/g)	Cumulative Pore Volume (cm^3/g)	Incremental Pore Area (m^2/g)	Cumulative Pore Area (m^2/g)
6164.8 - 671.1	730.977	0.001	0.001	0.070	0.070
671.1 - 286.7	342.605	0.001	0.002	0.079	0.149
286.7 - 212.2	237.958	0.000	0.002	0.078	0.227
212.2 - 207.3	209.705	0.000	0.003	0.031	0.258
207.3 - 165.2	181.268	0.000	0.003	0.101	0.359
165.2 - 120.6	135.631	0.002	0.005	0.452	0.812
120.6 - 117.8	119.200	0.001	0.005	0.194	1.006
117.8 - 101.7	108.474	0.001	0.006	0.492	1.498
101.7 - 76.9	85.602	0.008	0.014	3.631	5.129
76.9 - 67.3	71.413	0.009	0.023	4.842	9.971
67.3 - 57.7	61.713	0.016	0.039	10.466	20.437
57.7 - 49.0	52.578	0.022	0.061	16.534	36.971
49.0 - 43.0	45.536	0.019	0.080	16.659	53.629
43.0 - 38.0	40.147	0.018	0.097	17.475	71.104
38.0 - 34.0	35.781	0.020	0.117	22.489	93.593
34.0 - 29.9	31.635	0.056	0.173	70.752	164.345
29.9 - 26.5	27.935	0.002	0.176	3.567	167.912
26.5 - 23.2	24.589	0.001	0.176	1.024	168.936
23.2 - 21.6	22.308	0.000	0.177	0.266	169.203

Figure 11. Reduction in permeate flux over time

Figure 11 (a)

NF-90 with antiscalant		NF-90 without antiscalant	
Filtration time (hours)	Flux decline (J/Jo)	Filtration time (hours)	Flux decline (J/Jo)
0.5	1	0.5	1
1.0	1.00	1.0	0.99
2.5	0.93	2.0	0.87
3.5	0.92	3.5	0.77
5.0	0.90	4.5	0.77
18.5	0.83	6.0	0.77
30.0	0.70	8.0	0.77
43.0	0.69	12.0	0.69
50.0	0.67	24.0	0.64
68.0	0.67	27.0	0.63
70.0	0.69	30.0	0.61
73.5	0.66	33.0	0.60
74.4	0.66	36.0	0.59
		49.5	0.55

Figure 11 (b)

TMG-10 with antiscalant		TMG-10 without antiscalant	
Filtration time (hours)	Flux decline (J/Jo)	Filtration time (hours)	Flux decline (J/Jo)
0.3	1	0.5	1
0.5	1.00	1.0	0.88
1.0	0.97	2.0	0.84
2.0	95.48	3.5	0.81
3.0	0.94	4.5	0.80
4.0	0.92	6.0	0.80
6.0	0.90	8.0	0.77
8.0	0.89	12.0	0.76
20.0	0.87	24.0	0.75
22.0	0.83	27.0	0.75
24.0	0.80	30.0	0.73
26.0	0.79	33.0	0.72
28.0	0.80	36.0	0.70
44	0.78	49.5	0.64
46	0.78		
50	0.78		
53	0.78		
69	0.77		
71	0.77		
73	0.77		
77	0.77		

Figure 12. Reduction in permeate flux over time

Filtration time (hours)	Flux decline (J/Jo)	
	TFC-S	XLE
0.3	1	1
0.5	1	1
1	0.96	0.71
2	0.89	0.61
3	0.86	0.59
4	0.82	0.58
6	0.79	0.58
8	0.79	0.55
18.5	0.71	0.47
22.5	0.71	0.47
26.5	0.69	0.48
42.5	0.64	0.47
50.5	0.64	0.47
66.5	0.62	0.47
70.5	0.64	0.48
90.5	0.61	0.48
98.5	0.61	0.47
114.5	0.61	0.46
122.5	0.61	0.45
138.5	0.61	0.45
145.5	0.61	0.44

Figure 13. Reduction in permeate flux over time

TFC-HR		TFC-ULP		TMG10		ESNA		NF-90		TFC-S		XLE	
Time (hours)	J/Jo	Time (hours)	J/Jo	Time (hours)	J/Jo	Time (hours)	J/Jo	Time (hours)	J/Jo	Time (hours)	J/Jo	Time (hours)	J/Jo
0.5	1	0.3	1.00	0.3	1	0.5	1	0.5	1	0.3	1	0.3	1
1.0	0.96	0.5	1.00	0.5	1.00	1.0	0.93	1.0	1.00	0.5	1	0.5	1
2.0	0.96	1.0	0.92	1.0	0.97	2.5	0.92	2.5	0.93	1.0	0.96	1.0	0.71
3.0	0.92	2.0	0.91	2.0	95.48	3.5	0.90	3.5	0.92	2.0	0.89	2.0	0.61
6.0	0.92	3.0	0.91	3.0	0.94	5.0	0.84	5.0	0.90	3.0	0.86	3.0	0.59
8.0	0.88	4.0	0.89	4.0	0.92	18.5	0.85	18.5	0.83	4.0	0.82	4.0	0.58
25.0	0.83	6.0	0.89	6.0	0.90	30.0	0.83	30.0	0.70	6.0	0.79	6.0	0.58
31.0	0.81	8.0	0.89	8.0	0.89	43.0	0.81	43.0	0.69	8.0	0.79	8.0	0.55
49.0	0.77	20.0	0.87	20.0	0.87	50.0	0.80	50.0	0.67	18.5	0.71	18.5	0.47
55.0	0.77	22.0	0.85	22.0	0.83	68.0	0.78	68.0	0.67	22.5	0.71	22.5	0.47
61.0	0.77	24.0	0.84	24.0	0.80	70.0	0.79	70.0	0.69	26.5	0.69	26.5	0.48
79.0	0.77	26.0	0.84	26.0	0.79	73.5	0.77	73.5	0.66	42.5	0.64	42.5	0.47
		28.0	0.81	28.0	0.80	74.4	0.77	74.4	0.66	50.5	0.64	50.5	0.47
		44.0	0.79	44.0	0.78					66.5	0.62	66.5	0.47
		46.0	0.79	46.0	0.78					70.5	0.64	70.5	0.48
		50.0	0.77	50.0	0.78					90.5	0.61	90.5	0.48
		53.0	0.77	53.0	0.78					98.5	0.61	98.5	0.47
		69.0	0.77	69.0	0.77					114.5	0.61	114.5	0.46
		71.0	0.77	71.0	0.77					122.5	0.61	122.5	0.45
		73.0	0.77	73.0	0.77					138.5	0.61	138.5	0.45
		77.0	0.76	77.0	0.77					145.5	0.61	145.5	0.44

Figure 14. Correlation of normalized permeate flux (J/Jo) as a function of contact angle and surface roughness of virgin membranes

Membrane	TFC-HR	TFC-ULP	TMG-10	ESNA	NF-90	TFC-S	XLE
contact angle	35	38	54.5	57	63.2	57.4	66.3
roughness (nm)	64	42	44	29	64	73	73
J/Jo	0.77	0.765	0.776	0.77	0.66	0.63	0.47

Figure 19. Permeate flux of TMG-10 membrane at different stages of fouling, hydraulic cleaning, and chemical cleaning procedures

Fouling	Time (hours)	0.50	1.00	2.00	3.50	4.50	6.00	8.00	12.00	24.00	27.00	30.00	33.00	36.00	49.50
	J/Jo	1.00	0.88	0.84	0.81	0.80	0.80	0.77	0.76	0.75	0.75	0.73	0.72	0.70	0.64
DI	Time (hours)	54.67	55.00	55.33	55.67	60.00	65.00	75.17							
	J/Jo	0.77	0.76	0.74	0.73	0.72	0.70	0.65							
NaOH	Time (hours)	80.42	81.00	82.00	85.00	90.00	100.00	110.00	120.42	130.00	140.00	150.00	160.42		
	J/Jo	0.84	0.83	0.80	0.78	0.76	0.74	0.72	0.70	0.69	0.67	0.65	0.65		
HCl	Time (hours)	165.58	166.00	167.00	168.00	171.08									
	J/Jo	0.70	0.69	0.69	0.68	0.68									
Citric acid	Time (hours)	174.25	175.00	175.50	176.00	177.75									
	J/Jo	0.70	0.69	0.69	0.68	0.68									
NaOH	Time (hours)	182.92	183.20	183.70	185.00	187.00	200.00	209.92							
	J/Jo	0.86	0.85	0.78	0.74	0.70	0.61	0.60							
EDTA	Time (hours)	210.08	210.50	211.00	212.00	214.00	216.08	220.58							
	J/Jo	0.80	0.79	0.76	0.74	0.72	0.71	0.71							
SDS	Time (hours)	225.75	226.10	226.60	227.60	230.00	249.75								
	J/Jo	0.84	0.82	0.79	0.76	0.75	0.66								

Figure 20. Permeate flux of (a) TMG-10 and (b) NF-90 membranes at different stages of fouling, and cleaning procedures

Figure 20(a) TMG-10

Fouling	Time (hours)	0.50	1.00	2.50	3.50	5.00	18.50	30.00	43.00	50.00	68.00	70.00	73.50	74.40
	J/Jo	1.00	0.93	0.92	0.90	0.84	0.85	0.83	0.81	0.80	0.78	0.79	0.77	0.77
DI	Time (hours)	77.82	78.15											
	J/Jo	0.80	0.79											
NaOH	Time (hours)	81.65	82.40	83.40	85.40	96.65	98.65	102.65	106.65	120.65				
	J/Jo	0.99	1.00	0.99	0.98	0.93	0.93	0.90	0.90	0.84				
SDS	Time (hours)	124.15	126.65	130.15										
	J/Jo	1.00	0.98	0.88										

Figure 20(b) NF-90

Fouling	Time (hours)	0.50	1.00	2.50	3.50	5.00	18.50	30.00	43.00	50.00	68.00	70.00	73.50	74.40
	J/Jo	1.00	1.00	0.93	0.92	0.90	0.83	0.70	0.69	0.67	0.67	0.69	0.66	0.66
DI	Time (hours)	77.82	78.15											
	J/Jo	0.67	0.65											
NaOH	Time (hours)	81.65	82.40	83.40	85.40	96.65	98.65	102.65	106.65	120.65				
	J/Jo	0.75	0.74	0.69	0.67	0.67	0.65	0.64	0.62	0.59				
SDS	Time (hours)	124.15	126.65	130.15										
	J/Jo	0.75	0.72	0.66										

Figure 21. Rejection of TOC and UV absorbance at 254 nm in (a) FT and (b) IR flow regimes

Figure 21(a)				
Rejection (%)	NF90	TFC-HR	TFC-ULP	TMG10
TOC	84.0	73.8	84.5	84.3
UV 254	74.0	79.8	75.1	76.0
Figure 21(b)				
Rejection (%)	NF90	TFC-HR	TFC-ULP	TMG10
TOC	80.0	75.4	84.8	84.1
UV 254	77.3	85.7	82.3	84.4

Figure 22. Rejection of boron, barium, calcium, magnesium, sodium and silicon in (a) FT and (b) IR flow regimes

Figure 22(a)				
Rejection (%)	NF90	TFC-HR	TFC-ULP	TMG10
B	53.8	58.4	36.0	54.6
Ba	99.6	99.6	99.5	99.5
Ca	98.7	99.9	99.7	99.8
Mg	98.7	100.0	99.8	99.9
Na	93.3	98.7	97.6	98.2
Si	96.6	99.2	98.2	99.1
Figure 22(b)				
Rejection (%)	NF90	TFC-HR	TFC-ULP	TMG10
B	48.4	30.4	39.2	55.6
Ba	98.9	99.3	99.7	99.8
Ca	98.5	99.2	99.7	99.7
Mg	98.8	99.3	99.8	99.9
Na	91.1	96.0	96.9	97.8
Si	96.2	96.6	98.1	98.3

Figure 24. EC of CDT effluent during treatment of 500 mg/L NaCl at a flow rate of 250 mL/min

Time (min)	EC (uS/cm)
0	1097
5	1081
10	994
15	906
20	849
25	821
30	804
35	805
40	810
45	812
50	828
55	832
60	848
65	860
70	875
75	887
80	890
85	897
90	907
95	934
100	953
105	958
110	971
115	976

Figure 25. Treatment procedure of one cycle

Time (min)	EC (uS/cm)
0	10.2
5	10.19
10	10.18
15	10.18
20	10.15
25	10.13
30	10.08
45	8.49
50	8.7
55	9.2
60	9.41
65	9.57
70	9.67
75	9.74
80	9.79
85	9.82
90	9.84
140	11.89
150	11.89
155	10.98
160	10.28
165	10.16
180	8.51
185	8.77
190	9.29
195	9.41
200	9.67
205	9.74
210	9.81
215	9.86
220	9.9
225	9.92

Figure 26. Reduction in EC achieved after successive treatment of 10 mS/cm water

Time (min)	EC (uS/cm)	Time (min)	EC (uS/cm)
0	10.2	315	9.11
5	10.19	320	9.43
10	10.18	325	9.59
15	10.18	330	9.72
20	10.15	335	9.79
25	10.13	340	9.83
30	10.08	345	9.87
45	8.49	350	9.92
50	8.7	400	11.85
55	9.2	405	12.05
60	9.41	410	12.12
65	9.57	415	11.2
70	9.67	420	10.62
75	9.74	425	10.47
80	9.79	435	8.68
85	9.82	440	8.74
90	9.84	445	9.24
140	11.89	450	9.54
150	11.89	455	9.69
155	10.98	460	9.79
160	10.28	465	9.86
165	10.16	470	9.91
175	8.51	475	9.96
180	8.77	480	9.98
185	9.29	540	11.92
190	9.41	545	12.14
195	9.67	550	12.16
200	9.74	555	11.3
205	9.81	560	10.63
210	9.86	565	10.48
215	9.9	575	8.73
220	9.92	580	8.91
260	11.75	585	9.27
270	11.9	590	9.55
275	11.93	595	9.68
280	11.93	600	9.8
285	11.08	605	9.86
290	10.56	610	9.92
295	10.44	615	9.98
305	8.68	620	10
310	8.77		

Figure 27. Treatment of high salinity water using 10 mS/cm water for rinsing

Time (min)	EC (uS/cm)	Time (min)	EC (uS/cm)	Time (min)	EC (uS/cm)
0	10.06	310	**12.71**	672	5.92
11	8.37	315	**12.72**	673	5.96
12	8.37	325	10.6	674	5.95
13	8.4	330	10.35	675	5.94
14	8.44	346	7.25	680	5.9
15	8.48	347	7.26	685	5.9
16	8.52	348	7.28	690	5.96
17	8.59	349	7.27	695	6
18	8.65	350	7.24	745	12.6
19	8.75	355	7.19	750	**12.62**
20	8.85	360	7.23	760	**10.46**
25	9.21	365	7.32	765	10.28
30	9.39	370	7.44	781	5.7
35	9.52	420	11.34	782	5.7
85	11.52	425	11.21	783	5.71
90	11.53	435	10.32	784	5.68
100	10.5	440	10.21	785	5.67
105	10.21	451	6.73	790	5.6
121	8.1	452	6.71	795	5.56
122	8.12	453	6.71	800	5.57
123	8.12	454	6.7	805	5.62
124	8.12	455	6.68	855	12.62
125	8.11	460	6.65	860	12.62
126	8.1	465	6.7	875	10.37
127	8.12	470	6.78	880	10.29
128	8.15	475	6.85	901	5.62
129	8.16	525	12.57	902	5.58
130	8.19	530	**12.59**	903	5.56
135	8.37	540	**10.47**	904	5.52
140	8.55	545	10.31	905	5.47
145	8.66	561	6.53	910	5.37
195	12.35	562	6.46	915	5.29
200	12.38	563	6.42	920	5.31
215	10.55	564	6.38	925	5.33
220	10.33	565	6.33	970	10.43
236	7.7	570	6.22	975	10.43
237	7.7	575	6.06	1001	5.1
238	7.71	580	6.12	1002	5.05
239	7.7	585	6.18	1003	5.05
240	7.68	635	12.72	1004	5.05
245	7.67	640	12.72	1005	5.05
250	7.76	650	10.42	1010	4.95
255	7.88	655	10.25	1015	4.94
260	8	671	5.93	1020	4.93

Figure 29. Effect of temperature on removal of different constituents from produced water (Batch recycling operation using laboratory bench-scale unit)

	25 °C		12 °C	
	Rejection (%)	Std	Rejection (%)	Std
EC	6.7	0.8	7.0	1.0
I	69.7	2.3	65.8	4.9
Ca	22.0	18.5	16.4	17.1
Mg	21.7	15.3	16.3	14.2
Sr	22.5	17.8	18.0	16.8
Na	8.1	3.6	13.2	2.4
K	21.3	0.0	15.7	2.8
B	2.7	3.4	2.3	3.9

Figure 30. Effect of flow rate and feed concentration on operational sorption capacity and average sorption rate of the carbon aerogels using synthetic water. The error bars represent the standard deviation of 3 to 5 runs of each testing condition. (a) Feed flow rate 250 mL/min using laboratory bench-scale unit; (b) Feed TDS 500 mg/L using pilot-scale testing unit.

Figure 30 (a)					
Feed TDS concentration (mg/L)	500	1000	2000		5000
Sorption (mg TDS/g aerogel)	2.37	4.062	5.65		5.95
Sorption rate (mg TDS/g aerogel/min)	0.0395	0.0677	0.0941667		0.0991667
Figure 30 (b)					
Flow rate (mL/min)	700	1000	2000	2500	3000
Salt feeded (mg/min)	350	500	1000	1250	1500
Sorption (mg TDS/g aerogel)	3.17	2.94	2.81	2.44	2.46
Std	0	0.32	0.31	0.26	0.25
Average sorption rate (mg/g/min)	0.013	0.03559	0.0358	0.04031	0.05169
Std	0	0.00262	0.0016	0.00215	0.005

Figure 31. Effect of TDS loading on sorption rate of carbon aerogel. The error bars represent the standard deviation of 3 to 5 runs of each testing condition

TDS loading (mg TDS/g aerogel min)	0.056	0.081	0.161	0.202	0.242	0.554	0.923	1.258
Sorption rate (mg/g/min)	0.013	0.036	0.036	0.040	0.052	0.095	0.094	0.071
Std	0.000	0.003	0.002	0.002	0.005	0.018	0.027	0.006

Figure 32. Treatment of various constituents in the produced water using 1-stage two aquacells in series at flow rate of 560 mL/min and regeneration rate of 1,900 mL/min

Sample	Treatment Time		Conduct.	UVA_{254}	Concentration (mg/L)								
	(Hr:Min)	pH	(mS/cm)	(/cm)	Total Alkalinity (CaCO3)	TOC	Ca	Mg	B	Na	Cl	I	Br
Feed	0:11	8.27	11.4	0.1623	240		32.7	12.2	**3.8**	2430	4238	39	67
(Feed)	0:35	8.31	11.34				32.7	12.2					
Feed 2	1:51	8.3	11.42	0.1584	260		33.2	12.4	**3.8**	2406	4255	39	65
(Feed)	2:14	8.29	11.3				33.2	12.4					
(Feed)	3:47	8.21	11.25				33.2	12.4					
(Feed)	5:45		11.25				33.2	12.4				39	
Effl. 1	0	8.1	12.37	0.1497	278	1.06	36.9	13.9	**3.2**	2635	4598	32	75
Effl. 2	0:07	8.27	11.5	0.0963	278	1.07	31.0	12.0	**3.2**	2445	4324	23	65
Effl. 3	0:15	8.38	10.65	0.0569	264	0.80	25.5	10.2	**3.3**	2228	3986	16	49
Effl. 4	0:24	8.7	9.97	0.0431	254	0.72	22.0	9.0	**3.3**	2086	3667	13	41
Effl. 5	0:32	8.9	9.72	0.0368	260	0.69	19.9	8.2	**3.3**	2026	3658	12	40
Effl. 6	0:40	9	9.62	0.0347	272	0.64	19.8	8.2	**3.4**	2019	3556	11	37
Effl. 7	0:48	9.09	9.56	0.031	264	0.63	19.4	8.1	**3.5**	1984	3600	10	35
Effl. 8	0:57	9.11	9.75	0.0366	236	0.64	19.2	8.0	**3.4**	2075	3659	10	35
Effl. 9	1:06	9.06	10.01	0.0271	264	0.65	20.8	8.8	**3.6**	2111	3787	9	35
Effl. 10	1:14	9.07	10.12	0.0299	258	0.70	21.6	9.1	**3.6**	2188	3835	10	38
Effl. 11	1:23	8.98	10.57	0.0269	240	0.69	21.7	9.3	**3.5**	2208	3701	10	25
Effl. 12	1:31	8.58	11.65	0.0442	254	0.92	29.8	12.4	**3.5**	2300	3837	16	34
Effl. 13	1:40	7.97	13.41	0.2057	256	0.63	50.4	18.2	**3.9**	2429	4470	39	73
Effl. 14	1:48	8.24	12.68	0.3761	218	0.05	50.3	17.0	**4.6**	2600	4123	107	75
Effl. 15	1:55	8.62	11.64	0.2533	194	0.16	38.5	13.3	**4.5**	2424	3745	79	55
Effl. 16	2:01	8.85	10.95	0.1327	188	0.24	36.0	12.4	**4.6**	2337	3545	51	43
Effl. 17	2:09	8.68	10.5	0.1038	150	0.78	32.9	11.5	**4.8**	2218	3330	36	40
Effl. 18	2:17	8.01	9.98	0.0923	144	0.86	28.9	10.3	**4.9**	2145	2812	24	31
Effl. 19	2:27	7.9	9.42	0.0826	148	0.81	24.3	9.0	**4.7**	2083	2963	17	29
Effl. 20	2:41	7.87	9.16	0.0505	148	0.85	21.1	8.2	**4.2**	2012	2937	12	27
Effl. 21	2:53	8.17	9.16	0.0396	166	0.81	21.5	8.3	**4.5**	1927	2954	11	25
Effl. 22	3:03	8.3	9.29	0.0635	180	0.97	21.2	8.5	**4.1**	1958	3049	10	27
Effl. 23	3:18	8.58	9.57	0.0325	214	0.77	21.8	8.8	**3.9**	2183	3133	11	26
Effl. 24	3:29	8.66	9.86	0.0324	230	0.82	22.3	9.0	**3.7**	2207	3230	10	26
Effl. 25	3:36	8.01	10.92	0.0548	256	1.05	27.4	11.1	**3.6**	2389	3643	14	32
Effl. 26	3:45	7.66	12.1	0.1057	242	1.44	36.3	14.3	**3.4**	2846	4083	23	46
Effl. 27	3:53	7.57	13.18	0.2932	248	0.22	50.0	17.6	**3.6**	3085	4484	73	74
Effl. 28	4:01	7.76	12.35	0.3393	236	0.19	44.9	15.2	**3.8**	2785	4177	96	66
Effl. 29	4:09	8.04	10.98	0.1841	208	0.42	32.8	11.6	**3.9**	2417	3683	44	49
Effl. 30	4:17	8.27	10.34	0.0873	210	0.77	28.4	10.4	**3.9**	2417	3467	28	41

Figure 33. Multiple sorption and regeneration cycles of once-through operation by two-stage aquacells (two cells in series). (a) Conductivity; (b) Iodide

Date	sample #	Time sampled	Treatment time (Hr:Min)	Temp (ºC)	pH	Conductivity (mS/cm)	[I-] (mg/L)
8/20/2005	Feed	11:22	0:00	19.5	8.09	9.86	13.5
	Feed	12:56	1:34			9.86	13.5
	(Feed)*	13:03	1:41			11.31	40.0
	(Feed)	13:04	1:42	20.1	8.24	11.31	40.0
	(Feed)*	13:40	2:18			11.31	40.0
	Feed 2	13:43	2:21	22.2	8.56	9.65	13.2
	(Feed)*	14:54	3:32			9.65	13.2
	(Feed)	14:55	3:33	23.8	8.13	11.26	40.0
	(Feed)*	15:26	4:04			11.26	40.0
	(Feed)	15:27	4:05	24.2	8.47	9.66	13.5
	(Feed)*	15:40	4:18			9.66	13.5
8/22/2005	(Feed)	10:27	4:16	21.6	8.31	11.2	40.0
	Feed	10:35	4:24	21	8.56	9.86	14.4
	(Feed)*	12:19	6:08			9.86	14.4
	Feed 2	12:20	6:09	22.1	8.36	11.31	39.5
	(Feed)*	13:05	6:54			11.31	40.0
8/20/2005	Effl. 1	11:22	0:00	20.2	7.83	12.17	66.3
	Effl. 2	11:33	0:11	20.7	8.45	9.95	19.9
	Effl. 3	11:42	0:20	21.5	8.91	8.73	8.6
	Effl. 4	11:52	0:30	21.9	9.13	8.15	5.1
	(Effl)	11:59	0:37	22.3	9.2	8.01	4.5
	Effl. 5	12:02	0:40	22.3	9.29	7.83	3.9
	Effl. 6	12:13	0:51	23	9.29	7.88	4.0
	Effl. 7	12:24	1:02	23.5	9.19	8.01	3.7
	Effl. 8	12:35	1:13	24.2	9.17	8.21	4.1
	Effl. 9	12:44	1:22	24.2	9.12	8.45	4.2
	Effl. 10	12:56	1:34	23.5	8.59	9.5	4.3
	Effl. 11	13:02	1:40	22.5	8.26	10.75	13.0
	Effl. 12	13:12	1:50	22.5	7.98	12.37	23.5
	(Effl)	13:16	1:54	22.4	7.88	13.12	50.0
	Effl. 13	13:22	2:00	22.6	7.95	13.09	71.0
	(Effl)	13:29	2:07	23.6	8.45	12.79	77.0
	Effl. 14	13:36	2:14	24.2	8.71	11.53	85.5
	(Effl)	13:40	2:18	24	8.51	10.91	56.0
	Effl. 15	13:46	2:24	24.5	7.59	9.9	37.4
	(Effl)	13:52	2:30	24.9	7.25	9.18	25.0
	Effl. 16	13:56	2:34	25.4	7.25	8.77	18.4
	(Effl)	14:01	2:39	25.6	7.4	8.46	14.0
	Effl. 17	14:09	2:47	25.6	7.28	8.11	10.7
	(Effl)	14:15	2:53	26	7.66	8.04	9.5
	Effl. 18	14:21	2:59	26	7.95	8.1	8.6
	(Effl)	14:26	3:04	26.1	8.23	8.22	8.5
	Effl. 19	14:32	3:10	26.1	8.39	8.39	8.5

Figure 33. Multiple sorption and regeneration cycles of once-through operation by two-stage aquacells (two cells in series). (a) Conductivity; (b) Iodide

	(Effl)	14:37	3:15	26.2	8.46	8.53	8.3
	Effl. 20	14:46	3:24	26.3	8.68	8.75	7.8
	Effl. 21	14:56	3:34	25.1	7.89	10.37	16.9
	(Effl)	15:01	3:39	24.8	7.77	11.04	23.0
	Effl. 22	15:06	3:44	24.5	7.7	11.7	27.8
	(Effl)	15:10	3:48	25.1	7.64	12.27	50.0
	Effl. 23	15:17	3:55	25.2	7.63	12.45	73.3
	(Effl)	15:21	3:59	25.5	7.75	11.92	67.0
	Effl. 24	15:24	4:02	25.5	7.87	11.41	62.1
	(Effl)	15:30	4:08	26.6	8.08	10.72	50.0
	(Effl)	15:32	4:10	26.8	8.29	10.43	35.0
	Effl. 25	15:38	4:16	26.6	8.63	9.38	21.2
8/22/2005	(Effl.)	10:33	4:22	21.8	8.6	12.02	39.5
	Effl. 1	10:40	4:29	22.3	8.83	10.61	28.4
	Effl. 2	10:45	4:34	22.4	8.98	9.54	14.0
	Effl. 3	10:57	4:46	23.1	8.51	9.29	7.2
	Effl. 4	11:09	4:58	23.3	9.36	8.05	5.6
	Effl. 5	11:23	5:12	23.9	9.29	7.86	4.8
	Effl. 6	11:35	5:24	24.1	9.17	8.22	5.0
	Effl. 7	11:53	5:42	24.3	9.02	8.67	4.7
	Effl. 8	12:08	5:57	24.6	9.12	9.01	5.0
	Effl. 9	12:16	6:05	25	9.1	9.14	5.0
	Effl. 10	12:23	6:12	23.6	8.78	10.1	12.2
	(Effl.)	12:28	6:17	23.8	8.62	10.91	20.0
	Effl. 11	12:33	6:22	24	8.08	12.45	28.9
	Effl. 12	12:40	6:29	24.1	8.15	12.95	67.3
	(Effl.)	12:46	6:35	24.2	8.35	12.54	77.0
	Effl. 13	12:50	6:39	24.3	8.47	12.16	88.6
	(Effl.)	12:53	6:42	24.1	8.51	11.86	68.0
	Effl. 14	12:58	6:47	24.3	8.53	11.31	54.6
	(Effl.)	13:03	6:52	24.5	8.54	10.91	

Figure 34. Multiple sorption and regeneration cycles of once-through operation by three-stage aquacells (two cells in series). (a) Conductivity; (b) Iodide

Date	sample #	Time sampled	Treatment time (Hr:Min)	Temp (ºC)	pH	Conductivity (mS/cm)	[I⁻] (mg/L)
8/23/2005	Feed 1	11:47	0	23.8	8.83	6.72	5.99
	Feed 2	13:12	1:25			6.72	6
	Feed 3	13:15	1:28			11.53	45.05
	Feed 4	13:35	1:48	17.3	8.34	11.53	45.05
	Feed 5	13:47	2:00			11.53	45.05
	Feed 6	13:48	2:01			6.72	6
	Feed 7	14:07	2:20			6.72	6
	Feed 8	14:08	2:21			6.72	6
	Feed 9	15:00	3:13			6.72	6
	Feed 10	15:39	3:52			6.72	6
	Feed 11	15:40	3:53			11.53	45.05
	Feed 12	16:04	4:17			11.53	45.05
	Effl. 1	11:53	0:06	22.4	8.12	9.98	27.58
	(Effl.)	12:02	0:09	22.9	8.65	7.82	18
	Effl. 2	12:06	0:13	23.3	8.79	6.91	8.36
	Effl. 3	12:22	0:29	25.1	8.87	5.51	4.76
	(Effl.)	12:31	0:38	25.2	8.96	5.34	4.2
	Effl. 4	12:38	0:45	25.8	8.95	5.35	3.9
	(Effl.)	12:46	0:53	26	8.93	5.38	3.7
	Effl. 5	12:50	0:57	26.3	8.89	5.48	3.55
	Effl. 6	13:04	1:11	26.6	8.74	5.68	3.7
	Effl. 7	13:18	1:25	26.6	8.65	5.89	3.75
	Effl. 8	13:27	1:34	24.6	8.19	9.4	18.37
	(Effl.)	13:31	1:38	22.4	8.12	10.75	20
	(Effl.)	13:38	1:45	20.5	8.08	11.46	25
	Effl. 9	13:40	1:47	20.2	8	11.75	26.88
	Effl. 10	13:47	1:54	20.9	7.94	11.79	30.67
	Effl. 11	13:53	2:00	22.4	7.84	11.98	33.61
	(Effl.)	14:00	2:07	23.6	8.02	11.52	39
	Effl. 12	14:07	2:14	25.1	8.36	8.84	42.02
	(Effl.)	14:13	2:20	25.6	8.55	8	30
	Effl. 13	14:20	2:27	26.5	8.01	6.91	19.2
	Effl. 14	14:28	2:35	27	7.7	6.14	11.54
	Effl. 15	14:39	2:46	27.5	7.65	5.52	7.04
	Effl. 16	15:05	3:12	28.7	8.08	5.28	4.34
	Effl. 17	15:24	3:31	28	8.23	5.57	3.83
	Effl. 18	15:36	3:43	27.8	8.13	6.03	3.93
	(Effl.)	15:40	3:47	27.5	8.1	6.18	9
	Effl. 19	15:44	3:51	26.9	7.9	8.57	17.2
	Effl. 20	15:50	3:57	25.9	7.74	10.44	23.39
	(Effl.)	15:56	4:03	23.8	7.71	11.31	30
	Effl. 21	16:00	4:07	23.1	7.78	11.9	37.24
	Effl. 22	16:04	4:11	20.9	8.19	12.33	50.28

Analytes	Method	Detection limit	IR Permeate Concentration			
			TFC-HR	TFC-ULP	TMG10	NF-90
Inorganics- Cations						
Silver (mg/L)	Std Methods 3120B	0.0035	n.d.	n.d.	n.d.	n.d.
Aluminum (mg/L)	Std Methods 3120B	0.02	n.d.	n.d.	n.d.	n.d.
Arsenic (mg/L)	Std Methods 3114B	0.001	n.d.	n.d.	n.d.	n.d.
Boron (mg/L)	Std Methods 3120B	0.004	3.17	1.74	2.24	2.89
Barium (mg/L)	Std Methods 3120B	0.012	0.013	0.04	0.01	0.023
Beryllium (mg/L)	Std Methods 3120B	0.0003	n.d.	n.d.	n.d.	n.d.
Calcium (mg/L)	Std Methods 3120B	0.011	0.23	0.63	0.2	0.45
Cadmium (mg/L)	Std Methods 3120B	0.002	n.d.	n.d.	n.d.	n.d.
Cobalt (mg/L)	Std Methods 3120B	0.008	n.d.	n.d.	n.d.	n.d.
Chromium (mg/L)	Std Methods 3120B	0.005	n.d.	n.d.	n.d.	n.d.
Copper (mg/L)	Std Methods 3120B	0.002	0.056	0.03	0.04	0.026
Iron (mg/L)	Std Methods 3120B	0.002	n.d.	n.d.	n.d.	n.d.
Potassium (mg/L)	Std Methods 3120B	0.084	0.28	0.5	0.4	0.54
Lithium (mg/L)	Std Methods 3120B	0.001	n.d.	0.02	0.02	n.d.
Magnesium (mg/L)	Std Methods 3120B	0.0002	0.084	0.22	0.04	0.15
Manganese (mg/L)	Std Methods 3120B	0.0007	n.d.	n.d.	0.01	n.d.
Molybdenium (mg/L)	Std Methods 3120B	0.006	n.d.	0.01	n.d.	n.d.
Sodium (mg/L)	Std Methods 3120B	0.02	193	107.09	106.91	182
Nickel (mg/L)	Std Methods 3120B	0.007	n.d.	n.d.	n.d.	n.d.
Phosphorous (mg/L)	Std Methods 3120B	0.062	n.d.	0.01	n.d.	n.d.
Lead (mg/L)	Std Methods 3120B	0.023	n.d.	n.d.	n.d.	n.d.
Sulfur (mg/L)	Std Methods 3120B	0.05	0.60	0.09	0.03	0.51
Antimony (mg/L)	Std Methods 3120B	0.029	n.d.	n.d.	n.d.	n.d.
Selenium (mg/L)	Std Methods 3114B	0.001	n.d.	0.03	n.d.	n.d.
Silicon (mg/L)	Std Methods 3120B	0.11	0.11	0.73	0.46	0.13
Tin (mg/L)	Std Methods 3120B	0.03	n.d.	n.d.	n.d.	n.d.
Strontium (mg/L)	Std Methods 3120B	0.0002	n.d.	0.05	0.01	n.d.
Titanium (mg/L)	Std Methods 3120B	0.0008	n.d.	n.d.	n.d.	n.d.
Vanadium (mg/L)	Std Methods 3120B	0.0013	n.d.	n.d.	n.d.	n.d.
Zinc (mg/L)	Std Methods 3120B	0.0023	0.04	0.03	0.05	0.05
Inorganics- Anions						
Chloride (mg/L)	Std Methods 4110C	1.5	325.2	119.5	141.4	407.9
Bromide (mg/L)	Std Methods 4110C	1	12.4	2.27	2.85	15.3
Iodide (mg/L)	Ion selective probe	0.1	20.3	20.8	20.6	24
Organics						
TOC (total organic carbon) (mg/L)	Std Methods 5310C	0.06	0.12	0.2	0.2	0.07
UV-254 absorbance (m^{-1})	Std Methods 5910B	0.001	3.74	3.97	4.07	3.75
UV-272 absorbance (m^{-1})	Std Methods 5910B	0.001	2.46	3.03	3.16	2.51
Color (436 nm) (m^{-1})	Std Methods 2120C	0.001	1.07	1.23	1.29	0.95

Figure 35 and Summary of CDT testing results of one single industrial aquacell using synthetic NaCl solution

Flow rate (mL/min)	3000				3000			3000		
Average feed water conductivity (uS/cm)	3100				1926			1041		
Cycle	1	2	3	4	1	2	3	1	2	3
Total retained TDS during treatment cycle(mg)	10382	12936	12573	12033	20879	25246	23997	13573	15916	16438
Adsorption during treatment cycle (mg TDS/g carbon)	1.67	2.08	2.02	1.94	3.36	4.06	3.86	2.18	2.56	2.65
Retention rate during treatment (mg TDS/g carbon/min)	0.08	0.09	0.09		0.07	0.07	0.08	0.06	0.05	0.05
Released TDS during regeneration (mg)	12084	13045	13699	10283	21105	27096	21176	12486	13838	16005
Regeneration efficiency (%)	116	101	109		101	107	88	92	87	97
Treatment time (min)	21	24	23	23	48	57	48	38	54	53
Regeneration time (min)	16	17	17		20	22	22	25	16	18
downtime (%)	43	41	43	0	30	28	31	40	24	26
water recovery (%)	57	59	57		70	72	69	60	76	74
Max. conductivity reduction(us/cm)	455	504	486		467	473	511	266	283	306
Max removal (%)	15	16	16		24	25	27	25	27	29
Applied current during treatment	260	60	260	60	260	60	260	60	60	60
Applied current during regeneration	60	260	60	60	60	260	60	60	60	60
Energy consumption/product water (kWh/m^3)	1.59	1.10	1.52	0.27	1.41	0.89	1.26	0.30	0.38	0.20
Energy consumption/removed salts (kWh/g)	0.0775	0.0391	0.0561	0.0104	0.0154	0.0067	0.0119	0.0064	0.0048	0.0025

Flow rate (mL/min)	2500			2000		2000			1000			700	2000
Average feed water conductivity (uS/cm)	1041			1068		1053			1300			1053	1000
Cycle	1	2	3	1	2	1	2	3	1	2	3	1	1
Total retained TDS during treatment cycle(mg)	16947	14874	13726	23114	25454	19696	16524	16186	16725	17543	20455	17706	19556
Adsorption during treatment cycle (mg TDS/g carbon)	2.73	2.39	2.21	3.72	4.10	3.17	2.66	2.61	2.69	2.82	3.29	3.17	3.15
Retention rate during treatment (mg TDS/g carbon/min)	0.04	0.04	0.04	0.04	0.04	0.03	0.04	0.04	0.03	0.04	0.04	0.01	0.03
Released TDS during regeneration (mg)	12740	13916	13984	14273	14189	14854	13705	14757	20045	18926	29983	15028	23528
Regeneration efficiency (%)	75	94	102	62	56	75	83	91	120	108	147	85	120
Treatment time (min)	64	61	57	103	93	92	75	69	81	80	86	252	121
Regeneration time (min)	17	18	17	19	19	30	29	30	39	38	61	51	56
downtime (%)	21	23	23	16	17	25	28	30	32	32	41	17	32
water recovery (%)	79	77	77	84	83	75	72	70	68	68	59	83	68
Max. conductivity reduction(us/cm)	315	298	283	321	367	307	340	361	355	377	427	279	244
Max removal (%)	30	28	27	31	35	29	32	34	27	29	33	27	19
Applied current during treatment	60	60	60	60	60	30	30	30	30	30	30	30	15
Applied current during regeneration	60	60	60	60	60	30	30	30	30	30	30	30	15
Energy consumption/product water (kWh/m^3)	0.42	0.42	0.47	0.51	0.48	0.16	0.19	0.19	0.32	0.32	0.26	0.36	0.07
Energy consumption/removed salts (kWh/g)	0.0035	0.0042	0.0054	0.0015	0.0015	0.0007	0.0011	0.0012	0.0009	0.0008	0.0005	0.0002	0.0002

Appendix 2

ATR-FTIR spectra of virgin and fouled membranes: TFC-HR, TFC-ULP, TMG-10, TFC-S, and ESNA

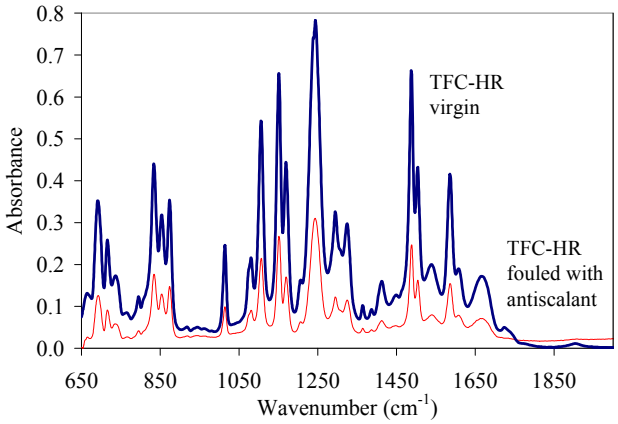

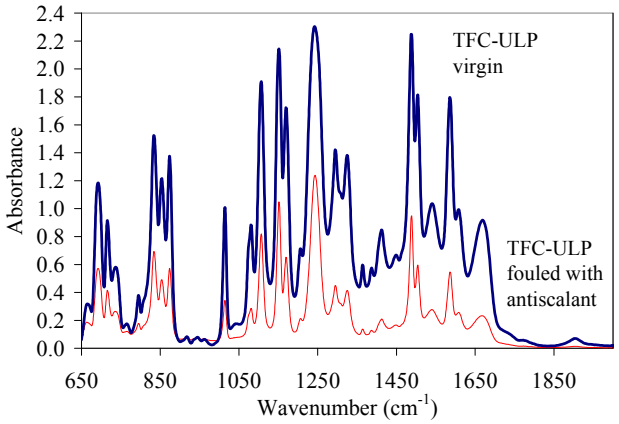

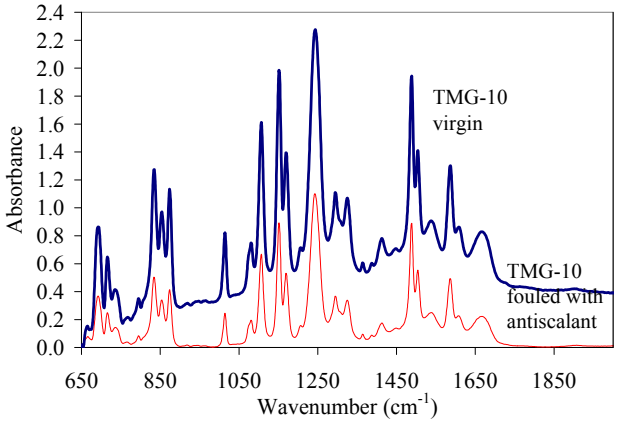

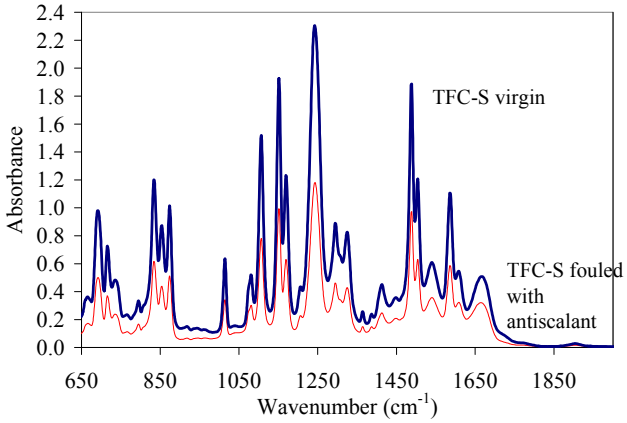

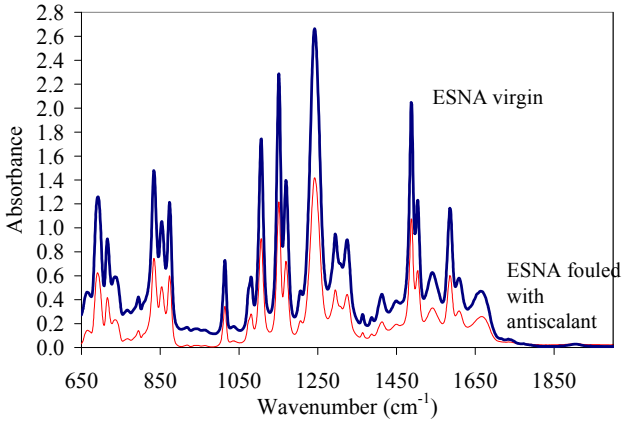

Appendix 3: Summary of Water Quality Data during Laboratory-Scale Membrane Testing

Analytes	Method	Detection limit	FT Feed Concentration			
			TFC-HR	TFC-ULP	TMG10	NF-90
Inorganics- Cations						
Silver (mg/L)	Std Methods 3120B	0.0035	n.d.	n.d.	0.22	n.d.
Aluminum (mg/L)	Std Methods 3120B	0.02	n.d.	n.d.	n.d.	n.d.
Arsenic (mg/L)	Std Methods 3114B	0.001	n.d.	n.d.	n.d.	n.d.
Boron (mg/L)	Std Methods 3120B	0.004	4.426	4.42	3.59	4.934
Barium (mg/L)	Std Methods 3120B	0.012	1.804	2.04	1.92	1.726
Beryllium (mg/L)	Std Methods 3120B	0.0003	n.d.	n.d.	n.d.	n.d.
Calcium (mg/L)	Std Methods 3120B	0.011	28.706	33.1	29.82	26.87
Cadmium (mg/L)	Std Methods 3120B	0.002	n.d.	n.d.	n.d.	n.d.
Cobalt (mg/L)	Std Methods 3120B	0.008	n.d.	n.d.	0.03	n.d.
Chromium (mg/L)	Std Methods 3120B	0.005	n.d.	n.d.	n.d.	n.d.
Copper (mg/L)	Std Methods 3120B	0.002	0.099	0.39	0.38	0.27
Iron (mg/L)	Std Methods 3120B	0.002	n.d.	0.01	0.01	n.d.
Potassium (mg/L)	Std Methods 3120B	0.084	7.8	9.71	5.4	9.2
Lithium (mg/L)	Std Methods 3120B	0.001	n.d.	0.3	0.36	n.d.
Magnesium (mg/L)	Std Methods 3120B	0.0002	11.728	11.78	11.03	10.92
Manganese (mg/L)	Std Methods 3120B	0.0007	n.d.	0.06	0.08	n.d.
Molybdenium (mg/L)	Std Methods 3120B	0.006	n.d.	0.01	0.06	n.d.
Sodium (mg/L)	Std Methods 3120B	0.02	1950.2	2186.1	2068	1825.6
Nickel (mg/L)	Std Methods 3120B	0.007	n.d.	n.d.	0.02	n.d.
Phosphorous (mg/L)	Std Methods 3120B	0.062	n.d.	0.23	n.d.	n.d.
Lead (mg/L)	Std Methods 3120B	0.023	n.d.	n.d.	n.d.	n.d.
Sulfur (mg/L)	Std Methods 3120B	0.05	5.54	5.11	0.78	5.89
Antimony (mg/L)	Std Methods 3120B	0.029	n.d.	n.d.	n.d.	n.d.
Selenium (mg/L)	Std Methods 3114B	0.001	n.d.	0.17	0.02	n.d.
Silicon (mg/L)	Std Methods 3120B	0.11	2.4400	2.88	2.29	2.98
Tin (mg/L)	Std Methods 3120B	0.03	n.d.	0.1	n.d.	n.d.
Strontium (mg/L)	Std Methods 3120B	0.0002	1.8	2.5	2.1	1.8
Titanium (mg/L)	Std Methods 3120B	0.0008	n.d.	n.d.	n.d.	n.d.
Vanadium (mg/L)	Std Methods 3120B	0.0013	n.d.	n.d.	n.d.	n.d.
Zinc (mg/L)	Std Methods 3120B	0.0023	0.19	0.61	0.79	0.51
Inorganics- Anions						
Chloride (mg/L)	Std Methods 4110C	1.5	3666.6	2260.2	3399.21	4980.53
Bromide (mg/L)	Std Methods 4110C	1.0	103.4	33.71	50.23	138
Iodide (mg/L)	Ion selective probe	0.1	54.52	66.36	65.06	58.2
Organics						
TOC (total organic carbon) (mg/L)	Std Methods 5310C	0.06	0.53	1.3	1.6	0.53
UV-254 absorbance (m^{-1})	Std Methods 5910B	0.001	13.29	15.01	14.99	12.86
UV-272 absorbance (m^{-1})	Std Methods 5910B	0.001	4.7	5.74	5.91	4.59
Color (436 nm) (m^{-1})	Std Methods 2120C	0.001	1.39	1.51	1.49	1.35
Specific UV absorbance (L m^{-1} mg^{-1})	Calculated as ratio between UV-254 and TOC	0.001	25.1	11.5	9.4	24.3

Analytes	Method	Detection limit	IR Feed Concentration			
			TFC-HR	TFC-ULP	TMG10	NF-90
Inorganics- Cations						
Silver (mg/L)	Std Methods 3120B	0.0035	n.d.	0.04	n.d.	n.d.
Aluminum (mg/L)	Std Methods 3120B	0.02	n.d.	n.d.	n.d.	n.d.
Arsenic (mg/L)	Std Methods 3114B	0.001	n.d.	n.d.	n.d.	n.d.
Boron (mg/L)	Std Methods 3120B	0.004	4.482	4.57	3.91	3.69
Barium (mg/L)	Std Methods 3120B	0.012	1.72	1.95	1.83	1.71
Beryllium (mg/L)	Std Methods 3120B	0.0003	n.d.	0.02	n.d.	n.d.
Calcium (mg/L)	Std Methods 3120B	0.011	25.945	32.21	29.69	25.939
Cadmium (mg/L)	Std Methods 3120B	0.002	n.d.	0.01	n.d.	n.d.
Cobalt (mg/L)	Std Methods 3120B	0.008	n.d.	0.03	0.03	n.d.
Chromium (mg/L)	Std Methods 3120B	0.005	n.d.	0.05	0.03	n.d.
Copper (mg/L)	Std Methods 3120B	0.002	0.313	0.82	0.5	0.329
Iron (mg/L)	Std Methods 3120B	0.002	n.d.	0.09	n.d.	n.d.
Potassium (mg/L)	Std Methods 3120B	0.084	8.6	13.86	8.53	8.8
Lithium (mg/L)	Std Methods 3120B	0.001	n.d.	0.83	0.25	n.d.
Magnesium (mg/L)	Std Methods 3120B	0.0002	10.696	11.34	10.74	10.67
Manganese (mg/L)	Std Methods 3120B	0.0007	n.d.	0.08	0.08	n.d.
Molybdenium (mg/L)	Std Methods 3120B	0.006	n.d.	0.62	0.06	n.d.
Sodium (mg/L)	Std Methods 3120B	0.02	1800	2070	1935	1757
Nickel (mg/L)	Std Methods 3120B	0.007	n.d.	0.04	n.d.	n.d.
Phosphorous (mg/L)	Std Methods 3120B	0.062	n.d.	n.d.	n.d.	n.d.
Lead (mg/L)	Std Methods 3120B	0.023	n.d.	0.07	n.d.	n.d.
Sulfur (mg/L)	Std Methods 3120B	0.05	4.696	3.65	4.4	7.087
Antimony (mg/L)	Std Methods 3120B	0.029	n.d.	0.01	n.d.	n.d.
Selenium (mg/L)	Std Methods 3114B	0.001	n.d.	0.67	0.42	n.d.
Silicon (mg/L)	Std Methods 3120B	0.11	2.991	3.62	2.24	2.971
Tin (mg/L)	Std Methods 3120B	0.03	n.d.	0.21	n.d.	n.d.
Strontium (mg/L)	Std Methods 3120B	0.0002	1.8	2.44	1.88	1.9
Titanium (mg/L)	Std Methods 3120B	0.0008	n.d.	0.01	0.01	n.d.
Vanadium (mg/L)	Std Methods 3120B	0.0013	n.d.	n.d.	n.d.	n.d.
Zinc (mg/L)	Std Methods 3120B	0.0023	0.48	0.72	0.87	0.501
Inorganics- Anions						
Chloride (mg/L)	Std Methods 4110C	1.5	4387.66	2676.80	2367.80	5955.46
Bromide (mg/L)	Std Methods 4110C	1.0	147.65	38.97	31.89	168.46
Iodide (mg/L)	Ion selective probe	0.1	51.06	62.51	63.46	57.9
Organics						
TOC (total organic carbon) (mg/L)	Std Methods 5310C	0.06	0.63	1.4	1.2	0.52
UV-254 absorbance (m^{-1})	Std Methods 5910B	0.001	13.37	14.75	13.75	13.02
UV-272 absorbance (m^{-1})	Std Methods 5910B	0.001	4.83	5.38	5.5	1.31
Color (436 nm) (m^{-1})	Std Methods 2120C	0.001	1.39	1.41	1.42	1.31
Specific UV absorbance (L m^{-1} mg^{-1})	Calculated as ratio between UV-254 and TOC	0.001	21.2	10.5	11.5	25.0

Analytes	Method	Detection limit	IR Feed Concentration			
			TFC-HR	TFC-ULP	TMG10	NF-90
Inorganics- Cations						
Silver (mg/L)	Std Methods 3120B	0.0035	n.d.	0.04	n.d.	n.d.
Aluminum (mg/L)	Std Methods 3120B	0.02	n.d.	n.d.	n.d.	n.d.
Arsenic (mg/L)	Std Methods 3114B	0.001	n.d.	n.d.	n.d.	n.d.
Boron (mg/L)	Std Methods 3120B	0.004	4.482	4.57	3.91	3.69
Barium (mg/L)	Std Methods 3120B	0.012	1.72	1.95	1.83	1.71
Beryllium (mg/L)	Std Methods 3120B	0.0003	n.d.	0.02	n.d.	n.d.
Calcium (mg/L)	Std Methods 3120B	0.011	25.945	32.21	29.69	25.939
Cadmium (mg/L)	Std Methods 3120B	0.002	n.d.	0.01	n.d.	n.d.
Cobalt (mg/L)	Std Methods 3120B	0.008	n.d.	0.03	0.03	n.d.
Chromium (mg/L)	Std Methods 3120B	0.005	n.d.	0.05	0.03	n.d.
Copper (mg/L)	Std Methods 3120B	0.002	0.313	0.82	0.5	0.329
Iron (mg/L)	Std Methods 3120B	0.002	n.d.	0.09	n.d.	n.d.
Potassium (mg/L)	Std Methods 3120B	0.084	8.6	13.86	8.53	8.8
Lithium (mg/L)	Std Methods 3120B	0.001	n.d.	0.83	0.25	n.d.
Magnesium (mg/L)	Std Methods 3120B	0.0002	10.696	11.34	10.74	10.67
Manganese (mg/L)	Std Methods 3120B	0.0007	n.d.	0.08	0.08	n.d.
Molybdenium (mg/L)	Std Methods 3120B	0.006	n.d.	0.62	0.06	n.d.
Sodium (mg/L)	Std Methods 3120B	0.02	1800	2070	1935	1757
Nickel (mg/L)	Std Methods 3120B	0.007	n.d.	0.04	n.d.	n.d.
Phosphorous (mg/L)	Std Methods 3120B	0.062	n.d.	n.d.	n.d.	n.d.
Lead (mg/L)	Std Methods 3120B	0.023	n.d.	0.07	n.d.	n.d.
Sulfur (mg/L)	Std Methods 3120B	0.05	4.696	3.65	4.4	7.087
Antimony (mg/L)	Std Methods 3120B	0.029	n.d.	0.01	n.d.	n.d.
Selenium (mg/L)	Std Methods 3114B	0.001	n.d.	0.67	0.42	n.d.
Silicon (mg/L)	Std Methods 3120B	0.11	2.991	3.62	2.24	2.971
Tin (mg/L)	Std Methods 3120B	0.03	n.d.	0.21	n.d.	n.d.
Strontium (mg/L)	Std Methods 3120B	0.0002	1.8	2.44	1.88	1.9
Titanium (mg/L)	Std Methods 3120B	0.0008	n.d.	0.01	0.01	n.d.
Vanadium (mg/L)	Std Methods 3120B	0.0013	n.d.	n.d.	n.d.	n.d.
Zinc (mg/L)	Std Methods 3120B	0.0023	0.48	0.72	0.87	0.501
Inorganics- Anions						
Chloride (mg/L)	Std Methods 4110C	1.5	4387.66	2676.80	2367.80	5955.46
Bromide (mg/L)	Std Methods 4110C	1.0	147.65	38.97	31.89	168.46
Iodide (mg/L)	Ion selective probe	0.1	51.06	62.51	63.46	57.9
Organics						
TOC (total organic carbon) (mg/L)	Std Methods 5310C	0.06	0.63	1.4	1.2	0.52
UV-254 absorbance (m^{-1})	Std Methods 5910B	0.001	13.37	14.75	13.75	13.02
UV-272 absorbance (m^{-1})	Std Methods 5910B	0.001	4.83	5.38	5.5	1.31
Color (436 nm) (m^{-1})	Std Methods 2120C	0.001	1.39	1.41	1.42	1.31
Specific UV absorbance (L m^{-1} mg^{-1})	Calculated as ratio between UV-254 and TOC	0.001	21.2	10.5	11.5	25.0

Appendix 4: Rotation of Cell Position through 4 Time Steps with the 700 mL/min System